Master of Science Thesis

Bi-directional Solid Oxide Cells used as SOFC for Aircraft APU system and as SOEC to produce fuel at the airport

Exergy evaluation of jet fuel and ammonia as fuel alternatives

Sana Fateh

15 Jan 2015

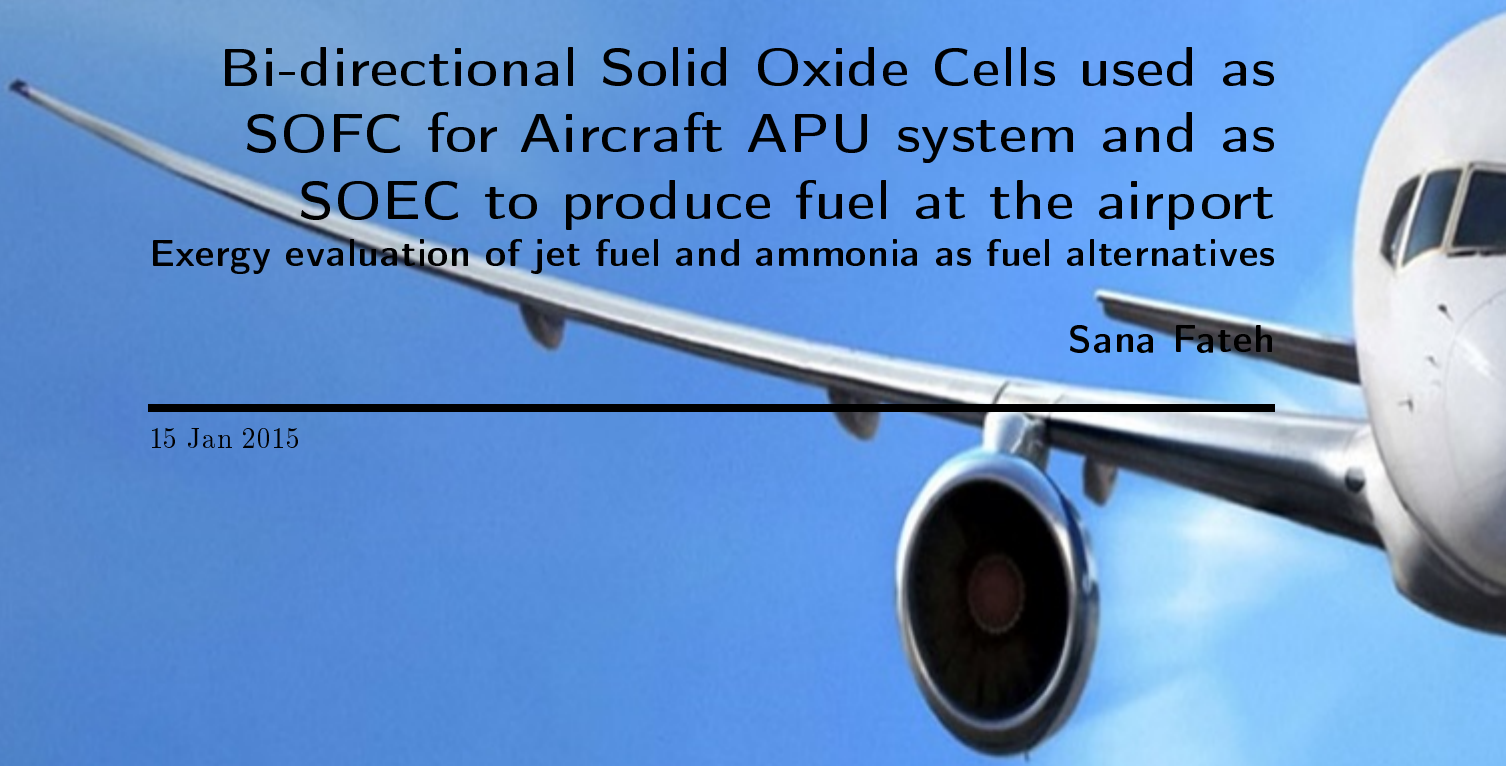

Faculty of Mechanical, Maritime and Materials Engineering · Delft University of Technology

Bi-directional Solid Oxide Cells used as SOFC for Aircraft APU system and as SOEC to produce fuel at the airport

Exergy evaluation of jet fuel and ammonia as fuel alternatives

Master of Science Thesis

For obtaining the degree of Master of Science in Mechanical, Maritime and Materials Engineering at Delft University of Technology

Sana Fateh

15 Jan 2015

Faculty of Mechanical, Maritime and Materials Engineering · Delft University of Technology

Delft University Of Technology
Department Of
Process and Energy Engineering

The undersigned hereby certify that they have read and recommend to the Faculty of Mechanical, Maritime and Materials Engineering for acceptance a thesis entitled **"Bi-directional Solid Oxide Cells used as SOFC for Aircraft APU system and as SOEC to produce fuel at the airport"** by **Sana Fateh** in partial fulfillment of the requirements for the degree of **Master of Science**.

Dated: 15 Jan 2015

Supervisor-1: _____
Prof.Dr.P.V. Aravind

Supervisor-2: _____
ir. Alvaro Fernandes

Examiner-1: _____
Prof. Burak Eral

Examiner-2: _____
Prof.Dr.Ad van Wijk

Abstract

Leaders of European union and G8 have set the target of 80% reduction in greenhouse gases emissions by 2050 by decarbonizing the power and transport sector. There are several pathways to achieve this, some of them being a) use of renewable power and biomass b) improvement in transport and building energy efficiency and c) replacement of fossil based fuel with sustainable fuel. This thesis is focussed on some of the measures which can be taken by Air Transportation Industry to reduce GHG emissions and carbon footprint. Although, there are many ways in which air transport industry can achieve this goal, this work mainly discusses a) increase in power generation efficiency of aircraft systems b) use of sustainable fuels for aircrafts and c) some ways for sustainable fuel production for aircrafts in an efficient and economic way. However, it is only starting point for discussion and can be further extended to include more efficient and cheaper technologies with reduced carbon foot-print.

In this study, use of bi-directional Solid-Oxide Cells (SOC) as auxiliary power unit (APU) on-board commercial aircraft is explored. These bi-directional SOC APU units can be used in the airport energy network either to produce cleaner energy or to produce sustainable fuels depending on the energy demand. This work focusses on use of these bi-directional SOCs as fuel cells during flight operations and as electrolysers to produce sustainable fuel at the airport when the aircrafts are parked. Hence, complete fuel production plant is designed to be situated at the airport. The scope of this thesis is limited to production of fuel for aircraft APU use only. Further extension of this project can include use of these bi-directional SOCs for providing electricity to the airport and fuel for other purposes.

For analysis, medium range aircrafts like A320 and B737 are considered. This system is designed and dimensioned for producing 500KW of electric power on-board aircarft. Jet fuel and ammonia are considered as fuel options for Solid Oxide Fuel Cell-Gas Turbine (SOFC-GT) based APU.

Small scale airports like Eindhoven are studied to understand the flight frequency and parking duration for the aircrafts. These bi-directional SOCs are operational as Solid Oxide Electrolyzer Cell (SOEC) only when the aircraft is parked. Co-electrolysis is performed to produce syngas and steam electrolysis is done to produce hydrogen at the airport. Jet

fuel is synthesized from syngas through Fischer Tropsch process and ammonia is synthesized from H_2 and N_2 through Haber Bosch process. Fuel synthesis plants are also designed as part of stationary fuel production plant at the airport.

The fact that electrolyzer operates on excess available renewable electricity only, needs a special mention here. Intermittent nature of excess renewable electricity requires implementation of another source of sustainable syngas for fuel production so that sufficient capacity to supply all demand is ensured and robustness against delivery risks is achieved. Biomass gasification is one other method for generating fossil-free fuel. It uses biomass (birch wood) to produce syngas for sustainable fuel production at the aiport alongwith electrolysers. This leads to three cases of fuel production:

- Case-1: Gasifier+fuel synthesis
- Case-2: SOEC+fuel synthesis
- Case-3: Gasifier+SOEC+Fuel synthesis

ASPEN PLUS is used for modelling SOFC and stationary fuel production plant models with both jet fuel and ammonia. Modelling procedure for all the models is explained in detail with input parameters and process conditions.

Thermodynamic analysis is carried out to compare the exergy efficiency of jet fuel and ammonia based SOFC-GT systems. It is observed that both jet fuel and ammonia based SOFC-GT systems give 62% and 58% exergy efficiency respectively which is higher than the conventional APU systems. Similarly, section by section exergy analysis is carried out for jet fuel and ammonia production plants to understand the exergy destructing processes. Comparison is made between exergy efficiency of jet fuel and ammonia production plants at the airport to understand thermodynamic behavior of both. Jet fuel synthesis produces significant amount of hydrogen and gasoline alongwith jet fuel as product. Therefore, two scenarios are analysed for exergy comparisons.

a) *Ammonia and jet fuel considered as product:* Ammonia shows higher exergy efficiency than jet fuel production for all three cases enumerated above.

b) *Ammonia and (jet fuel, gasoline, hydrogen) are considered as useful products:* For case-1 and case-3, jet fuel plant is exergetically more favorable than ammonia plant. However, for case-2, ammonia plant has higher exergy efficiency than jet fuel plant.

Acknowledgements

This thesis has been a team work and I would like to thank all those who have helped me through the duration of my thesis and helped me complete this tremendous amount of work. I would like to thank Dr. P.V. Aravind for giving me an opportunity to work with his team and allow me to take up a project of my choice. I would specially like to thank my daily superviser Álvaro Fernandes, who guided me at each step and provided me with every possible help to complete the thesis successfully. I would like to thank the Process and Energy department for providing the facilitites to carry out my thesis. At last I would like to thank my parents and friends for supporting me mentally and morally thorughout the thesis period and for motivating me to keep going through all the ups and downs.

Delft, The Netherlands
15 Jan 2015

Sana Fateh

Contents

List of Figures

List of Tables

Nomenclature

Roman Symbols

A	Total cell area	[sqm]
ASR	Area specific Resistance	[Ω/sqm]
dG	Change in Gibbs free energy	[KJ]
dH	Change in Enthalpy	[KJ]
dS	Change in entropy	[KJ/K]
dU	Change in internal energy	[KJ]
dV	Change in control Volume	[cum]
Ex	Exergy flow	[KW]
F	Faraday's constant	[c/mol]
f	Empirical coefficients to calculate liquid fuel chemical exergy	
H	Enthalpy	[KJ]
h	Altitude	[m]
I	Current	[Amp]
J	Current density	[Amp/m2]
LHV	Lower Heating Value	[KJ/kg]
m	Mass flow	[kg/s]
N	Total number of units	
n	Number of moles of a substance	[mol]
O	Oxygen flow	[kmol/hr]
P	Power	[KW]
p	Partial Pressure	[bar]
p1	Total pressure	[bar]
Q	Heat	[KJ]
R	Ideal gas constant	[kJ/kmolK]

S	Entropy	[KJ/K]
T	Temperature	[K]
UF	Fuel utilization	
V	Voltage	[V]
W	Work	[KJ]
z	Number of eletrons exchanged per electrochemical reaction event	

Greek Symbols

η	Efficiency	
$\triangle g$	Change in molar Gibbs free energy	[KJ/mol]
$\triangle h$	Change in molar enthalpy	[KJ/kmol]
$\triangle s$	Change in molar entropy	[KJ/kmol-K]
$\triangle V$	Overpotential	[Volt]
β	Empirical coefficient to calculate chemical exergy for solid fuels	

Abbreviations

AEA	All Electric Aircraft
APU	Auxilliary Power Unit
ATR	Auto thermal reformer
FICFB	Fast Internal Circulating Fluidized Bed
MEA	More Electric Aircraft
NOx	Nitrous oxide
OCV	Open Circuit Voltage
OLGA	Oil and Gas Simulation
RWGS	Reverse water gas shift
SOC	Solid Oxide Cell
SOEC	Solid Oxide Electrolyzer Cell
SOFC-GT	Solid Oxide Fuel Cell- Gas Turbine
SOFCPU	Solid Oxide Fuel Cell Power unit
WGS	Water gas shift

Subscripts

a	Anodic value
am1	Ammonia based fuel production plant (case-1)
am2	Ammonia based fuel production plant (case-2)
am3	Ammonia based fuel production plant (case-3)
aux	Auxilliary components
bio	biomass
c	Cathodic value
cell	Cell units in SOFC
chem	Chemical

dest	Destruction
elec	Electrical
Ex	Exergy based value
f	Functional
gasifier	Gasifier based values
H2	Hydrogen based value
H2O	Water based value
i	Represents any element
in	Inlet value
jf	Jet fuel based
jf1	Jet fuel based fuel production plant (case-1)
jf2	Jet fuel based fuel production plant (case-2)
jf3	Jet fuel based fuel production plant (case-3)
k	Number of gaseous species
lf	Liquid fuel
N2	Nitrogen based values
net	Net value
NH3	Ammonia based
nst	Nernst potential
O2	Oxygen based value
out	Outlet value
phy	Physical
rev	Thermodynamic reversibility
rxn	Reaction based quantity
S	Sulphur based values
s	Solid fuel
SOEC	Electrolyzer cell based values
SOFC	SOFC based values
total	Total
turb	Turbine value
u	Universal

Superscripts

0	Standard condition (1 bar, temperature of reaction)
ec	Electrolysis value
mol	Molar basis
v	Stoichiometric coefficients of specie in global reaction

Chapter 1

Introduction

In July 2009, the leaders of the European Union and the G8 announced an objective to reduce greenhouse gas emissions by at least 80% below 1990 levels by 2050 [12]. According to Roadmap 2050, 95 to 100% decarbonization of power sector is required to achieve this goal. Carbon capture and storage, nuclear energy and mix of renewable technologies are considered as pathways for decarbonizing the power sector keeping in mind energy security, environmental and economic goals of the European Union. To reach the target of 80% GHG reduction by 2050, transport and building sectors should switch to clean fuels such as biofuels or biomass, carbon-free hydrogen and decarbonized electricity from fossil fuels. To reduce fuel consumption, noise and exhaust emissions, aircraft industry has to move towards newer technologies for primary and secondary power production. Fuel cells is one such technology which show a high potential for future realization because of the unmatched efficiency and environmental performance. This chapter, therefore, deals with explanation of aircraft APU systems and why it is a good idea to replace conventional APU turbine systems with SOFC. To make it more greener and cleaner, use of sustainable fuel in SOFC based APU system is suggested. For production of these fuels, one of the many ways is to use bi-directional SOC APU from aircraft when they it is parked or use biomass gasification technology to produce biofuel. Hence, this chapter also gives the motivation and aim of the thesis, which just scratches the surface of otherwise enormous task.

1.1 Aircraft APU systems

Typical Auxiliary Power Units (APUs) are gas turbine engines located in the tapered tail cone section of the rear fuselage in commercial jet aircraft. Figure 1.1 shows the shematic for a typical turbine based aircraft APU system. They are used primarily during aircraft ground operation to provide electricity, compressed air, and/or shaft power for main engine start, air conditioning and other aircraft systems. APUs can also provide backup electric power during in-flight operation. Basic APU functions are as described below:

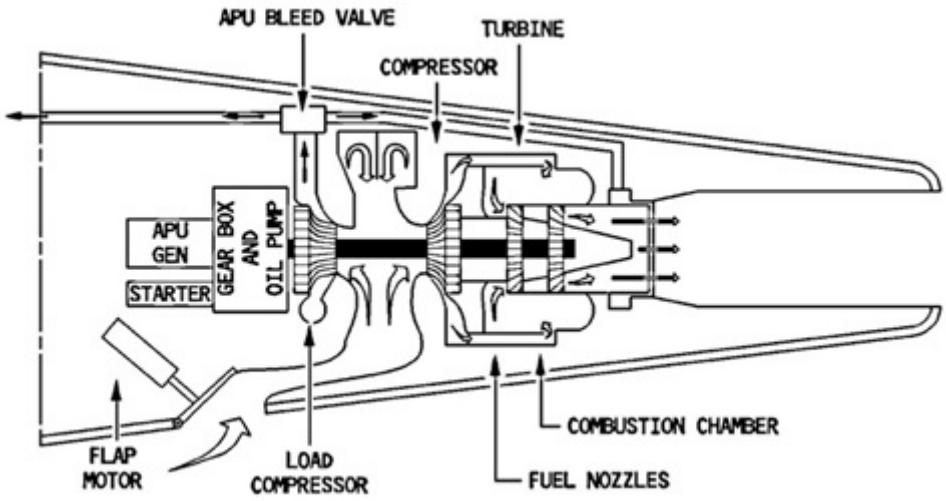

Figure 1.1: Aircraft APU schematic (gas turbine APU) [1]

- On the ground
  - It supplies bleed air for starting the engines and for the air conditioning system
  - It supplies electrical power to the electrical system.
- During takeoff
  - It supplies bleed air for air conditioning, thus avoiding a reduction in engine thrust caused by the use of engine bleed air for this purpose
- In flight
  - It backs up the electrical system
  - It backs up the air conditioning
  - It can be used to start the engines

Currently, the propulsion engines are utilized for electrical power loads during the cruise operation and a separate tail mounted gas turbine based APU system for ground operations. In flight, the marginal efficiency of electric power generated by the main engines and their generators is at most 40-45% [13], however, recent studies [9] have claimed efficiencies for state-of-art B787 achievable to 50% due to advances in power electronics and high efficiency power conversions. The separate gas turbine based APU, used during ground operations, has an average fuel efficiency of 15% [13] and undesirable noise and gaseous emissions [14]. Due to their relatively smaller size as compared to propulsion gas turbines, turbine-based APUs have not been focussed on for improvement. They produce almost 20% of the aircraft NOx emissions and a significant amount of noise [15]. Therefore, a fulltime duty APU with solid oxide fuel cell-gas turbine hybrid (SOFC-GT) technology promises a substantial improvement in system efficiency and overall NOx emissions. SOFC-GT based APU systems will provide electric power both on ground and cruise altitudes and operate continuously at full load. Therefore SOFC-GT based APU system

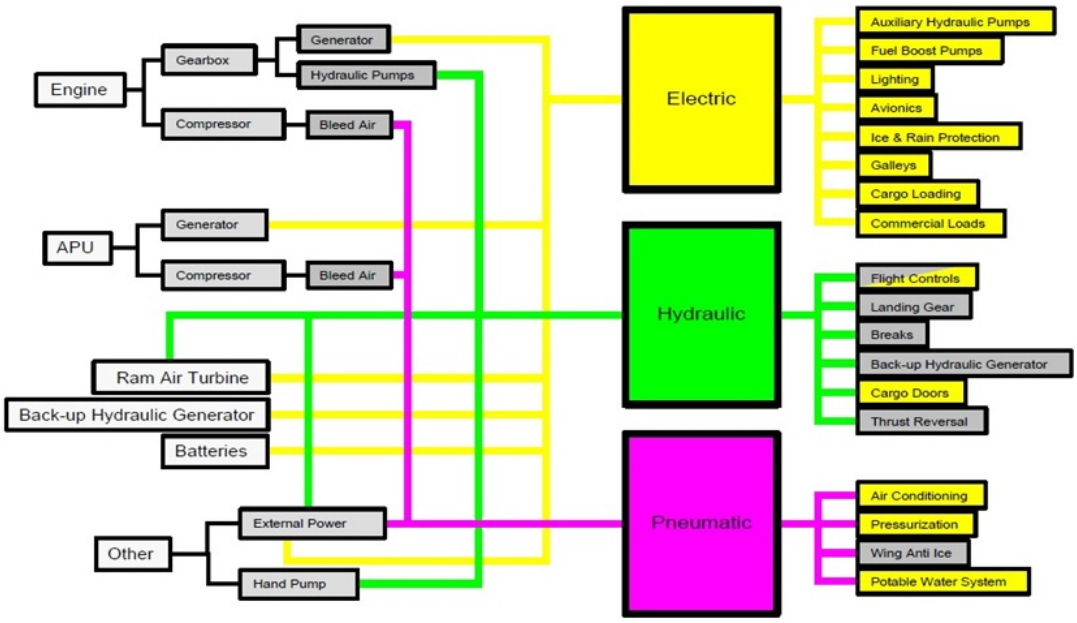

Figure 1.2: Energy Supply and Consumers with Future Electric Systems (yellow) in More Electric Aircrafts [2]

should achieve efficiencies greater than maximum achievable efficiencies by conventional systems providing electric power.

1.2 State of art technology

Future aircraft designs are projected to require a significant increase in auxiliary electrical loads due to increased application of electromechanical actuators, passenger services, and communications [15]. The aircraft system concept behind this is referred as more electric aircraft (MEA), which completes to an all electric aircraft (AEA) if all systems are electric. According to the power requirements and characteristics of modern aircrafts, the electric power demand of a MEA is displayed in figure 1.2.

The transition is already being realized in new generation aircrafts, for example the A380 with electro-hydraulic and electromechanical actuators for secondary flight control systems [2]. This increase in power demand will be met by incorporation of APU systems which are operational continuously both on ground as well as during cruise operations. Hence, a highly efficient, cleaner and quieter APU becomes the need of the hour. Much higher demand for electrical power in MEA and AEA cannot be fulfilled by APU systems available today. This presents a need for alternative options for APU.

Fuel cells can offer solutions for these requirements with their main advantages:[2, 16]

- Higher fuel efficiency
- Lower to zero emissions
- Direct current generation

- Decentralization of power generation and potential water recovery.
- Water produced as a byproduct which allow the aircraft to generate its own water supply
- No moving parts, hence easier and cheaper to maintain than fossil-fuel powered APUs
- Low noise

In MEA, electrical loads are run by electrical generators off the main engine shaft and bleed air from engine is minimally used. SOFC can generate electrical power at higher efficiency than is achieved by using power from the main engine shaft to run a generator. Hence, a solid oxide fuel cell power unit (SOFCPU) can be operated throughout the flight to maximize fuel savings unlike current APU systems.

1.3 Motivation of the thesis

To achieve the goal of 80% reduction of greenhouse gases, many energy efficiency measures are planned like decarbonization of the power sector, a fuel shift from oil and gas to power and biomass, afforestation and many others. Aggressive energy efficiency measures in transport, building, industry, agriculture etc. are required. In transport sector, this is done by replacing fossil fuels with decarbonized electricity and low CO_2 fuels (e.g., 2nd-generation biofuels). Use of renewable energy to power the airport, use of bio-waste from airport and aircraft to produce biofuel, use of sustainable fuel for aircraft operations and installation of energy efficient aircraft systems are some of the pathways which can result in greener air transport industry. Air transport is expected to rely on bio-kerosene for decarbonization. Air and sea transport can reduce emissions by 0.1 $GtCO_{2e}$ per year by switching to biofuels [12]. This thesis, therefore, will focus on one of these pathways which includes use of multi-purpose efficient aircraft APU system which can also be used for production of sustainable, fossil-free fuels.

Biofuel can be a complex mixture of hydrocarbons and impurities such as sulfur-based species. Solid Oxide Fuel Cell (SOFC) is tolerant to impurities upto a certain limit and requires reforming to convert hydrocarbons to carbon dioxide or carbon monoxide which act as fuel. Therefore, SOFC has been chosen as APU system for this analysis. Although SOFC-based system is heavier than gas turbine unit, when the fuel mass saved from the difference in efficiency is accounted for, the system compares favorably with a gas turbine system. Even higher efficiencies can be achieved by incorporating smaller gas turbine unit as a bottoming cycle to SOFC.

SOC can be used in electrolysis mode to produce hydrogen, which can further act as source of sustainable fuel production, thus completing the cycle. Solid oxide electrolysis cells (SOEC) can be made to run on excess electricity available from renewable source to make the complete process fossil fuel free. Since excess electricity might not be available throughout the year, SOEC will work on part-load most of the time during the year and may not even be operational during some parts of the year. To overcome this shortcoming, a mix of technology is considered. Using mix of technologies ensures sufficient capacity

to supply all demand and a mix of technologies is more robust against delivery risks. Therefore, biomass gasification is also considered as an alternative to produce fuel for aircrafts. Biomass gasification is a promising technology which can be used to produce biofuels. Following reasons justify combining of biomass gasifiers with SOEC unit to produce biofuel:

- It has high conversion efficiency
- High temperature operations, hence reactions are faster resulting in low resident time
- They are compact and hence more economical
- Gasification technology is well developed and commercially available

According to Roadmap 2050, 40% of the biomass potential is assumed to go to road transport, 40% is assumed to be used for power generation and 20% is assumed to be used for air and sea transport justifying the use of biomass gasifier for biofuel production.

For this analysis, jet fuel and ammonia are considered as fuel options. The advantage of choosing jet fuel is:

- Lower volume and higher energy density
- Easy to transport and store, hence suitable for use in aircrafts
- No extra jet fuel storage tank required as it is similar to the fuel used for main propulsion engine as well
- Jet fuel can be produced from Fischer Tropsch process by using biomass to produce syngas, hence making the process fossil free

Liquid ammonia with an energy density of 11.5 MJ/L [17] has emerged as a promising fuel for SOFCs due to its many advantages as compared to hydrogen.

- Ammonia presents a cheap and convenient way of storing hydrogen, and suitable for transportation
- Pure ammonia is easily liquefied at room temperature by the application of modest pressures and has a comparatively narrow combustion range[18]
- Ammonia can be directly input into the SOFC system without any pre-treatment
- Ammonia can be produced from different feedstocks such as natural gas, oil, coal, as well as biomass

Jet fuel and ammonia, therefore prove to be best available fuel options for comparison and the fact that they can be produced via biomass gasification technique and Electrolysis, make their production fossil free.

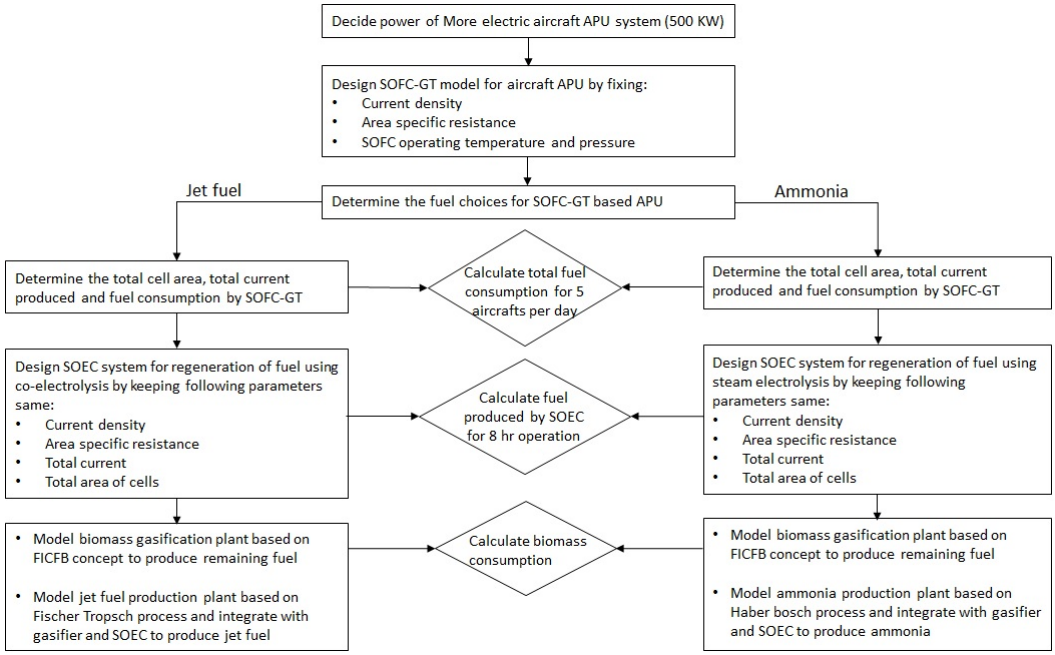

Figure 1.3: Steps followed to achieve aim of the thesis

1.4 Aim of thesis

This thesis focuses on modelling and simulation of jet fuel and ammonia production plants at the airport using bi-directional SOC which are used as APU in small distance 200 passenger commercial aircrafts and as electrolysis cells at the airport. In other words, production of sustainable fuel by reversing the function of fuel cells when aircraft is parked at the airport.

To accomplish this, a SOFC-GT system is modelled for aircraft APU for producing 500 KWe. The model is used to predict the size of the SOC unit which has to be used reversibly as electrolysis cell for the stationary fuel production plant. The algorithm followed for modelling and calculations for the thesis is shown in figure 1.3.

Solid oxide electrolysis cells produce either syngas or hydrogen which has to be further processed to produce jet fuel or ammonia. For this purpose, jet fuel synthesis unit and ammonia synthesis unit are also to be designed and modelled. A biomass gasification unit, as a source of syngas, is also modelled and integrated with fuel synthesis unit for stationary plant. This report considers three cases which are modelled and compared thermodynamically for each fuel type.

- **CASE-1**: Biomass gasification based fuel production plant
- **CASE 2**: SOEC based fuel production plant
- **CASE 3**: SOEC and biomass gasification integrated fuel production plant

The main steps of the thesis are as mentioned below:

1. Modelling and simulation of solid oxide fuel cell system which can be used as auxilliary power unit (APU) for a More Electric Aircraft (A320 or B737) and generates 500KW of net electric power.

2. Sizing of fuel cell stack size for SOFC unit for Jet fuel and ammonia based on sensitivity analysis done for different altitudes, temperature and pressure conditions.

3. Modelling and simulation of solid oxide electrolysis cell (SOEC) to produce syngas and hydrogen through co-electrolysis and steam electrolysis respectively. Stack size and number of cells are same as SOFC unit designed.

4. Gasification unit is modelled as another option for fuel production. Biomass composition is decided and amount is calculated to produce the required fuel when gasification plant runs on full load. Gasification, gas cleaning and tar removal technologies are discussed and modelled to produce pure syngas.

5. Modelling and simulation of jet fuel synthesis unit based on Fischer Tropsch process. Step by step process is followed to produce jet fuel blend from mixed alcohol synthesis to hydrogenation and distillation of paraffins. Reactors are modelled to carry out specific reactions at controlled temperature and pressure conditions to process syngas to produce jet fuel.

6. Ammonia production model is designed with gas processing, ammonia synthesis and ammonia recovery units. Syngas processing is carried out to achieve appropriate nitrogen/hydrogen ratio for ammonia synthesis and removal of CO_2. Ammonia synthesis consists of Haber Bosch process for ammonia formation, product recovery and storage.

7. Integration of gasification unit and/or SOEC with Fischer Tropsch unit for jet fuel production and with ammonia synthesis unit for ammonia production for all cases.

8. Thermodynamic analysis for SOFC-GT, integrated jet fuel production plant and ammonia production plant. For thermodynamic analysis, exergy efficiency of all the models will be calculated. SOFC-GT and stationary production plants for jet fuel and ammonia will be compared based on exergy efficiency and destruction observed.

9. Exergy flow diagrams for integrated jet fuel and ammonia production plants will be produced, compared and results will be drawn.

For modelling all the plants and systems, ASPEN PLUS is used. It is thermodynamic simulation software and allows modelling of reactors and processes with the help of inbuilt components. Equation solver can be chosen to model appropriate processes and reactors.

1.5 Thesis structure

This report consists of 7 chapters which discuss concepts of bi-directional SOC units used as aircraft-APU systems. It also focusses on production of sustainable fuel from these bi-directional SOC APU systems when aircrafts are parked at the airport. Chapter-1 provides introduction about the concept of MEA, need for moving to SOFC-GT systems

for aircraft APU, requirement and possible pathways to produce biofuels for SOFC-based aircraft APU, motivation and aim of the thesis. Chapter-2 outlines literature reviewed for technical concepts of SOC electrochemistry and thermodynamics. It also highlights the exergy calculation for different types of fuels and systems. Chapter-3 explains choice of fuel to be used in SOC and fuel production methods. Gasification technology, tar removal processes and syngas cleaning is studied. Fischer Tropsch for jet fuel production and Haber Bosch processes for ammonia prodcution are discussed and process steps are shown. Chapter-4 deals with modelling of SOFC-GT system for aircrafts and sensitivity analaysis is carried out for different parameters. This chapter also provides results for SOFC-GT systems for both fuel types. Results mainly highlights voltage, current, active cell area and stack dimensions for SOFC-GT based aircraft APU. Chapter-5 discusses modelling of fuel production plants including gasification unit and SOEC unit. Underlying assumptions used for modelling and calculations are also highlighted in this section. Results of simulation are also discussed in this chapter. Chapter-6 shows thermodynamic analysis and exergy efficieny calculations for integrated jet fuel and ammonia production plants. It also gives the comparison of jet fuel and ammonia production plants based on exergy analysis and exergy flow diagrams. Chapter-7 concludes the thesis work and results are provided based on simulation carried out on software ASPEN PLUS. Future recommendations are also discussed in this chapter.

Chapter 2

Theoretical background

This chapter deals with the literature review for the thesis work. It presents working principles for SOFC and SOEC in section 2.1. Section 2.2 shows basic thermodynamic and electrochemical principles and equations behind working of SOFC and SOEC. Section 2.2 also investigates losses observed in SOC and their main reasons. Section 2.3 explains the concept of exergy, describing methods to calculate physical and chemical exergy for different fuels (solid, liquid, gaseous). Section 2.3 also provides equation which are used to calculate exergy efficiency for different components and systems.

2.1 SOC electrochemistry

Solid oxide cells are reversible electrochemical devices which convert chemical energy of a fuel into electrical energy and vice versa. When this unit produces electric power by oxidation of fuel, it is called solid oxide fuel cell (SOFC). Conversely, when an external electric power source is provided for reduction reaction, it is renamed solid oxide electrolysis cell (SOEC). Equation 2.1 shows reversible SOFC and SOEC reaction.

$$H_2 + 1/2O_2 \leftrightarrow H_2O \tag{2.1}$$

SOFC and SOEC reactions are Redox reactions and occur through exchange of ions and electrons. During operation of fuel cell, hydrogen is oxidised to water and oxygen reduction takes place according to equations 2.2 and 2.3 respectively.

$$H_2 + O^{2-} \rightarrow H_2O + 2e^- \tag{2.2}$$

$$1/2O_2 + 2e^- \rightarrow O^{2-} \tag{2.3}$$

Similarly, when SOEC is operated, steam is reduced to hydrogen and oxide ions are oxidised to oxygen as shown in equations 2.4 and 2.5 respectively.

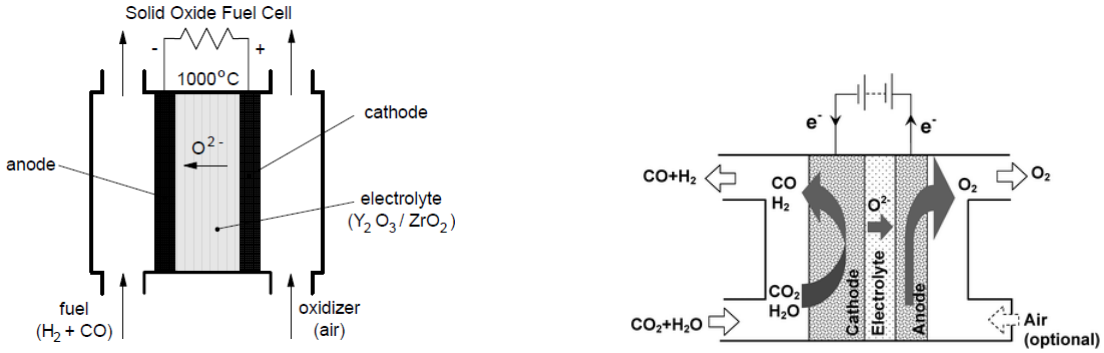

(a) Working principle of Solid oxide fuel cell (SOFC)

(b) Working principle of Solid oxide electrolysis cell (SOEC) for co-electrolysis

Figure 2.1: Working principle of solid oxide cells [3]

$$H_2O + 2e^- \rightarrow H_2 + O^{2-} \tag{2.4}$$

$$O^{2-} \rightarrow 1/2O_2 + 2e^- \tag{2.5}$$

These two half reactions are separated and occur at different sites in the cell called electrodes. Figure 2.1 depicts the working principle of SOFC and SOEC with ionic and electronic flows between anode and cathode sides. Oxidation is always performed at the anode while reduction takes place at the cathode. Electrons move from anode to cathode whereas oxide ions move from cathode to anode [4]. When solid oxide cell operates as electrolysis cell, electrodes exchange their respective reactions and hence names. However, steam/hydrogen and oxygen/air mixture are always provided to the same side of the cell.

Usually, hydrogen/steam electrode is fabricated with a cermet of nickel metal (Ni) and ceramic yttria-stabilized-zirconia (YSZ), while electrolyte is based on pure YSZ and oxygen/air electrode on YSZ mixture with lanthanum-strontium-manganite (LSM) [4].

2.2 Thermodynamics of SOC

This section describes the thermodynamic principles associated with both solid oxide fuel cells and electrolysis cells. Standard reversible voltage is derived from basic thermodynamics laws followed by definition and calculation of Nernst potential with SOC losses.

2.2.1 Thermodynamic potentials

The first law of thermodynamics, also known as the law of conservation of energy, states that internal energy (dU) of a closed system must be equal to heat transfer (dQ) to the system minus the work done by the system (dW). Work considered here is mechanical and is accomplished by expansion of system against pressure. Electric work will be considered when fuel cell thermodynamics is discussed in the section 2.2.2.

$$dU = dQ - dW = dQ - pdV \tag{2.6}$$

The second law of thermodynamics defines the randomness of a system, which is also known as entropy of the system. A system's entropy is calculated by equation 2.7 based on how heat transfer causes the entropy of a system to change at a constant temperature.

$$dS = \frac{dQ}{T} \tag{2.7}$$

Based on equations 2.6 and 2.7, thermodynamic potentials based on temperature, pressure (T,p) and on entropy, pressure (S,p) are defined. These thermodynamic potentials are Gibbs free energy (G) and Enthalpy (H) of the system [19].

$$dU = TdS - pdV \tag{2.8}$$

$$G = U - TS + pV \tag{2.9}$$

$$H = U + pV \tag{2.10}$$

Therefore, Gibbs free energy is defined as the total energy to create the system and make room for it minus energy provided by the environment. In other words, Gibbs free energy represents the exploitable energy potential or work potential of the system. Enthalpy of a system is the sum of energy needed to create a system and work needed to make room for it [19]. The variation of G and H leads to equations 2.11 and 2.12.

$$dG = -SdT + Vdp \tag{2.11}$$

$$dH = TdS + Vdp \tag{2.12}$$

Maximum heat energy which can be extracted from a fuel is given by its enthalpy of reaction. For constant pressure process (dp=0), by manipulating equations 2.6, 2.7 and 2.12

$$dH = TdS = dQ = dU + dW \tag{2.13}$$

This equation shows that change in enthalpy is due to change in internal energy of system and work done towards the system.

Similarly by using equations 2.9 and 2.10, Gibbs free energy can be related to enthalpy and entropy of a system.

$$G = H - TS \tag{2.14}$$

$$dG = dH - TdS - SdT \tag{2.15}$$

Considering isothermal operation (dT=0), equation 2.15 can be written as

$$dG = dH - TdS \tag{2.16}$$

Internal energy, entropy and enthalpy of a system are extrinsic quantitites and scale with the system, hence are denoted in uppercase (U, S, H). However, molar quantities like molar enthalpy, molar entropy and molar Gibbs energy are intrinsic and do not scale with the system, therefore, they are denoted in lower case (h, s, g). Energy changes due to reaction is calculated on a molar basis: Δh_{rxn}, Δs_{rxn} and Δg_{rxn}. The symbol Δ represents change during thermodynamic process and gives difference between final and initial state properties [19]. Therefore, equation 2.16 for an isothermal reaction at temperature, T, can be written in terms of molar quantities as

$$\triangle g_{rxn} = \triangle h_{rxn} - T\triangle s_{rxn} \tag{2.17}$$

2.2.2 Standard reversible voltage

A reversible fuel cell voltage is the voltage produced by fuel cell at thermodynamic equilibrium. As soon as current is drawn from fuel cell, its equilibrium is lost and these equations are not applicable.

For fuel cell, electric work needs to be included with mehanical work to calculate work potential. Therefore, by expanding equation 2.8, equation 2.12 can be re-written as

$$dU = TdS - (pdV + dW_{elec}) \tag{2.18}$$

$$dG = -SdT + Vdp - dW_{elec} \tag{2.19}$$

Since fuel cells operate at constant pressure and temperature (dT, dp =0) this equation reduces to

$$dG = -dW_{elec} \tag{2.20}$$

Since there is no mechanical work involved in SOC, W_{elec} is the maximum electric work that can be obtained from a fuel cell. Considering a reaction using molar quantitites, this equation can be written as

$$W_{elec} = -\triangle g_{rxn} \tag{2.21}$$

Electrical work can be calculated as the product between charge and potential. If z electrons are exchanged per mole of reacted hydrogen, then multiplying it with Faraday's constant, F (96485 C/mol), will give the amount of charge. Hence, electrical work can

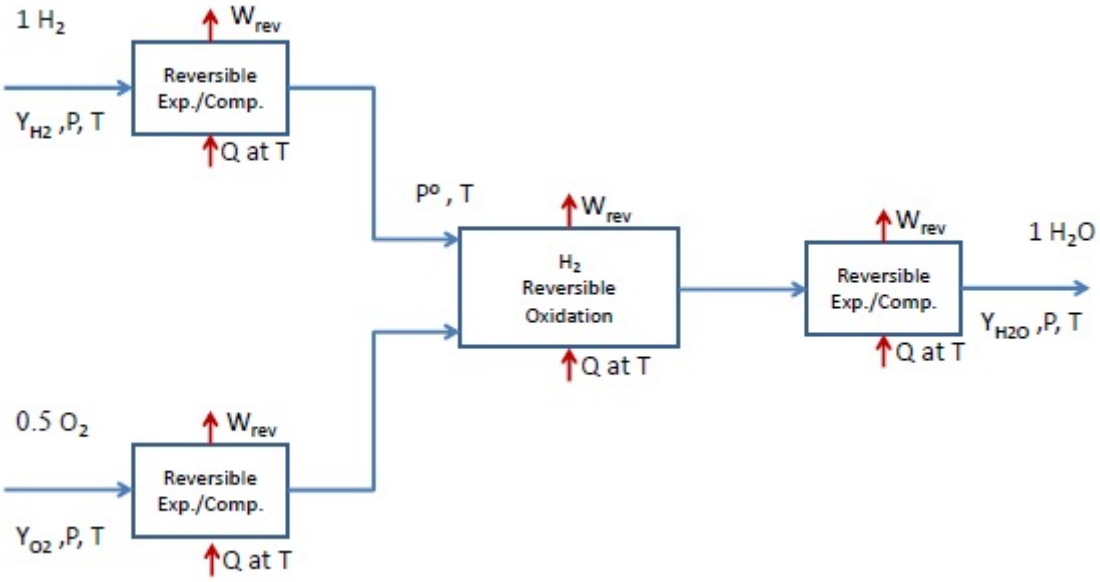

Figure 2.2: Thermodynamic model for oxidation of hydrogen at arbitrary pressure, temperature and composition going through compression and expansion states [4]

be calculated as shown in equation 2.22 which is also equivalent to change in Gibbs free energy.

$$W_{elec} = zFV_{rev} \tag{2.22}$$

Deducting from equations 2.21 and 2.22,

$$V_{rev} = \frac{-\triangle g_{rxn}}{zF} \tag{2.23}$$

If reactants and products are assumed at standard state (reaction temperature (T), atmospheric pressure (p_0) and molar quantities), standard reversible voltage can be calculated by equation 2.24 where $\Delta g^0{}_{rxn}$ is the standard state free energy change for the reaction. This reversible voltage is only dependent on temperature of the reaction.

$$V^0_{rev} = \frac{-\triangle g^0_{rxn}}{zF} \tag{2.24}$$

2.2.3 Nernst voltage

A shift from standard pressure and concentration can cause variation in previously calculated work since reactants and products have to be compressed or expanded to their partial pressures. Figure 2.2 shows complete process defining the thermodynamic state of components entering the system and their consequent compression and expansion which is considered additional work of the sytem.

Compression or expansion work for an ideal gas can be represented by equation 2.25.

$$W_{rev} = -nRT \int_{p_{in}}^{p_{out}} \frac{dp}{p} = nRTln\left(\frac{p_{in}}{p_{out}}\right) \tag{2.25}$$

Equations 2.26 and 2.27 show expansion/compression work for hydrogen and oxygen to achieve standard pressure from their partial pressure and equation 2.28 shows expansion/compression work for H_2O from standard pressure to its partial pressure [4].

$$W_{rev,\mathrm{H2}} = RTln\left(\frac{p_{\mathrm{H2}}}{p_0}\right) \tag{2.26}$$

$$W_{rev,\mathrm{O2}} = 0.5RTln\left(\frac{p_{\mathrm{O2}}}{p_0}\right) \tag{2.27}$$

$$W_{rev,\mathrm{H2O}} = RTln\left(\frac{p_0}{p_{\mathrm{H2O}}}\right) \tag{2.28}$$

Combining all these equations, a new formula for total electrical work 2.29 and hence voltage is calculated. This voltage 2.30 is called Nernst voltage.

$$W_{elec} = -\triangle g^0_{rxn} + RTln\left(\frac{p_{\mathrm{H2}}p^{0.5}_{\mathrm{O2}}}{p_{\mathrm{H2O}}}\right) \tag{2.29}$$

$$V_{nst} = V^0_{rev} + \frac{RT}{zF}ln\left(\frac{p_{\mathrm{H2}}p^{0.5}_{\mathrm{O2}}}{p_{\mathrm{H2O}}}\right) \tag{2.30}$$

Equation 2.30 can also be written in general form as shown below [20]:

$$V_{nst} = \frac{-\triangle g^0_{rxn}}{zF} + \frac{RT}{zF}ln\left(\prod \frac{p^{v(k)}_{reactants}}{p^{v(k)}_{products}}\right) \tag{2.31}$$

Here p_k is the partial pressure of species k (in atmospheres), and v(k) are the stoichiometric coefficients in the global reaction. Assuming chemical equilibrium exists, the Nernst potential can be written in terms of the oxygen partial pressures in the anode and cathode channels [20] as shown in equation 2.32.

$$V_{nst} = \frac{RT}{4F}ln\left(\frac{p_{\mathrm{O2},c}}{p_{\mathrm{O2},a}}\right) \tag{2.32}$$

The same procedure can be applied for calculating potential for electrolysis cell as well. Inversion of products and reactants leads to a sign variation of both standard Gibbs free energy change and reaction quotient logarithm. Therefore, negative reversible voltages emerge for the electrolysis process [4]. The Nersnt potential for electrolysis cell looks like in equation below.

$$V^{ec}_{nst} = V^0_{rev} + \frac{RT}{zF}ln\left(\frac{p_{\mathrm{H2O}}}{p_{\mathrm{H2}}p^{0.5}_{\mathrm{O2}}}\right) \tag{2.33}$$

2.2.4 Energy losses in SOC

In earlier sections, thermodynamically reversible fuel cells were discussed, which means that there were no energy losses. However, in reality, the measured voltage shows deviation from theoretical Nernst voltage. This deviation is usually called either voltage drop or overpotential (ΔV) and is caused by energy losses. These losses tend to decrease SOFC Nernst potential and increase SOEC one [4].

Since electrolyte is not a perfect insulator, some internal current is present. However, this internal current is weakened at high temperature and leakage can be assumed negligible with proper sealing. Therefore, for high temperature and properly sealed fuel cells, open circuit voltage (OCV) is almost similar to Nernst potential [4]. When the circuit is closed, the measured voltage is lower than OCV due to losses. SOC losses are categorised into three regions and types:

1. Activation loss: This represents the voltage that is sacrificed to overcome the activation barrier to extract a net current from an electrochemical reaction. The over-potential is the extra voltage needed to reduce the energy barrier of the reaction (usually the rate determining step) so that the reaction proceeds at a desired rate. Thus, higher is the voltage sacrificed, higher is the current density obtained [21].

2. Ohmic loss: It arises due to electrical resistance in the cell components, including resistance to the flow of ions in the electrolyte (ionic resistance), resistance to the flow of electrons and ions in the catalyst layer (ionic and electronic resistance), resistance to the flow of electrons through the gas-diffusion layer (electronic resistance) and resistance to the flow of electrons through the interface contact and the terminal connections (electronic resistance) [21].

3. Concentration loss: Finally, another limiting step could be the mass transport of gaseous agents. Reactants must reach the reaction zone and products should be removed. If the cell is operated at very high currents, diffusion may not be fast enough to efficiently bring reactants and remove products from reaction sites. This causes a drop in the local reversible voltage, which depends on product and reactant concentrations. Commonly, these losses are called either diffusion, mass transport or concentration losses [21].

Figure 2.3 shows the effect of the irreversibilities in the cell voltage for fuel cell. Ohmic losses represent the most significant losses and activation losses are less significant at higher temperatures.

2.3 Exergy definitions

The exergy of a portion of matter is equal to the maximum useful work obtainable when taken from its given state to the thermodynamic equilibrium with the environment, without intervention rather than its own and the one of the environment. Such a final state of equilibrium is known as dead state. From another point of view, the exergy can be

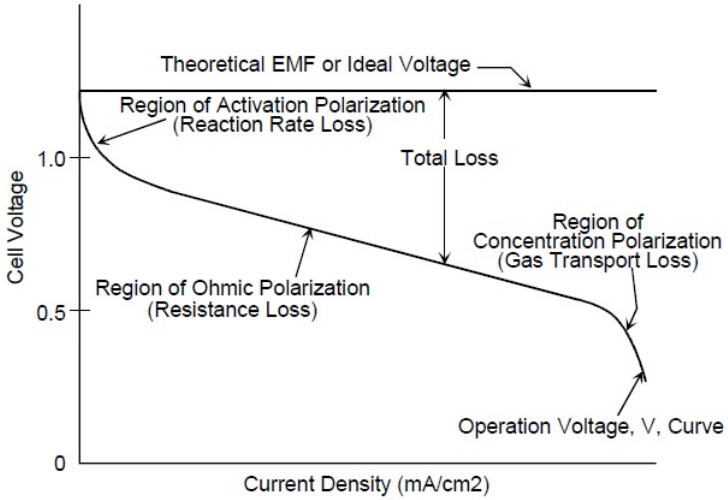

Figure 2.3: Theoretical and actual fuel cell voltage/current characteristics [5]

considered as a measure of the existing disequilibrium between the considered matter and the environment.[22] Exergy analysis enables one to evaluate quantitatively the causes of thermodynamic imperfections of thermal and chemical processes. Poor thermodynamic performance is the results of exergy losses in combustion and heat-transfer processes.[23]

The exergy of a substance is defined in two separate variables: **physical exergy** which is associated with changes in temperature and pressure with respect to the reference environment; and **chemical exergy** which is related to changes in chemical compositions. Therefore, the calculation of the physical exergy involves the definition of the temperature and the pressure of environment, and chemical exergy requires an environment composition with reference substances.[6] The total exergy of a substance can therefore be calculated as:

$$Ex_{total} = Ex_{phy} + Ex_{chem} \tag{2.34}$$

2.3.1 Physical Exergy

Physical exergy of a stream of matter can be defined as the maximum work (useful energy) that can be obtained from it in taking it to physical equilibrium (of temperature and pressure) with the environment.[24]

$$Ex_{phy} = (H - H_0) - T_0(S - S_0) \tag{2.35}$$

Where the enthalpy and the entropy of the substance have to be evaluated at its temperature and pressure conditions (T, p) and at the temperature and pressure of the environment (T_0,p_0). Enthalpy and entropy at the stream and reference conditions are evaluated for the same chemical composition of the stream of matter.[24]

Table 2.1: Mole fractions of components of air: Baehr reference environment

Components	Mole Fraction
N_2	0.7565
O_2	0.2030
CO_2	0.0003
H_2O	0.0312
Ar	0.0090

2.3.2 Chemical Exergy

Chemical exergy of a stream of matter can be defined as the maximum work (useful energy) that can be obtained from it in taking it to chemical equilibrium (of composition) with the environment. The enthalpy and the entropy have to be evaluated for the chemical composition of the substance (X) and for the chemical composition (X_0) of the environment products obtained from the substance by reacting with environment components; normally at the environment conditions (T_0,p_0)[24]

There are two methods for calculating chemical exergy based on reference environment, namely Szargut and Baehr. In this analysis, Baehr environment is taken as reference since it is used for evaluating energy conversion systems. Baehr's method is based on mole or mass fractions of gaseous components in air at a reference temperature and pressure of 25^0C and 1 atm respectively as shown in table 2.1 .

The procedure of calculation of the chemical exergy of a mixture (state 1) can be summarized as shown in figure 2.4:

1. **Decomposition of the mixture (2)**: Components are separated and compressed and become available at (T_0,P_0). In case of a single compund, it is not requirred to separate the components therefore $W_{rev,2}$=0. (For a mixture, equation 2.38 can be used)

2. **Chemical conversion into environmental components (3)**: Components are converted into environmental components (e.g. CO_2, H_2O) by reacting with environmental components (e.g. O_2) [Reverse formation reaction]

$$W_{rev,3} = (H_{in} - H_{out}) - T_0(S_{in} - S_{out}) \tag{2.36}$$

3. **Expansion (or compression) of the environmental components (4)**: Expansion of environmental components to their partial pressure, p_i, in the environment

$$W_{rev,4} = -R^{mol}T_0 ln\frac{p_i}{p_0} \tag{2.37}$$

4. **Compression of environmental components for the reactions (usually O2) (4a)**: Compression of environmental component (transfer from environment trough reversible membrane and compression) of separated component to environmental pressure. [6]

$$W_{rev,4a} = R^{mol}T_0 ln\frac{p_i}{p_0} \tag{2.38}$$

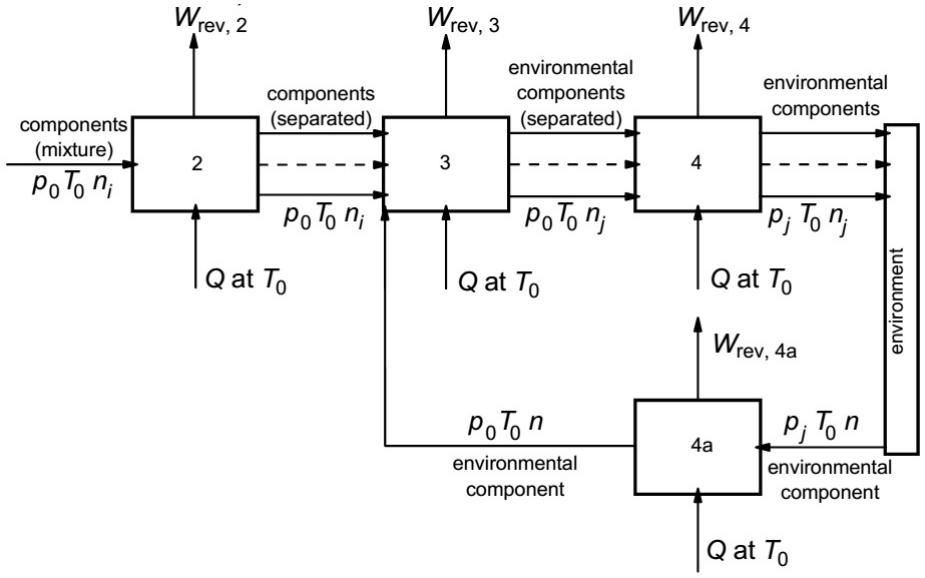

Figure 2.4: Steps for calculation of chemical exergy of a mixture [6]

The chemical exergy of the mixture is the sum of all the exergies calculated for the substeps:

$$Ex_{chem} = W_{rev,2} + W_{rev,3} + W_{rev,4} + W_{rev,4a} \tag{2.39}$$

For calculation of chemical exergy of liquid fuel oils, an approximate determination can be easily carried out through empirical coefficients f_l and f_h , which relate it to the lower or higher heating values, where LHV and HHV respectively represent the lower and higher heating values.[22]

$$Ex_{chem,fuel} = f_l.LHV_{fuel} \tag{2.40}$$

f_l can be calculated based on atomic composition as calculated by Szargut, shown in equation 2.41 where mass fractions represent weight percent of hydrogen, oxygen and sulphur in the compond with respet to carbon.

$$f_l = 1.0401 + 0.1728\frac{m_{H_2,lf}}{m_{C,lfl}} + 0.0432\frac{m_{O_2,lf}}{m_{C,lf}} + 0.2169\frac{m_{S,lf}}{m_{C,lf}}(1 - 2.0628\frac{m_{H_2,lf}}{m_{C,lf}}) \tag{2.41}$$

Similarly for calculating chemical exergy of solid fuels like biomass equations 2.42 and 2.43 are used [10].

$$Ex_{chem,bio} = m_{bio}\beta.LHV_{bio} \tag{2.42}$$

$$\beta = \frac{1.044 + 0.016\frac{m_{H2,s}}{m_{C,s}} - 0.3493\frac{m_{O2,s}}{m_{C,s}}\left(1 + 0.0531\frac{m_{H2,s}}{m_{C,s}}\right) + 0.0493\frac{m_{N2,s}}{m_{C,s}}}{1 - 0.4124\frac{m_{O2,s}}{m_{C,s}}} \tag{2.43}$$

2.3.3 Exergy efficiencies

Exergy efficiency can be defined in two ways according to the process in consideration.

- Universal exergy efficiency
- Functional exergy efficiency

Universal exergy efficiency is the ratio of exergy of flows leaving the system and exergy of flows entering the system.

$$\eta_{ex,u} = \frac{\sum Ex_{out}}{\sum Ex_{in}} \tag{2.44}$$

Functional efficiency, on the other hand, is the ratio of sum of exergies of all the product flows and sum of exergies of all source flows. Product exergy represents the total amount of useful work obtained from the system as product and source exergy is the amount of exergy input to the system [25].

$$\eta_{ex,f} = \frac{\sum Ex_{product}}{\sum Ex_{souce}} \tag{2.45}$$

Functional exergy efficiency is highly used for thermodynamic analysis as it provides more realistic results than universal efficiency . However, if it is not possible to calculate functional efficiency for a component, universal exergy effiiency can also be used.

Functional efficieny for different components is shown in the table 2.2 [25].

Table 2.2: Functional exergy efficiencies of different components

Component	Exergy efficiency
Turbine	$\frac{W}{Ex_{in}-Ex_{out}}$
Compressor	$\frac{Ex_{out}-Ex_{in}}{W}$
Heat exchanger	$\frac{Ex_{cold,out}-Ex_{cold,in}}{Ex_{hot,in}-Ex_{hot,out}}$
Adiabatic Combustor	$\frac{Ex_{phy,fluegas}-Ex_{phy,fuel}-Ex_{phy,air}}{Ex_{chem,fuel}+Ex_{chem,air}-Ex_{chem,fluegas}}$

Exergy efficiency also leads to the concept of exergy losses and exergy destruction. Exergy destruction occurs in a component and occurs due to following reasons [26]:

- Transformation of the binding energy that is released by burning fossil fuels into thermal energy
- Flow of heat from a higher temperature to a lower one during heat transfer
- Friction arising from the flow of the energy carriers by the different apparatus

Exergy destruction in a process is calculated from exergy balance equation.

$$Ex_{mass,in} + Ex_{power,in} - Ex_{mass,out} - Ex_{power,out} = Ex_{dest} \tag{2.46}$$

Exergy loss, on the other hand, occurs in the form of exhaust gases and waste product streams which cannot be utilized for further energy conversions.

2.4 Conclusion

The SOC electrochemistry describes the working principle of SOFC and SOEC highlighting the difference between the two modes. Thermodynamics of SOC shows the equations to calculate Nernst potential and its derivation. These equations will be used to calculate voltage and current for SOFC in chapter-4 and for SOEC in chapter-5. Exergy definitions clearly indicate ways to calculate exergy for different fuels- liquid, solid and gaseous. The exergy efficiency concept explained will be used to calculate exergy efficiency of SOFC-GT system and fuel production plants.

Chapter 3

Basics of subsystem technology

This chapter explains in detail the basics of technology adopted to design different subsystems for the thesis. The ASPEN PLUS models are developed based on the concepts explained in this chapter. Section 3.1 investigates the two types of fuels used for this analysis. Section 3.2 defines gasification technology to produce syngas which can further be used to produce either jet fuel or ammonia. Section 3.3 highlights the process steps for Fischer Tropsch process to produce jet fuel and last section 3.4 is about ammonia production from Haber Bosch process and its consequent recovery.

3.1 SOFC fuels for aviation

Hydrogen and carbon based fuels as well as ammonia are the main fuels which can be used in Solid oxide fuel cells. In this project, jet fuel and ammonia are studied as SOFC fuels based on their ease of availability, energy content and convenience in storage and transportation. These fuels can be directly used for SOFCs unlike proton exchange membrane (PEM) fuel cells which requires pure hydrogen as fuel. For fuels containing higher hydrocarbons and sulphur species, desulpherisation and reforming is required for SOFCs. Co-electrolysis to produce syngas for jet fuel and steam electrolysis to produce hydrogen for ammonia through solid oxide cells in electrolyzer mode are also investigated.

3.1.1 Jet fuel

The two main types of aviation fuels are gasoline and jet fuel (C_8-C_{16}) [8]. They are composed mainly of paraffins and cycloparaffins and smaller amounts of aromatics and olefins along with some additives specified by each category of aviation fuel. Air transport sector is dominated by jet engine which uses jet fuel. Jet fuel is further categorised into military (e.g. JP4 and JP8) and commercial (e.g., Jet A1 and Jet B), since each service has its own operational requirements [8]. However, jet fuel cannot be directly used in SOFC system since heavy hydrocarbons ($>C_4$) can cause significant deactivation and

coking problems associated with most anode catalysts for SOFC [27]. The choice of fuel and fuel cells has a significant impact on the fuel processing strategies for on-board fuel pre-processor. An adiabatic pre-reformer is used to breakdown most C_8-C_{16} hydrocarbons to C_1-C_2 compounds to produce final reformates (mainly H_2 and CO, with some CO_2). Pre-reforming takes place in the low temperature range, typically from 400 °C to 550 °C [27].

3.1.2 Ammonia

Ammonia, an important basic chemical, is produced at a scale of 150 million tons per year. It is used for production of nitrogen based fertilizers, metal treating operations, petrochemical, refrigerant, pulp & paper industry and many other chemical industries. Ammonia containing 17.5 wt% hydrogen is an ideal carbon-free fuel for fuel cells [17]. Ammonia works very well in an SOFC system based on nickel anodes and also incorporating nickel or iron-based catalysts [18]. As one of the largest produced chemical, ammonia production technologies are matured and infrastructure for ammonia already exists as compared to hydrogen which requires new investments.

3.2 Gasification technology

Gasification technology includes gasification of biomass followed by gas cleaning unit to produe pure syngas. Gasification is a thermochemical process for converting carbonaceous material, such as coal and biomass, to a combustible or synthetic gas by partial oxidation at elevated temperatures. The gasification of solid fuel involves a series of heterogeneous and homogeneous reactions. Generally the final desired components in the syngas are H_2, CO, and CH_4. Mixtures of H_2 and CO at various ratios in the syngas are necessary for many syntheses [28].

3.2.1 Gasification of biomass

Biomass as a term covers a wide range of materials, encompassing all kinds of plants, animals, and their wastes and residues, especially utilized to produce energy and chemicals. In this study, birch wood is considered as the source of biomass. Main components of biomass are carbon, hydrogen, oxygen, nitrogen and sulfur in traces; these elements can be converted to fuel and chemicals using the gasification technology [6]. Biomass usually has high volatile and oxygen contents, but low carbon content and heating value as compared to solid fuels like coal [28]. Gasification converts biomass to gaseous fuel by heating it in a gasification medium such as air, oxygen, steam, or their mixture.

Biomass gasification follows two main processes, namely, drying and pyrolysis followed by oxidation and gasification. As heat is added to the the fuel in gasifier, dried biomass is obtained. With increasing temperature, pyrolysis takes place converting dry fuel into char and volatiles[28].

$$\text{fuel} + \text{heat} \rightarrow \text{dryfuel} + H_2O \tag{3.1}$$

$$\text{dryfuel} + \text{heat} \rightarrow \text{volatiles} + \text{char} \tag{3.2}$$

In general, some oxygen is injected into the gasifier to oxidize pyrolysis products to provide thermal energy for gasification reactions. The following main reactions may take place when the pyrolysis products are burned. When the temperature reaches 600-700 °C, remaining particles are gasified by other agents like H_2O and CO_2. Oxidation and gasification reactions are shown below. [28]

$$C + 1/2O_2 \rightarrow CO + \text{heat} \tag{3.3}$$

$$CO + 1/2O_2 \rightarrow CO_2 + \text{heat} \tag{3.4}$$

$$CH_4 + 2O_2 \rightarrow CO_2 + 2H_2O + \text{heat} \tag{3.5}$$

$$C + 2H_2 \rightarrow CH_4 + \text{heat} \tag{3.6}$$

$$CO + 3H_2 \rightarrow CH_4 + H_2O + \text{heat} \tag{3.7}$$

$$CO + H_2O \rightarrow CO_2 + H_2 + \text{heat} \tag{3.8}$$

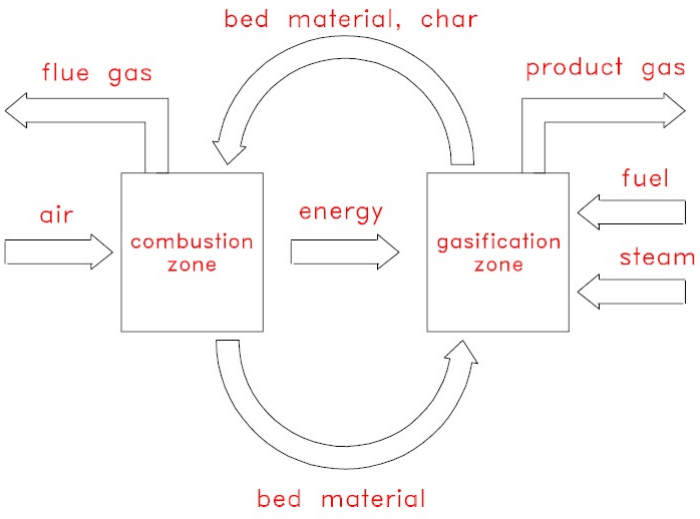

Figure 3.1: FICFB gasification concept diagram [7]

Gasifiers used today can be divided into three maincategories: moving bed, fluidized bed, and entrained flow gasifiers [28]. The gasifier considered for modeling is based on Fast

Internal Circulating Fluidized Bed (FICFB). The principle is shown graphically in Figure 3.1.

The basic idea is to divide the gasifier into two zones, a gasification zone and a combustion zone. Bed material, which acts as heat carrier from combustion to gasification zone is circulated between these zones with gases kept separated[7]. Gasification of fuel is done with steam such that the gas produced is almost free from nitrogen. Combustion zone is fluidized with air which partly burns char circulated from gasification zone. The exothermic reaction in the combustion zone provides the energy for the endothermic gasification with steam. The flue gas will be removed without coming in contact with the product gas [7]. Product gas is primarily composed of hydrogen, carbon monoxide, carbon dioxide, methane, and steam including moderate amounts of higher hydrocarbons, nitrogen, tars, as well as others [10].

3.2.2 Gas cleaning unit

Tar, sulfur compounds, solid particulates, and higher hydrocarbons are present in low concentrations in the outlet stream from the gasifier. Factors such as deposition, agglomeration, obstruction, and catalyst deactivation make them undesirable; therefore, a gas cleaning unit is implemented [10]. The gas cleaning unit comprises of : hot filter, OLGA unit, desulphurizer and chlorine removal unit. Hot gas filters are widely used in industrial processes to remove solid particles from gas streams. For tar removal, OLGA process, developed by Energy Research Center of Netherlands (ECN), is used. It avoids mixing of water and tar so that after tar removal, commercially available cleaning systems can be used to remove inorganic components. OLGA is based on dew point control and consists of two sections of multiple stage scrubbers as shown in figure 3.2. These scrubbers use special scrubbing oil.

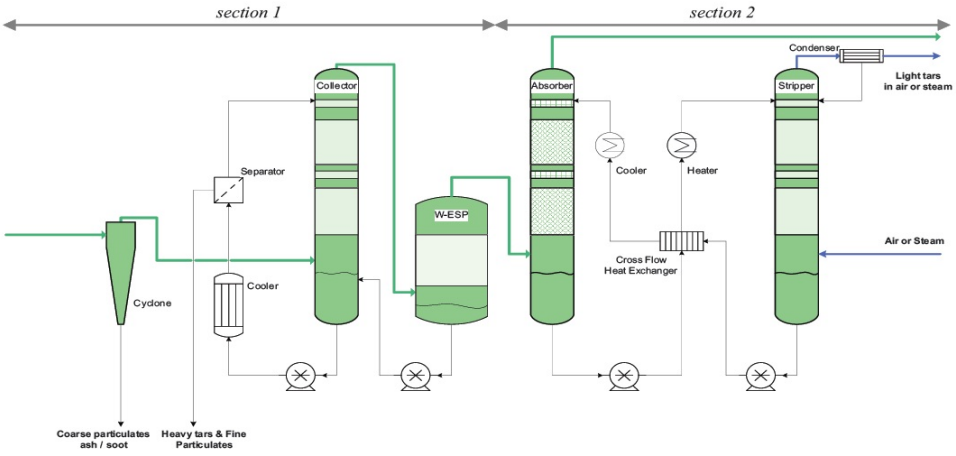

Figure 3.2: OLGA process scheme[7]

First section deals with condensation of heavy tar particles followed by separation from oil and recycling. In second section, hot air is used to strip light gaseous tar absorbed by scrubbing oil. All heavy and light tars can be recycled to the gasifier where they are destructed and contribute to the energy efficiency [29].

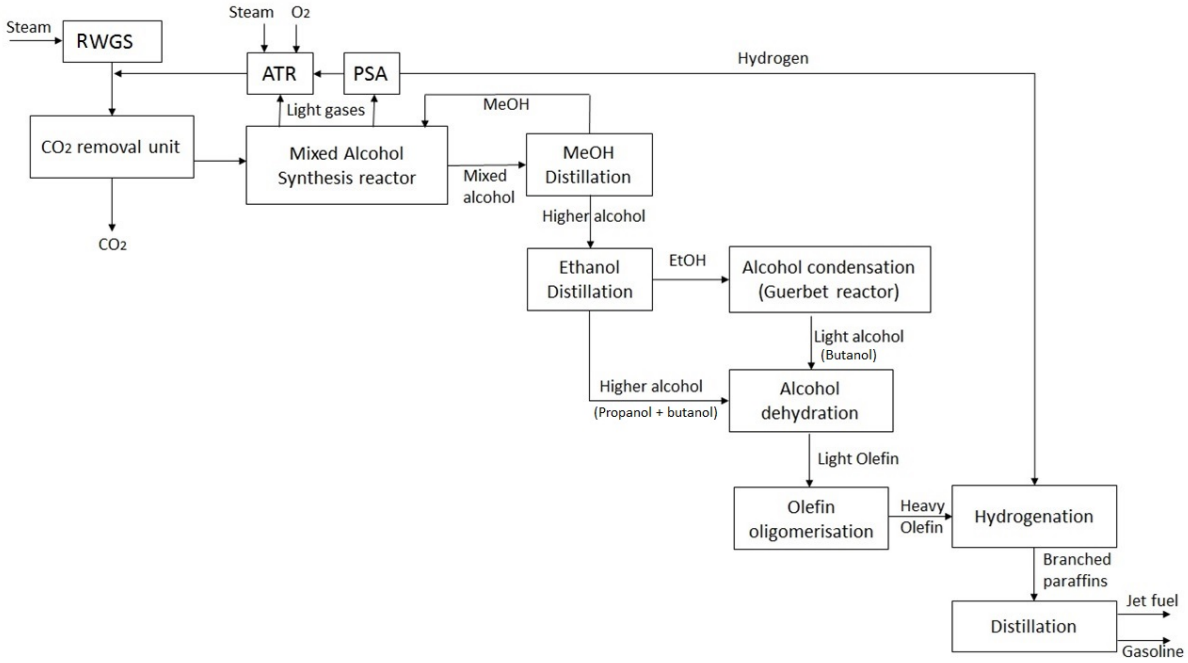

Figure 3.3: Jet fuel production from mixed alcohol process steps

After tar removal, the syngas is made free of sulphur compounds like H_2S, which is considered poisonous for most of the catalysts. Fixed bed reactors using metal oxides like Zn oxide as catalyst are used for desulphurization. The process occurs at 673 K [10]. As the last step, chlorine, which is found in form of HCl in syngas is removed. Although it has lower concentration as compared to other contaminants, it can cause harm to nickel catalysts and so its removal becomes necessary. In hot gas cleanup, a sorbent is employed to remove HCl and is most efficient between 500-550C. Carbon, alumina and alkali oxides are used as catalysts in fixed bed reactors to remove chlorine from syngas.

Cleaned syngas is processed further to be sent to fuel synthesis units. Process steps and principles for both jet fuel and ammonia production from syngas are discussed in next sections.

3.3 Fischer Tropsch for jet fuel production

This section describes in detail, processes associated with gas processing followed by jet fuel synthesis using Fischer Tropsch. The main conventional method for aviation fuels production is through refining of crude oil which is upgraded to fuels through fractional distillation, hydrotreating and hydrocracking. Fischer Tropsch Synthesis (FTS) is another method where biomass is converted into a H_2/CO gas mixture (syngas) via gasification, followed by hydrocarbons synthesis mainly of long chain paraffins, olefins, alcohols and aldehydes [8]. Fischer Tropsch process converts syngas into liquid hydrocarbons based on catalyst activity. The complete process for jet fuel synthesis is shown in figure 3.3.

3.3.1 Gas Processing

Syngas from biomass is cleaned and conditioned before entering the Fischer Tropsch reactor. Entering this process area, the syngas has been reformed, quenched, compressed and treated to have acid gas concentrations (H_2S, CO_2) reduced. Syngas from gasification unit and electrolyzer unit undergoes reverse water gas shift (RWGS) reaction to form CO such that H_2/CO ratio of 1-1.2 is achieved before syngas enters mixed alcohol synthesis reactor. This ratio is required due to the fact that the catalyst used for mixed alcohol synthesis maintains significant water-gas shift (WGS) activity and will generate its own H_2 from CO and H_2O [30]. Syngas after RWGS still contains carbon dioxide which is removed through Rectisol process using methanol. Methanol (CH_3OH), classifiable as a polar protic solvent, is capable of preferentially dissolving H_2S and CO_2. As a result, it can selectively remove those two acid gases from a syngas stream. Compared to Selexol, it has two important advantages: Solubilities of H_2S and CO_2 considerably increase at low temperatures and it can operate at very low temperatures to boost its methanol acid gas solubility, in turn, decreasing the solvent flow rate and absorber size. It is also commercially available on a large scale [31] . After CO_2 removal, syngas enters mixed alcohol synthesis reactor for further processing and alcohol formation.

3.3.2 Mixed alcohol synthesis

Research on alcohol synthesis catalysts has waxed and waned over many decades. Based on literature review[8], a modified Fischer-Tropsch catalyst was used for this process design, specifically a molybdenum-disulfide-based (MoS_2) catalyst. These catalyst types promote the formation of higher alcohols, mainly ethanol. Modified fischer tropsch catalyst produces a mixture of linear alcohols.

The synthesis of mixed alcohol is conducted under high pressure (>40 bar) and at temperature 250–320^{0}C in presence of catalyst (MoS_2) that favors the reactions of alcohol synthesis:[8]

$$nCO + 2nH_2 \rightarrow C_nH_{2n+1}OH + (n-1)H_2O \tag{3.9}$$

Water gas shift also takes place as water is formed by the alcohol formation reactions.

$$CO + H_2O \rightarrow CO_2 + H_2 \tag{3.10}$$

Higher alcohol synthesis results into variety of products, mainly low carbon chain alcohols (C_2-C_4), methanol, hydrocarbons and CO_2 which are separated into two streams: mixed alcohols and light gases. The composition of different products is determined by the catalyst selectivity and process conditions. Mixed alcohols stream comprises mainly of methanol, ethanol, propanol, butanol and other higher alcohols in trace amounts. Methanol is separated in the distillation column and recirculated to the mixed alcohol synthesis reactor to be reused and higher alcohols are sent to another distillation column for ethanol separation. Ethanol is one of the main alcohols produced which is further distilled to produce higher alcohols (butanol) through alcohol condensation. Almost 85% hydrogen is recovered from the light gases obtained from alcohol synthesis using pressure

swing adsorption (PSA) [32]. The PSA process works at basically constant temperature and uses the effect of alternating pressure and partial pressure to perform adsorption and desorption. This hydrogen is further used for hydrogenation of oligomers later in the process. The light gases obtained are reformed in an autothermal reformer (ATR) to convert methane into hydrogen and carbon monoxide before recirculating it to mix with syngas. Autothermal reforming process is explained in detail in forthcoming sections.

3.3.3 Alcohol condensation (Guerbet reaction)

Pure ethanol is sent to Guerbet reactor, where dimerisation of ethanol occurs with loss of water molecule. This is the first step of fuel upgrading where ethanol is converted to higher alcohols. Ethanol can be converted into 1-butanol over alkali earth metal oxides and modified MgO catalysts. The reaction is proposed to proceed through a mechanism in which a $C-H$ bond in the β-position in ethanol is activated by the basic metal oxide, and condenses with another molecule of ethanol by dehydration to form 1-butanol [33].

$$2C_2H_5OH \rightarrow C_4H_9OH + H_2O \tag{3.11}$$

From the literature review [8], it is observed that good ethanol conversion and high n-butanol selectivity is also achieved by using $RuCl_2$ catalyst.

3.3.4 Alcohol dehydration

Higher Alcohols obtained from Guerbet reactor undergo alcohol dehydration to form olefins. Alcohol dehydration is a process in which alcohols undergo unimolecular or bimolecular elimination mechanisms to lose water and form a double bond. Dehydration of butanol isomers (1-butanol, 2-butanol and isobutanol) produces butenes, such as 1-butene, cis-2-butene, trans-2-butene and isobutene, hence butene product depends on butanol isomer which undergoes dehydration [34].

$$C_3H_7OH \rightarrow C_3H_6 + H_2O \tag{3.12}$$

$$C_4H_9OH \rightarrow C_4H_8 + H_2O \tag{3.13}$$

Several relevant studies have proved that catalysts such alumina, Ru, Amberlyst acidic resins and ZSM-5 zeolites have an efficient effect on alcohols dehydration under high pressure [8] and show increased olefin selectivity at temperatures greater than 240^0C.

3.3.5 Olefin oligomerisation

Oligomerization is a process that converts light olefins, usually ethylene, propylene, butylene or their mixtures, from catalytic or steam cracking or Fischer-Tropsch units into gasoline or jet fuel after hydrogenation. In the net reaction, one olefin reacts with one or more of the same or different olefins to form a heavier olefinic compound. [35]

$$nC_4H_8 \rightarrow C_{4n}H_{8n}, n = 2, 3, 4 \tag{3.14}$$

Jet fuel is usually composed of higher alkanes (C_{12}-C_{16}) and formation of these alkanes requires hydrogenation of higher olefins. n-Butene attracts the interest of many studies for further upgrading such as oligomerization, mainly on the grounds that this C_4 isomer mainly is derived from biochemical processes through fermentation [8]. Recent patent by Wright et al. suggests quantitative conversion of 1-butene to a Schultz-Flory distribution of oligomers by use of Group 4 transition-metal catalysts in the presence of methylaluminoxane (MAO). The oligomerization reaction is carried out at ambient temperature in a sealed reaction vessel with complete conversion of 1-butene. The combination of high catalyst activity without production of high polymer led to a highly efficient production of new hydrocarbon jet fuel candidates [36].

3.3.6 Oligomer hydrogenation

Higher olefins are hydrogenated to form paraffins for jet fuel and gasoline production by addition of H_2. These reactions are accomplished effectively in the presence of Pd alloy catalysts in relative high pressure (>20 bar), at 200–350^{0}C[8].

$$C_nH_{2n} + H_2 \rightarrow C_{2n}H_{2n+2}, n = 8, 12, 16 \tag{3.15}$$

Finally, these paraffins are distilled to separate heavier alkanes (jet fuel) which consists of mainly C_{12}-C_{16}hydrocarbons from lighter paraffins (Gasoline) consisting of higher percentage of C_8 hydrocarbons.

3.4 Ammonia production

This section deals with gas processing and ammonia synthesis processes with subsequent ammonia recovery. Syngas containing hydrocarbons can damage catalyst used for ammonia synthesis, therefore syngas obtained from gasification unit undergoes gas processing to remove these species and also achieve N_2 /H_2 ratio of 1/3. Hydrogen produced from SOEC can be directly sent to the ammonia synthesis unit. Gas processing and ammonia synthesis technologies are discussed in following sections.

3.4.1 Gas Processing

Syngas from gasification section after cooling and cleaning mainly consists of CO, H_2, CO_2, small amounts of CH_4 and nitrogen. The objective of gas processing unit is to enhance the concentration of H_2 in the syngas to optimize the ammonia production. Air is also added during gas processing to maintain the nitrogen in ratio required to carry out ammonia synthesis. Another important target is to purify the synthesis gas and remove the species which might be poisonous for ammonia synthesis, such as sulfur compounds and oxygen compounds: CO and CO_2 [6].

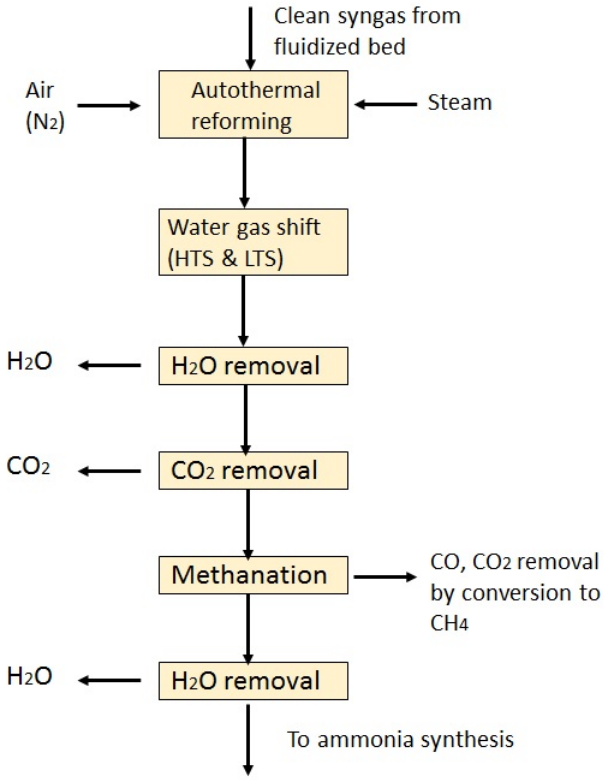

Figure 3.4: Syngas processing steps for ammonia synthesis (fluidized bed gasification) [6]

In this study, syngas is produced by fluidized bed technology, therefore, the gas processing steps are in accordance to that as shown in the figure 3.4.

Syngas is a mixture of hydrogen and carbon monoxide with the ratio depending on the desired product. It also contains compounds such as methane, nitrogen, carbon dioxide, and so forth. The reforming of syngas uses a nickel-based catalyst to promote the reaction. It proceeds in parallel with the water-gas shift reaction according to the following reactions [37]:

$$CH_4 + H_2O \rightarrow CO + 3H_2 \tag{3.16}$$

$$CO + H_2O \rightarrow CO_2 + H_2 \tag{3.17}$$

Reaction of methane and steam is highly endothermic and water-gas shift, is slightly exothermic, therefore the overall reaction is endothermic. Since the reaction is endothermic, a source of heat is needed to keep the energy balance of the system. The heat can be provided by supplying oxygen to the reformer for oxidation reactions inside the reactor, which give the heat required for the steam reforming (direct heating). This process is called "autothermal" reforming (ATR), and it is usually performed by adding air to the steam/gas mixture.[6]

$$CH_4 + 1/2O_2 \rightarrow CO + 2H_2 \tag{3.18}$$

An ATR reactor contains a combustion zone at the top and a catalyst filled bed at the bottom. The syngas is mixed with a limited amount of oxidant and burned in the combustion zone. They are suited for making synthesis gas with relatively low H_2/CO ratios such as 1.5/1 – 3/1 [37]. ATR is an attractive option for ammonia synthesis because the amount of air added to the reactor can be controlled to maintain the nitrogen entering the system.

The product gas from ATR contains large amount of CO which will be converted to produce hydrogen through water-gas shift (WGS) reaction. WGS reactor is implemented through a series of high temperature shift (HTS) followed by a low temperature shift (LTS) catalyst based reactors with intercooling stage to increase the overall conversion to hydrogen. The HTS usually is an iron oxide – chromium oxide based catalyst. Operational temperatures vary from 310ºC to 450ºC [38]. Inlet temperatures are usually kept at 350ºC to prevent the catalyst bed temperature from damage. LTS reactors are copper based catalyst. Typical compositions include Cu, Zn, Cr and Al oxides. Recent catalysts can be operated at medium temperatures around 300ºC. Typical exit concentration is of 0,1% of CO [38].

The process gas from the low temperature shift converter contains mainly H_2, N_2, CO_2 and the excess process steam. Acid gases must be removed as they can poison the catalyst of ammonia synthesis . After cooling the gas, most of the excess steam is condensed and is removed before it enters the CO_2 removal system [6]. Carbon capture and removal technology is discussed in section 3.3.1. Rectisol process developed by Lurgi and Linde is used for carbon dioxide removal.

To further purify the synthesis gas and remove traces of CO and CO_2, syngas is made to undergo methanation. The methanation reactions take place at around 250-450°C in a reactor filled with a nickel containing catalyst. The reactions to convert CO and CO_2 into methane are shown below:

$$CO + 3H_2 \rightarrow CH_4 + H_2O \tag{3.19}$$

$$CO_2 + 4H_2 \rightarrow CH_4 + 2H_2O \tag{3.20}$$

Water must be removed before entering the ammonia synthesis unit and is usually removed after methanation by cooling and condensation or by adsorption on molecular sieves [6]. After processing, syngas is ready to be mixed with hydrogen from Electrolyzer cell before entering into ammonia synthesis unit. SOEC concept has already been discussed previously. Next section deals with ammonia production from synthesis gas.

3.4.2 Ammonia synthesis and recovery

The Haber–Bosch process is an artificial nitrogen fixation process and is the main industrial procedure for the production of ammonia. The process converts nitrogen (N_2) to ammonia (NH_3) by a reaction with hydrogen (H_2) using a metal catalyst under high temperatures between 350-550°C and pressures in the range of 100-250 bar [6].

$$N_2 + 3H_2 \rightarrow 2NH_3 \tag{3.21}$$

Figure 3.5 shows the Haber Bosch process steps for synthesis of ammonia from syngas.

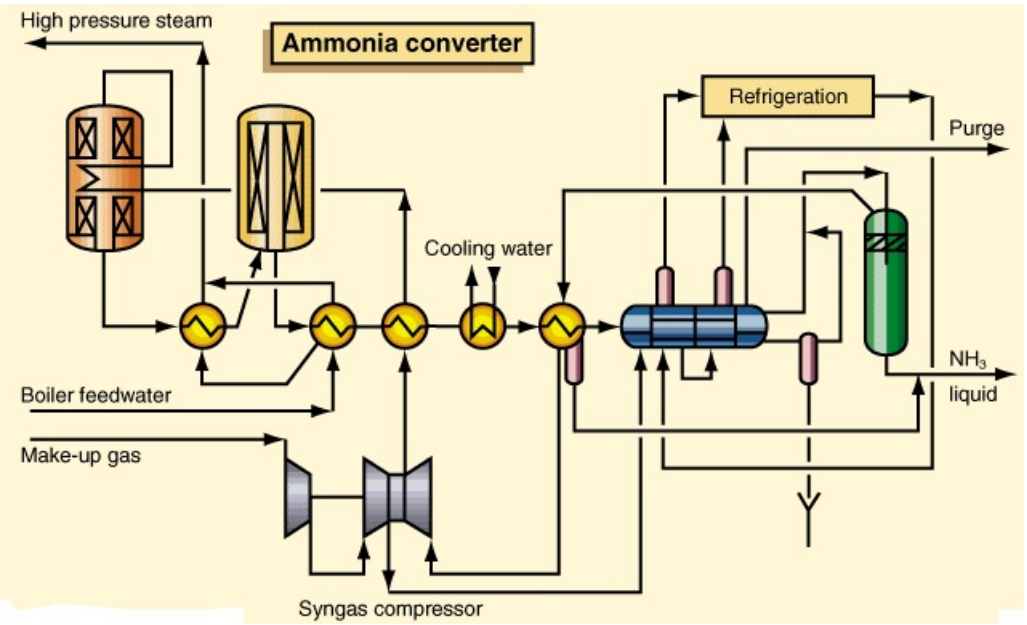

Figure 3.5: Haber Bosch Process- Ammonia synthesis [6]

The syngas coming from the gas processing is compressed to required pressure and mixed with recirculated stream from ammonia converter. This stream is preheated before it enters the reactor. The gas leaving the converter has an ammonia content between 15-25% depending on the operative parameters of the synthesis. Only 20-30% of the reactants per pass are converted in the reactor due to the unfavourable equilibrium conditions. The formation of ammonia is an exothermic reaction with release of heat. Ammonia synthesis is favoured at high pressure and low temperatures. However, high temperatures are used in the presence of an iron-based catalyst to lower the activation energy of the reaction, required to break nitrogen molecule. The ammonia formed is separated by cooling, refrigeration and condensation. A purge is required in the loop to avoid accumulation of inerts and nitrogen in the loop. The liquid ammonia separated in the process is sent to the product recovery section. [6].

Ammonia recovery Liquid ammonia from ammonia synthesis unit contains dissolved gases which are removed partially by flashing in pressure flash tank operating at 20 bar. The product obtained is further flashed in second flash tank at ambient pressure. Ammonia is obtained as product from this flash tank and is further sent to ammonia storage tank. The gases released from first and second pressure flash tanks are treated with wash water to recover ammonia. This aqueous ammonia is distilled in a column to obtain NH_3 vapour which is then sent to ammonia storage tank. Purge obtained can be used as fuel.

3.5 Conclusion

The technologies discussed in this chapter provide the concept for designing and modelling of various processes. Gasifier unit is modelled based on FICFB model and gas cleaning unit is modelled based on OLGA unit design in chapter-5. Fischer Tropsch process is adopted to produce jet fuel. All reactions and processes like mixed alcohol synthesis, alcohol dehydration, oligomerisation, dehydrogenation and distillation are explained with operating conditions. Similarly ammonia synthesis based on Haber bosch process is modelled based on processes and design conditions described in this chapter.

Chapter 4

SOFC based aircraft APU system

This chapter deals with modelling of SOFC-GT based aircraft APU-system using jet fuel and ammonia. The design parameters adopted to model the system are taken from [9], with an objective to validate the model, determine the fuel cell stack size and fuel consumption. Section 4.1 discusses the modelling paradigms of the SOFC describing the basic underlying modelling concepts, equations and assumptions. Section 4.2 deals with model development for jet fuel and ammonia. Sensitivity analysis is performed in section 4.3 to validate operating pressure of SOFC for optimum operation. Sensitivity analysis also helps in determining air inlet conditions and size of the stack for SOFC-GT system based on power produced by SOFC and total cell area for SOFC operation at different times and different altitudes. In section 4.4 results for Nernst potential, current and dimensions of SOFC are discussed with total power produced by SOFC and turbine and power consumption by auxilliary units. Section 4.5 concludes the chapter with result summary and comments.

4.1 Modelling paradigms

SOFC-GT models are developed for two different cases, operating with jet fuel and ammonia as fuels. Assumptions are same for both the models. Previous studies [2, 14, 9] have already discussed modelling of SOFC-GT for aircraft APU systems as shown in figure 4.1.

For this study, the model designed by [9] will be taken as reference and SOFC parameters are set according to those described by Whyatt et al. in his work. However, before defining the assumptions and describing the model, internal equations to calculate various parameters of SOFC system will be discussed.

4.1.1 SOFC internal equations

The modelling of the fuel cell is done based on design data from Whyatt et al. [9] to size the system and calculate fuel consumed for producing required power. It is required

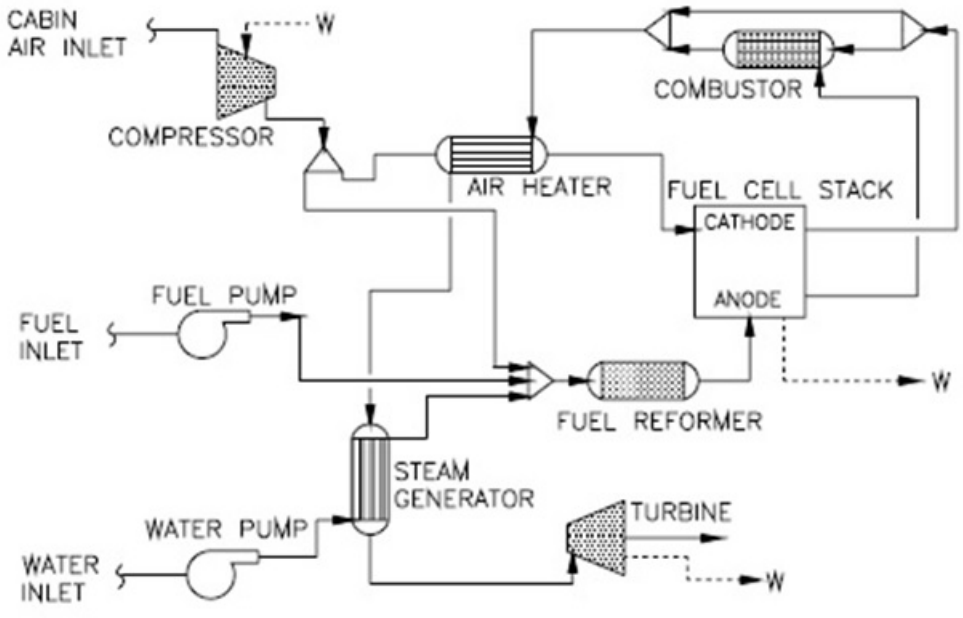

Figure 4.1: Schematic of SOFC-GT based aircraft APU system [2]

to relate electric power and heat flow with molar flows at their actual inlet and outlet thermodynamic conditions. According to equation 4.1 this power can be expressed as product of operative voltage and current.

$$P_{SOFC} = V.I \tag{4.1}$$

Mole flows and concentration equations are formed to compute voltage and current for calculating power. Current can be releated to the equivalent inlet molar flow of hydrogen, fuel utilization factor and the Faraday constant. Equation 4.2 shows the fuel cell relationship while equation 4.3 shows fuel utilization factor, which represents the actual consumption of the fuel per pass in the fuel cell, over the total fuel supply.

$$I = 2.F.UF.n_{H2eq} \tag{4.2}$$

$$UF = \frac{fuel_{consumed}}{fuel_{supplied}} = \frac{H_{2,consumed}}{H_{2,supplied}} \tag{4.3}$$

Once the current density is fixed, total active area of SOFC can be calculated by using total current as shown in equation 4.4. Flow of oxygen ions from cathode to anode in the fuel cell can be determined by using equation 4.5.

$$A = \frac{I}{J} \tag{4.4}$$

$$O_{flow} = \frac{I}{4F} \tag{4.5}$$

Nernst potential or V_{nst} can be calculated using partial pressures of oxygen at anode and cathode as previously shown in equation 2.32. Since V_{nst} is maximum achievable voltage of a fuel cell for a given fuel composition, actual voltage (V) is calculated by considering losses encountered in the cell. Operative cell voltage can be represented as a function of Nernst potential and lumped voltage drop which is result of all dissipative phenomenon occuring within the cell. To define the losses, some assumptions are made for simplification. Activation losses are assumed negligible at high temperatures of SOFC and non linear region due to concentration losses can be excluded while modelling a reversible SOFC model [4]. Therefore operations are carried out within the ohmic losses region, hence operative cell voltage can be expressed linearly as shown in equation 4.6. ASR is an equivalent area specic resistance, which might include ohmic, activation and concentration losses.

$$V = V_{nst} - J.ASR \tag{4.6}$$

4.1.2 Assumptions

To model the SOFC, certain assumptions need to be made which are listed below:

- Steady state operation
- Constant utilization factor
- Isobaric electrochemical reaction at SOC inlet pressure
- Same equivalent area specific resistance (ASR) assumed for both SOFC models
- Same current density assumed for both SOFC models
- Temperature difference of 100K between inlet and outlet of SOFC

4.2 SOFC models

The SOFC is based on the Gen4 Delphi planar SOFC with assumed modifications based on information obtained from literature [9]. An estimate of electrical power of A320 and B737 is made, assuming them as MEA. As a futuristic approach, 500 KW power SOFC-GT are designed to work as APU systems for these more electric aircrafts. Both jet fuel and ammonia based systems have to be designed keeping in mind the power requirements and basic parameters of SOFC-GT used for the present study.

According to Whyatt et al [9], engine generators produce 230VAC power which is converted to +/-270VDC to drive the largest loads. Therefore, SOFC-GT system should be designed to produce +/- 270 V to run the electric loads. Calculations performed by them also show that most optimum point of operation for SOFC is achieved at 8 bar and cell voltage of 0.825 V. The optimum condition is the point where fuel saved from increased efficiency of SOFC-GT system balances the excess fuel used by main engines to carry heavier SOFC-GT system. Therefore SOFC for both the models will be designed to operate at 8 bar and

800^0C. This model is based on jet fuel, however, these values can change with respect to different fuels. Some of the modifications assumed for designing the SOFC as assumed by [9] are shown below:

- Power density in the active area of the cell is estimated to be 0.76 watt/cm^2 at 0.825 V/cell which results in current density of 9212 A/m^2. This high power density can be attributed to the fact that a recently developed material set showing higher power densities is assumed to be used, SOFC is operated at higher pressure of 8 bar and anode recycle steam reforming is used. More than half of the anode exit gas is recycled which improves the overall fuel utilization.

- As temperature of fuel cell increases, Vnst or Vrev decreases. According to figure 4.2 , Vnst of 1.015 V is assumed at 800^0C (1073 K) for SOFC at 0.825V/cell. Therefore, ASR can be calculated by dividing the difference of Vnst and V by current density. This value comes out to be 0.2056 Ω/cm^2.

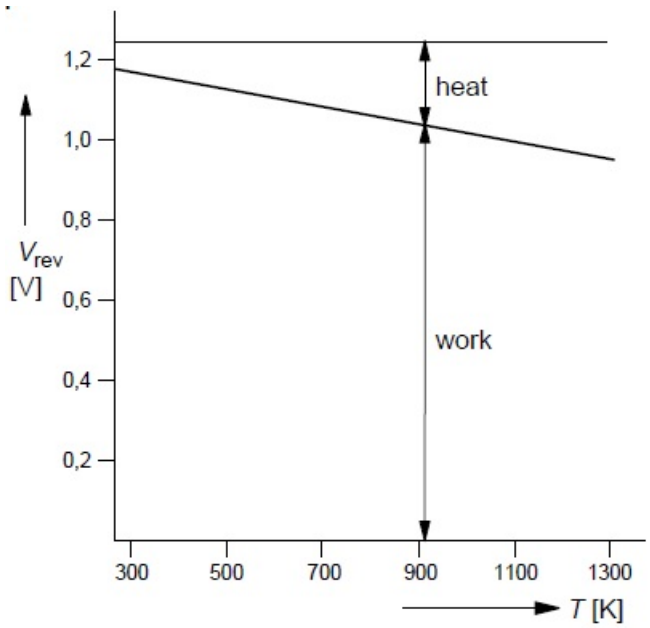

Figure 4.2: Nernst potential vs temperature graph

- The cells are organised into stacks and stacks are organised to make towers to produce specific power. A cell stack is an array of cells connected in series to produce 90 V, which gives number of cells in each stack as per equation 4.7. A module is an array of stacks connected in series to produce total voltage of 270 V, which makes total number of cells in an independent module 3 times than that in one stack. A number of such modules are then connected in parallel to produce required power. Figure 4.3 shows the configuration of stacks in a module.

$$N_{cell} = 90/V \tag{4.7}$$

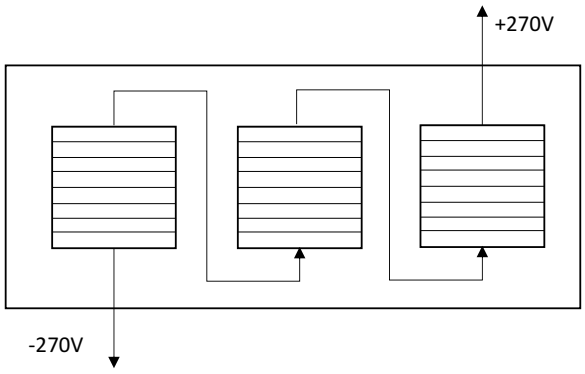

Figure 4.3: Configuration of cells in stacks and stacks in a module. Conceptual layout of one independent module.

- Total area of cells can be calculated by using current and current density. Equation 4.8 will then give active area of each cell. Number of modules is decided by using a design specification block such that the number of modules are just enough to produce the required amount of power for SOFC.

$$A_{cell} = \left(\frac{I}{3.J.N_{cell}.N_{module}}\right) \tag{4.8}$$

$$P_{SOFC} = V \times J \times A_{cell} \times N_{cell} \times 3 \times N_{module} \tag{4.9}$$

With these specifications in mind, model can be designed in ASPEN PLUS.

4.2.1 Jet fuel SOFC

First of all, to model jet fuel SOFC, jet fuel composition is decided. Based on data obtained from [8], jet fuel composition is assumed to be a mixture of various higher hydrocarbons shown in table 4.1.

Table 4.1: Jet fuel composition [8]

Component name	Chemical formula	Mole fraction
Octane	C_8H_{18}	0.70%
Do-decane	$C_{12}H_{26}$	41.50%
Hexadecane	$C_{16}H_{34}$	58.55%

SOFC-GT system consists of basic components such as compressors, pumps, heat exchangers, SOFC unit and turbine. To increase the efficiency of the system, SOFC is designed as hybrid system with gas turbine unit. Figure 4.4 shows complete SOFC-GT system designed in ASPEN PLUS to produce power from Jet fuel.

The fuel enters the system at ambient condition. It is then compressed to 8 bar and mixed with steam and recirculated stream from anode. This mixture is sent to steam reformer for

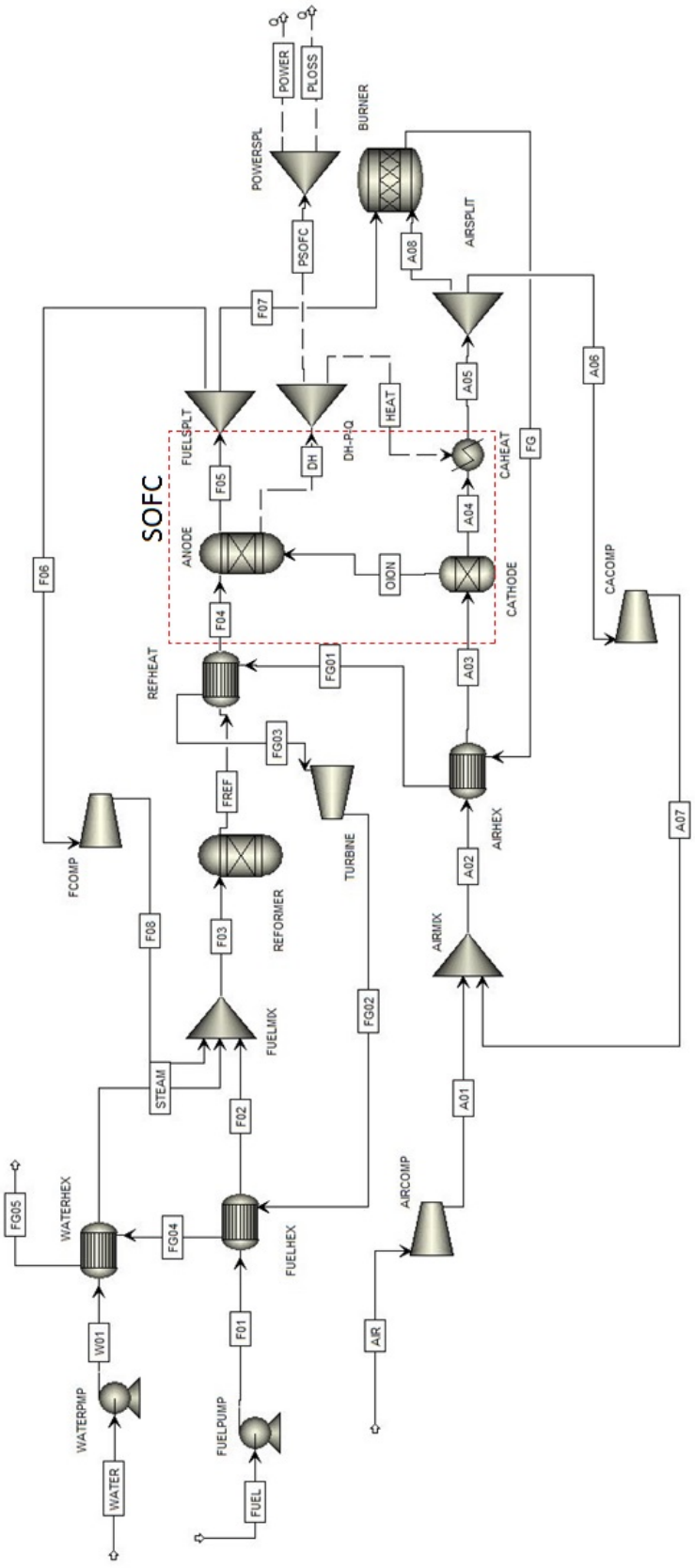

Figure 4.4: ASPEN PLUS model for 500 KW SOFC-GT system designed for aircraft APU using jet fuel

converting jet fuel into syngas. Since higher hydrocarbons might lead to coke formation if fed directly to SOFC as fuel, pre-reforming is recommended. The reformer is designed as equilibrium block (R-Gibbs) with process parameters as shown in table 4.2. Typically, a steam reformer is used to convert methane into H_2 and CO. In this process, practical H_2O/C ratios are 2.5-3 [10]. For this project steam to carbon ratio of 2.5 is adopted. In the reformer, the mixture of anode waste gas, steam and fuel reacts over a catalyst consisting of a small amount of rhodium metal dispersed onto a magnesia-alumina spinel support which is then coated onto a FeCrAlY metal foam [9]. Reactions taking place in steam reformer are endothermic, thus reducing the temperature of the reaction. However, as the reaction proceeds, some CO forms CO_2 through water gas shift, which is then followed by methanation reaction. These reactions are exothermic and thus balance the temperature of the reactor making steam reforming an adiabatic process. Steam reforming, unlike auto thermal reforming, requires only steam. This type of steam reformer operation is important to achieving the high efficiency of the overall SOFC power system.

Table 4.2: Reformer stream results and process parameters

Mole Flow (kmol/hr)	Stream in	Stream out
H_2	0.52	2.26
H_2O	9.18	6.27
CH_4	0.0003	2.94
C_8H_{18}	0.0022	0.00
$C_{12}H_{26}$	0.13	0.00
$C_{16}H_{34}$	0.18	0.00
CO	0.18	0.21
CO_2	0.91	2.35
Total Flow (kmol/hr)	11.11	14.04
Temperature (C)	561.89	535.08
Pressure (bar)	8.16	8.08

The reformate is then heated to a temperature of 700^0C through heat exchanger using the heat of flue gases from the combustor. SOFC block consists of number of reactors which include equilibrium reactor (R-Gibbs) as anode and separator block as cathode. Air entering at ambient condition is compressed and heated before it enters cathode. Oxygen ion flow is represented by OION stream in figure 4.4. Fuel utilization is assumed as 0.75 for SOFC model. Input parameters for determining voltage, current and size of SOFC as discussed previosuly is shown in table 4.3.

Table 4.3: Input variables for SOFC [9]

Variable	Value	Unit
J	9212	A/sqm
ASR	2.06E-05	ohm/sqm
SOFC temperature	800	C
SOFC pressure	8	bar
UF	0.75	

Product gas leaving anode is split. Approximately 75% of the gas is mixed with fuel and recycled back to the reformer. Rest of the gas is sent to combustor along with air from cathode for combustion. Flue gas at high temperature from combustor is then used to produce power in a gas turbine. Flue gas from combustor leave at high temperature and therefore can be used to heat up fuel and air from ambient conditions to SOFC temperature through heat exchangers. Combustor is designed as stoichiometric block with water formation reaction. SOFC produces power as well as heat. Since SOFC is designed to be adiabatic, heat streams from anode reactor are used to connect anode reactor to the cathode flow.

4.2.2 Ammonia SOFC

Ammonia based SOFC-GT system is designed in the same way as jet fuel based SOFC-GT system with only difference being the absence of steam reformer and water input. Ammonia is stored in the aircraft in liquid form at -40^{0}C. It is compressed and heated to 700^{0}C before it enters SOFC. Air is taken at ambient condition, compressed and sent to cathode. The reactions taking place at anode and cathode in case of ammonia respectively, are shown below:

$$2NH_3 \rightarrow N_2 + 3H_2 \tag{4.10}$$

$$H_2 + O^{2-} \rightarrow H_2O + 2e^- \tag{4.11}$$

$$O_2 + 2e^- \rightarrow 2O^{2-} \tag{4.12}$$

Input parameters like current density, area specific resistance etc. for ammonia based SOFC is same as that for jet fuel based SOFC and can be seen in table 4.3.

4.3 Sensitivity analysis

This section compares various scenarios for SOFC operation to determine the size of the fuel cell stacks. It provides data to ensure that model is designed to operate at maximum capacity required by aircrafts at different times and different altitudes. This analysis is performed for jet fuel SOFC only. The trend of results can vary with different fuel types, however, we assume similar conditions for ammonia as well to simplify the study.

4.3.1 Influence of ambient environment

According to Airbus A320-Pilot's operating handbook, the maximum altitude that A320 and similar aircrafts can achieve is 28000 feet or 8615.3 metres above sea level. Due to change in ambient conditions, the pressure and temperature of incoming air as well as outgoing flue gases will change, which will change the power produced and consumed by different units of the system. To understand this, simple equations 4.13 and 4.14 are used

to calculate pressure and temperature respectively at different altitudes of the aircraft [39].

$$p1 = p_0 \left(1 - 0.0065 \frac{h}{T_0}\right)^{5.2561} \tag{4.13}$$

$$T = T_0 - 6.5 \frac{h}{1000} \tag{4.14}$$

Here, pressure (p1) is in bar, temperature (T) is in K and altitude (h) is in metre. Ambient temperature T_0 and pressure p_0 are 288.15K and 1.013 bar respectively. Based on above equations, power requirements for SOFC are considered for 4 different altitudes as shown in table 4.4 by changing pressure and temperature of incoming air and outgoing flue gas.

Table 4.4: Sensitivity analysis for SOFC power by changing ambient conditions

Temperature (C)	Pressure (bar)	Altitude (m)	P_{SOFC} (KW)	Current (Amp)	Total cell area (sqm)
-41	0.325	8615.3	450.75	546649	59.34
-35	0.371	7692.3	452.69	548906	59.58
-10	0.628	3846.2	461.50	559452	60.73
15	1.013	0	472.11	572113	62.10

It is clear from table 4.4 that SOFC is required to produce maximum power when it is at sea level (on ground). During cruising at higher altitudes, the power required is less and therefore, current produced is less. Due to lower currents, active cell area required to produce the current is also small at higher altitudes. Therefore, SOFC is designed for ambient conditions at sea level to have maximum cell area such that it can produce required amount of current to achieve 500 KW both at cruise altitude as well as sea level. Since this analysis is done to size the SOFC only, power of the turbine and auxilliaries are not mentioned.

4.3.2 Influence of SOFC pressure on power

To understand reasons for 8 bar operation pressure for SOFC, sensitivity analysis was done by changing the operating pressure of SOFC from 2 to 8 bar and observing the effect on power production or consumption by different components. Figure 4.5 shows the change in power production by turbine and SOFC and consumption by auxilliaries with changing operating pressures.

From figure 4.5, it can be seen that increasing the pressure leads to decrease in electric power produced by SOFC. This reduces SOFC current. Lower current leads to reduction in SOFC stack size in turn reducing the weight of the SOFCPU. In addition, lower current also means lesser fuel consumption. This implies an increased fuel cell efficiency. The increase in the operating pressure of SOFC also causes an increase in the turbine inlet pressure, because of which the turbine is able to provide a substantial amount of excess power. For different fuels, operating pressures can vary depending on the optimum point of operation for aircraft with SOFC-GT based APU.

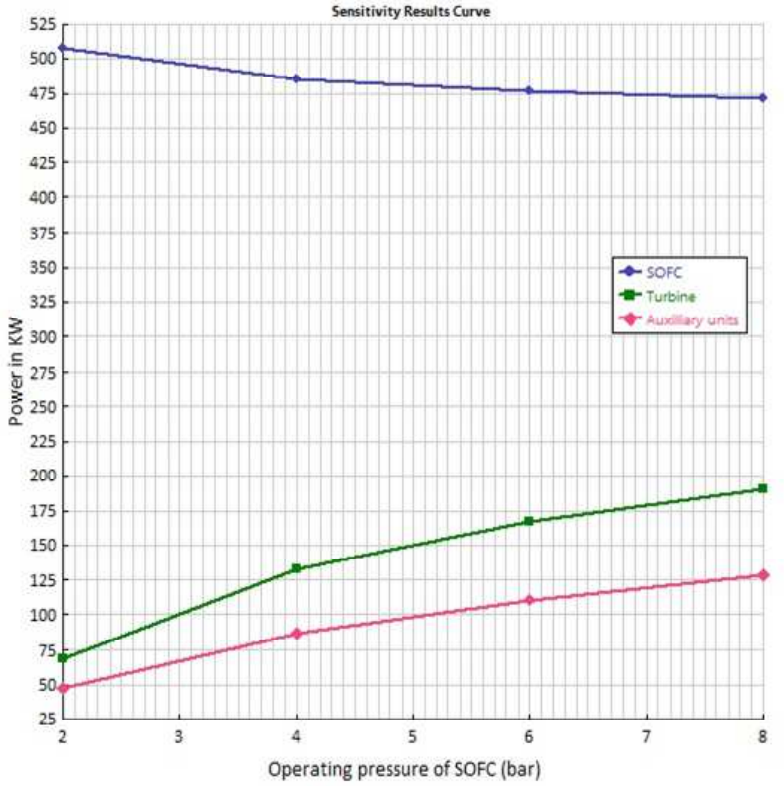

Figure 4.5: Changes in power requirements with operating pressure change. The auxilliary, turbine and SOFC power considered before DC-DC converter.

4.4 Results and discussion

The results of SOFC-GT model are required as inputs in order to model the SOEC for stationary fuel production plant, and will be discussed within this chapter. Exergy efficiency and comparisons for SOFC-GT systems will be discussed in chapter-6.

4.4.1 Results: Jet fuel SOFC

Calculator blocks are used to calculate the amount of steam to enter reformer for required results. Also design specification blocks are used to adjust air flow in SOFC and fuel consumption for producing 500 KW power. The results after simulation are presented in table 4.5.

Table 4.5: Inlet conditions for various input streams for SOFC (jet fuel)

	Mole flow (kmol/hr)
Jet Fuel	0.308
Water	6.822
Air	47.165

The table 4.6 gives the power produced by SOFC, auxilliary components and turbine before and after DC-DC converter. An efficiency of 0.95 is chosen for DC-DC converter. Neet power produced by the SOFC-GT system is defined by equation 4.15 which includes power produced by SOFC, turbine and consumed by auxilliary components like compressors.

$$P_{net} = P_{SOFC} + P_{turb} - P_{aux} \tag{4.15}$$

Table 4.6: Power requirements for jet fuel SOFC based APU system before and after DC-DC converter

	Before DC-DC conversion	After DC-DC conversion	Units
Auxiliary components power	123.18	129.66	KW
Turbine power	190.7	181.16	KW
PSOFC	472.11	448.5	KW
Power achieved	--	500	KW

Table 4.7 shows calculated SOFC voltage and current values respectively. The table also gives dimensions of each cell as well as the number of stacks and modules required to produce required power.

Table 4.7: SOFC voltage and current calculations for jet fuel as fuel source

Variable	Value	Unit
V_{nst}	1.02	Volt
V	0.825	Volt
I	572113	A
N_{cell} /module	327	
A_{cell}	0.0474	sqm
N_{module}	4	

By keeping all the assumptions in sync with literature [9], the voltage achieved for jet fuel is obtained as 0.825 V. Hence the model is validated.

4.4.2 Results: Ammonia SOFC

Design specification blocks are used to adjust air flow in SOFC and fuel consumption for producing 500 KW net power for SOFC-GT system. The results after simulation are presented in table 4.8.

Table 4.8: Input parameters for inlet streams of ammonia SOFC- APU system

	Mole flow (kmol/hr)
Ammonia	9.04
Air	63.80

Table 4.9 shows voltage and current calculation performed for ammonia SOFC which also highlights the cell area and number of cells per module.

Table 4.9: SOFC voltage and current calculations for ammonia as fuel source

Variable	Value	Unit
V_{nst}	1.02	Volt
V	0.827	Volt
I	605535	A
N_{cell} /module	327	
A_{cell}	0.0403	sqm
N_{module}	5	

Table 4.10 shows power requirements and power production from ammonia SOFC.

Table 4.10: Power requirements for ammonia SOFC based APU system before and after DC-DC converter

	Before DC-DC conversion	After DC-DC conversion	Units
Auxiliary components power	176.91	186.22	KW
Turbine power	221.7	210.6	KW
PSOFC	500.64	475.6	KW
Power achieved	--	500	KW

4.5 Conclusions

This chapter can be concluded by saying that the SOFC-GT based APU systems can prove to be more efficienct than conventional turbine based APU systems for the aircrafts. SOFC-GT system for aircraft APU was designed to produce 500 KW electric power. Typically used temperature of 800^0C was assumed for SOFC modelling. Pressure of 8 bar was chosen based on literature review and sensitivity analysis was done to show that at 8 bar SOFC has to produce less power than it has to at lower pressures. Simulations revealed that voltage of 0.825 V is achieved with jet fuel and 0.827 V is obtained with ammonia as fuel source for SOFC. Sensitivity analysis was also done to determine the dimensions of the SOFC-GT unit. It is concluded that SOFC system has to be designed based on sea level ambient conditions to fulfill maximum current requirements. Total active cell area of 62.1 m^2 and 65.7 m^2 is required for jet fuel and ammonia based SOFC respectively. In case of jet fuel, the flue gas stream releases 4.4 kmol/hr (7.8%) carbon dioxide in the ambient, whereas, while using ammonia as a fuel, there are no carbon emissions. There is nitrous oxide present in flue gas in almost negligible amounts. Using Solid oxide fuel cells for more electric aircrafts can be a way to reduce carbon emissions and increase the fuel efficiency. In chapter-6, exergy calculation for both jet fuel and ammonia operated SOFC will be undertaken to understand exergy efficiencies of these APU systems and provide a comparison between conventional and SOFC based APU system efficiencies.

Chapter 5

Stationary fuel production plant modelling

Stationary sustaianble fuel production plant at the airport is one of the many methods which can help air transport industry in decarbonizing and reducing emissions. In this chapter, two technologies namely- electrolysis and biomass gasification, and their mix is considered for sustainable fuel production. Although there can be many other efficient ways to produce sustainable fuel, this thesis investigates only above mentioned pathways. This work focusses on production of fuel for aircraft APU use only.

This chapter discusses system assumptions in section 5.1, modelling of stationary fuel production plant (both jet fuel and ammonia) in section 5.2, section 5.3 discusses the results and section 5.4 concludes the chapter. Modelling of each individual unit is discussed in detail in section 5.2. Subsection 5.2.5 discusses the concept of integrated model design where SOEC, gasifier and fuel synthesis units are integrated to form a plant. The three fuel production cases: gasifier+fuel synthesis, SOEC+fuel synthesis and gasifier+SOEC+fuel synthesis, as mentioned in chapter-1, are discussed in this subsection. Results for these cases are also shown section by section. The focus is not only on operating conditions of SOEC and major reactors for jet fuel or ammonia production but also on the necessary auxiliary components such as pumps, compressors and distillation columns.

5.1 System configurations

ASPEN PLUS modeling software was used to model SOEC, gasifier and fuel synthesis units to produce jet fuel and ammonia. Figure 5.1 shows the three cases considered for jet fuel and ammonia production with the necessary process steps.

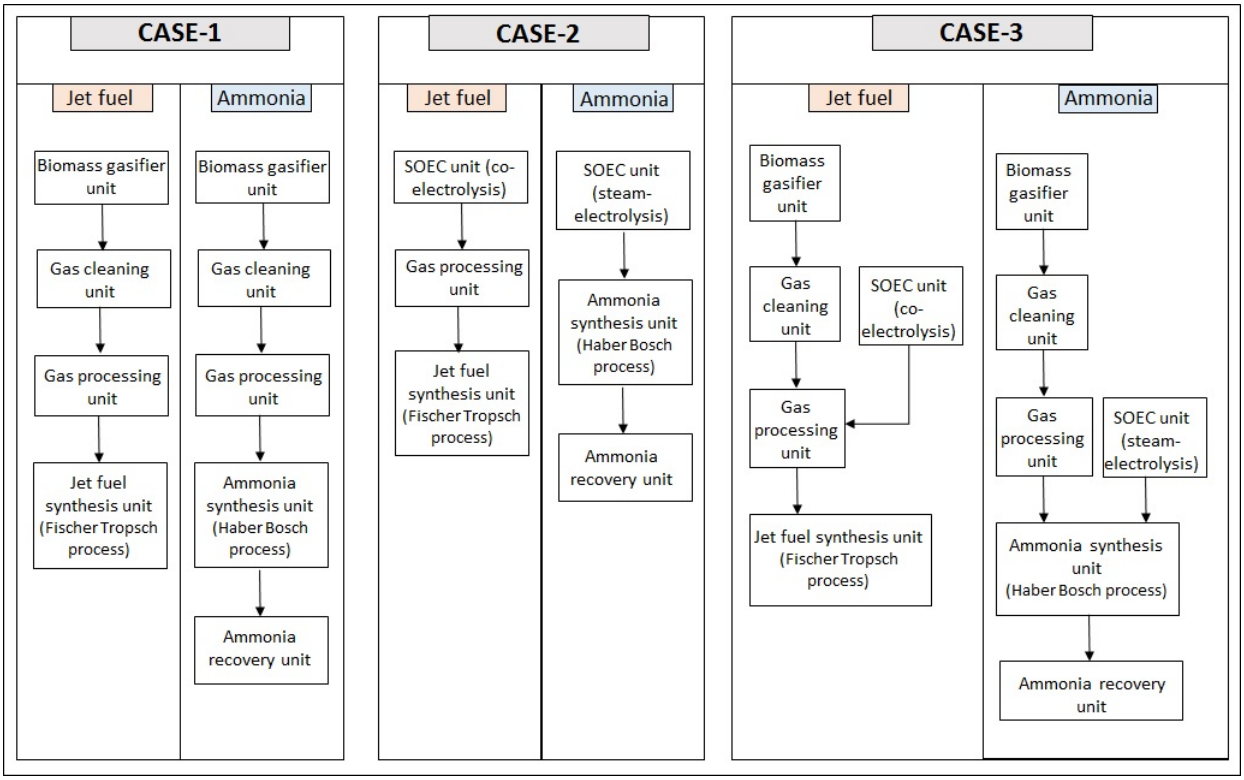

Figure 5.1: Fuel production pathways for biofuel production. Cases considered for modelling of stationary fuel production plant. *Reasons for choosing these configurations are mentioned below.

CASE-1: According to Roadmap 2050, 20% of biomass potential is dedicated to air and sea transport. Therefore, for this scenario, only gasification system is designed which uses biomass to produce biofuel for aircrafts. Gasifier modelled for this case operates at full capacity producing entire fuel used for one day operation of aircraft APUs.

Model description: The model is based on fluidized bed gasifier to produce syngas which is further processed to produce either jet fuel or ammonia. The gasifier model uses similar processing assumptions and unit operation configurations as those used by [10].

CASE-2: This scenario considers fuel production through SOEC units only. It is assumed that SOEC operates for 8 hours, when aircrafts are parked at the airport, on excess available electricity from renewable sources. The intent here is to analyze fuel regenerated by SOC used as electrolyzer when aircraft is parked, hence only 1 bi-directional unit is modelled and analyzed as each aircraft is supposed to regenerate its own fuel.

Model description: SOEC performs either co-electrolysis or steam electrolysis to produce syngas and hydrogen respectively. Syngas from SOEC is sent to the jet fuel synthesis unit after processing to form jet fuel. For ammonia production, hydrogen from SOEC is sent to ammonia synthesis and recovery unit.

CASE-3: Since biomass is limited and excess electricity from renewable sources has intermittent nature, both energy sources are expected to contribute for biofuel production for aircraft industry. According to forecast by [40], The Netherlands will be confronted

with 2 TWh of excess electricity in the year 2020, if the target of installing ~17 GW of wind and solar energy is reached and other options of dealing with oversupply are not available (e.g. export). However, excess electricity will only be available for 1000 hours throughout the year [40] with an average of 2.7 hours/day. Assuming sufficient power is available to run 5 SOEC units on full capacity for 2.7 hrs/day, amount of fuel produced is comparable to that produced by one SOEC unit operating for 8 hours/day. Therefore, to simplify the modelling process, one SOEC unit operating for 8 hours/day is considered. Since SOEC operation is limited to 8 hours only (when aircraft is parked), biomass gasifier working at full capacity is used to produce fuel for rest of the day. Since gasifier unit cannot be shut down and is designed for constant capacity production, the SOEC unit is combined with gasifier operating at full capacity.

Model description: Integrated plant for fuel production includes contribution from both biomass gasification and SOEC units. Due to full capacity operation of gasifier and 8 hour operation of SOEC, the fuel produced will be slightly more than required for 5 aircraft APUs per day. Detailed jet fuel and ammonia production plant schematic for case-3 are shown in figure 5.2 and 5.3 respectively.

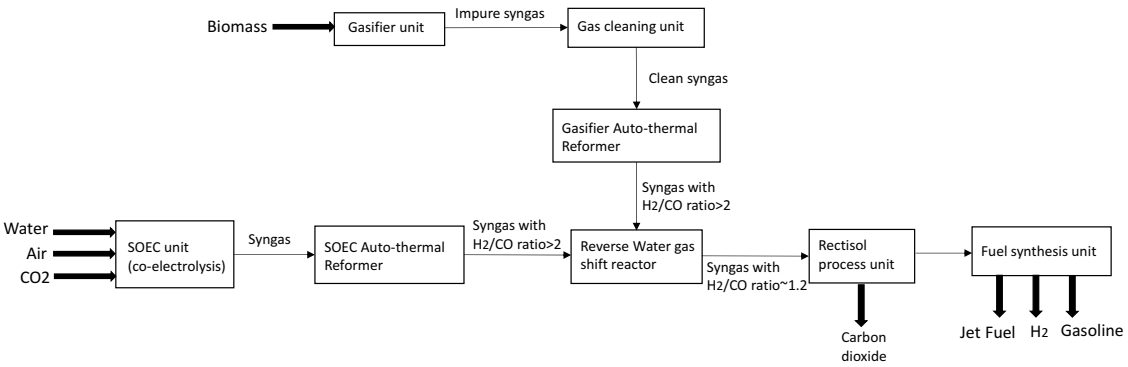

Figure 5.2: (CASE-3) Schematic of integrated Jet fuel production plant showing major process steps

Detailed schematic for jet fuel synthesis unit (Fischer Tropsch) is provided in chapter-3, figure 3.3. The Fischer Tropsch process plant to produce jet fuel is based on model developed by [8] in terms of composition and process operative conditions.

In case of ammonia production, syngas from biomass gasifier is cleaned and processed before entering ammonia synthesis unit. Gas processing unit is explained in detail in chapter-3, figure 3.4. Ammonia production and gas processing plant compares to work done by [6] in his master thesis report.

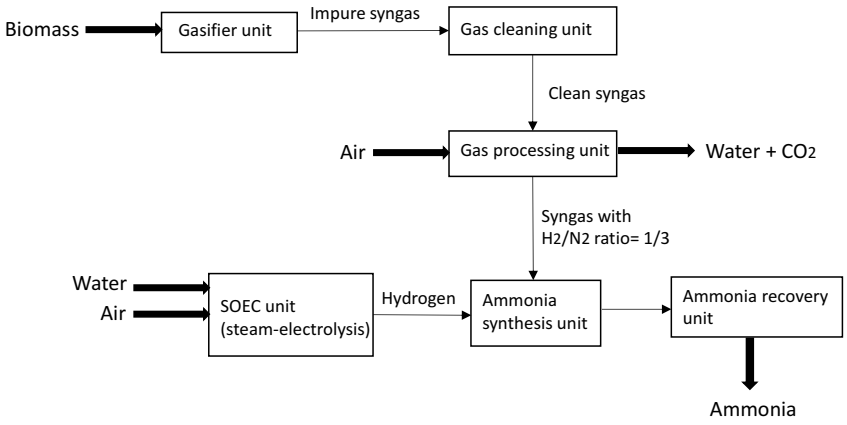

Figure 5.3: (CASE-3) Schematic of integrated ammonia production plant showing major process steps

5.1.1 General assumptions

Before modelling the SOEC and fuel production processes, it is necessary to make few assumptions based on which plant capacities and working conditions are determined.

- For present analysis, Eindhoven airport was chosen as basis of study.
  - Short to medium range aircrafts with a capacity of 150-200 passengers like A320 and B737 are considered for the analysis. Since Eindhoven is a relatively smaller airport and handles traffic only within Europe, only short to medium range aircrafts are operated from there.
- Fuel consumption and production is considered for 5 aircraft APUs only
  - Flights operate everyday from 7am till 11pm from Eindhoven airport. From 11pm to 7am (8 hours), 5 aircrafts are parked at the airport on an average. This was concluded after data analysis of flight arrivals and departures at Eindhoven airport on a daily basis for a week.
- It is assumed that an aircraft is performing activities like cruising, taking off, landing and taxing for a total of 10 hours/day with 100% fuel consumption. 30% fuel consumption is assumed during preparation for passenger boarding and un-boarding for 6 hours/day at the airport.
  - According to the calculated fuel consumption in kmol/hr for an aircraft to produce 500KW in chapter-4, fuel consumption for five aircrafts can be calculated. Equation 5.1 can be used to calculate the amount of fuel required to be produced by stationary fuel production plant per day.

$$Fuel_{day} = 5.\,(10 \times Fuel_{SOFC} + 6 \times 0.3 \times Fuel_{SOFC}) \tag{5.1}$$

Table 5.1 shows the fuel consumption on a daily basis for five aircrafts (jet fuel and ammonia).

Table 5.1: Fuel consumption calculations for jet fuel and ammonia based aircraft SOFCPU systems on per day basis

	Jet fuel	Ammonia	Units
SOFC fuel consumption	0.31	9.04	kmol/hr
Fuel consumed during flight	3.08	90.37	kmol/day
Fuel consumed during passenger boarding/ unboarding	0.55	16.26	kmol/day
Total fuel consumed	3.63	106.64	kmol/day
Total fuel for 5 aircrafts	18.18	533.20	kmol/day

While modelling the plant components, assumptions are made to design reactors and heat exchangers. The common assumptions applicable for all models include the following:

- All subsystems are in steady-state
- Air composition is on molar basis 21% oxygen and 79% nitrogen for all models.
- Environmental conditions are assumed for all plants to be 25^0C (298.15 K) and 1.013 bar (1 atm) .
- Heat and pressure losses occurring within the pipeline system are neglected
- Compressors are assumed isentropic with an efficiency of 80% and a mechanical efficiency of 90%. Pumps are assumed with efficiency of 80% and driver efficiency of 80% as well.
- Isentropic efficiency of gas turbine is assumed as 90% same as mechanical efficiency
- Heat exchangers are assumed to be counter current and adiabatic
- Generally, a pressure drop of 1.5% of the inlet pressure is assumed for heat exchangers, heaters, separators and other reactor blocks like Gibbs or Stoichiometric reactor.
- The gasifier operates in isothermal conditions

The values of mole flows of syngas or other streams shown in following sections are those obtained from integrated jet fuel or integrated ammonia plants where both SOEC and gasifier are connected to the fuel synthesis units to produce fuel (case-3).

5.2 Modelling of stationary plant units

This sections deals with modelling of different units for stationary fuel production plant. The design and model of gasification and gas cleaning unit is same for both jet fuel and ammonia for all cases. Only the input and output quantities will differ based on the amount of syngas required from gasification unit. These inlet and outlet quantities are generated as results after the model is run and will be discussed in section 5.3.

Input conditions and modelling parameters for SOEC are discussed for both syngas and hydrogen production. Modelling parameters for SOEC unit remain same for case-2 & case-3. Outputs from SOEC will differ for jet fuel and ammonia production and will be tabulated as results in section 5.3.

Jet fuel synthesis based on Fischer Tropsch and ammonia synthesis based on Haber Bosch process are modelled. Input conditions and parameters such as operating temperatures and pressures of reactors will remain same for all three cases. Outputs and calculated values for these models will be discussed and compared in section 5.3.

5.2.1 Gasifier and gas cleaning unit

The gasifier is based on fast internal circulating fluidized bed as explained in chapter-3. Birch round wood is considered as biomass input for the gasifier with a composition depicted in table 5.2 .

Table 5.2: Biomass composition used for simulation [10]

Biomass	wt%
C	48.7
H	6.4
O	44.5
N	0.08
H20	11.1

Biomass enters gasifier GF-GSF (R-Gibbs block) to break down biomass into H_2, CO, CO_2, water and other hydrocarbons with unreacted carbon, hydrogen and oxygen. The outlet composition is defined by carbon distribution for outlet species as obtained through experiments done with gasifier using olivine catalyst [41].

Gasifier model is shown in figure 5.4. The outlet stream from GF-GSF is sent to the GF-CSEP (Separator block) to separate raw syngas from char and ashes. The unreacted C, H_2 and O_2 are remitted to combustor GF-COMB (R-Stoic block). Steam is added to the gasifier block after heating water through number of heat exchangers using heat of flue gas from combustor and raw syngas from GF-CSEP block. The amount of steam supplied to the gasifier is calculated with a steam to carbon ratio S/C = 0.63 [41]. Additional fuel and extra air is added to the combustor to produce enough heat for Gasifier and GF-CSEP blocks.

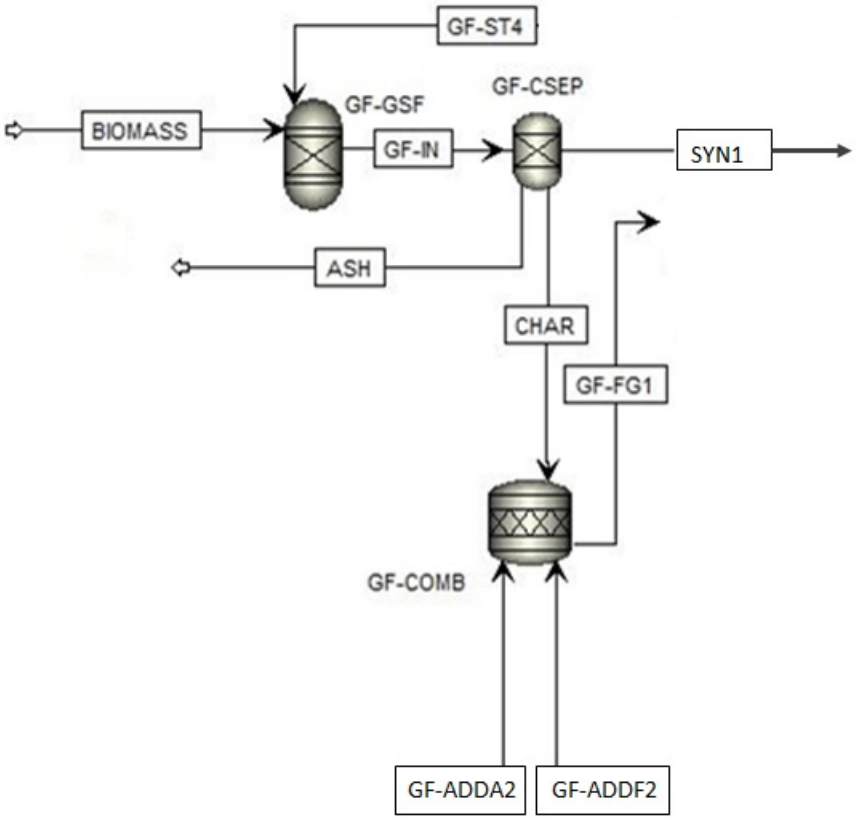

Figure 5.4: Gasifier and combustor with biomass, fuel and air inlet and syngas outlet

It is required to achieve a ratio of 1.2 between oxygen entering and leaving the combustor. This calculation is done using Calculator block in ASPEN PLUS and amount of air (GF-ADDA1) to be added is calculated. Before entering OLGA process for tar removal, 30.5% of the total syngas is recirculated to the combustor. The split is performed after removing solid particulates in hot gas filter. Hot gas filter is designed as a separator block (GC-HGF) which produces purge and particle free syngas at 350^0C. This purge gas mainly composed of hydrogen, methane, ammonia and inerts is also added to combustor block. Basic input parameters for gasifier unit are available in table 5.3.

Table 5.3: Basic input parameters for gasifier and combustor reactors

	Jet Fuel	Ammonia	Units
Gasifier			
Temperature	850	850	C
Pressure	1.3	1.3	bar
Combustor			
Temperature	920	920	C
Pressure	1.3	1.3	bar

The cooled syngas sent to OLGA unit should have a temperature above the dew point

temperature (277°C) of tars to prevent condensation on heat exchanger surfaces [29]. Product gas enters the OLGA process at a temperature of 280°C and leaves the process cleaned by tars at a temperature of around 80°C. OLGA process uses biodiesel as scrubbing liquid [6]. Figure A.1 highlights the OLGA process in gas cleaning unit and can be found in appendix.

The scrubbing liquid leaves absorber block OL-ABS modelled as separator block at 217°C. It is then cooled to 80°C and mixed with nitrogen to be sent to a filter for cleaning dust and particles. The clean scrubbing liquid obtained from the filter is heated again and stripped by hot air in desorber block OL-DABS (separator block). The air coming out of desorber block is mixed with ambient air (GF-ADDA1) and sent to gasifier combustor. Scrubbing oil received from desorber block is recirculated by mixing with biodiesel input stream. Since thermodynamic analysis is considered, modeling is done to reproduce the similar pressure and temperature profile of the original process, with proportional mass flows [6, 10].

Since, gasification process modelling is assumed free of sulphur and chlorine components, desulphurizer and HCl removal units are not simulated. Rather, temperature increase and pressure drop is considered instead of modelling any reactors for desulphurizer and dechlorination. The cleaned syngas is then sent to gas processing unit for further processing.

5.2.2 SOEC unit

The solid oxide fuel cell is reversibly used as electrolysis cell for stationary fuel production plant at the airport. SOEC for jet fuel and ammonia are modelled in different ways. For jet fuel, co-electrolysis is performed, which uses both steam and carbon dioxide as input to produce syngas. For ammonia, steam electrolysis is performed and only steam is input in the cell. Input temperature, pressure and compositions for both the processes are different and are tabulated in table 5.4.

Table 5.4: Input conditions for water air and carbon dioxide for SOEC

	Recirculated Hydrogen	Water inlet	Recirculated water	Carbon dioxide inlet	Recirculated CO2	Air	Units
Jet fuel SOEC							
Temperature	800	350	800	25	800	25	C
Pressure	20	20.6138	20	150	20	1.013	bar
Ammonia SOEC							
Temperature	800	25	800	--	--	25	C
Pressure	1.013	1.013	1.013	--	--	1.013	bar

- Fuel utilization factor, current density and cell resistance is equal for both.
- Operating temperature is same for both at 800°C but operating pressure varies.
- Active cell area, number of cells and current for SOEC are same corresponding to the jet fuel based or ammonia based SOFC.
- For both the electrolysis cells, reversible voltage is calculated based on the output concentration of oxygen molecules at cathode and anode. Equation 2.32 is used.

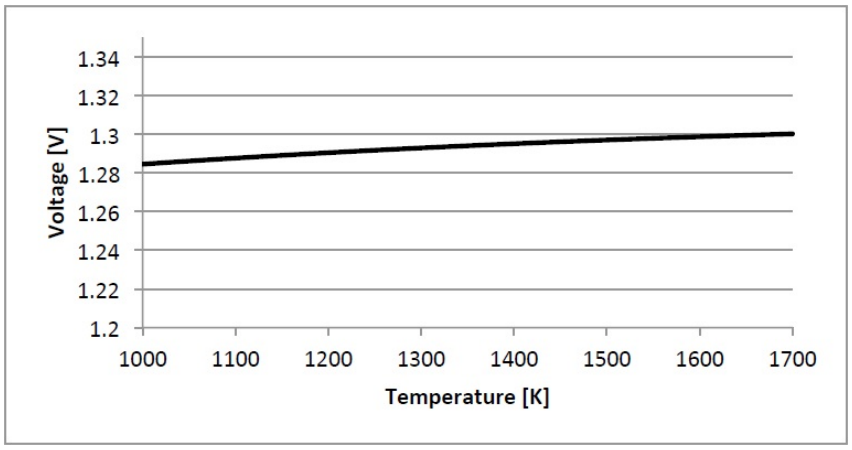

Figure 5.5: Thermoneutral voltage from 1000K to 1500 K [5]

- For both the electrolysis processes, SOEC block (R-Stoic) is made adiabatic by heat integration between anode and cathode.
- Air is added to both the electrolysis cell to maintain the temperature of cells at 800°C. This air can be at a temperature higher or lower than operating temperature of the SOEC based on thermal behaviour of the SOEC.
  - Electrolysis process can be endothermic, thermoneutral or exothermic. If it is endothermic, extra thermal energy is required to maintain the temperature of the system as electric energy is used for electrolysis only. In case of thermoneutral process, electric energy performs both the electrolysis process and heats the system. Electrolysis is exothermic when there is excess of energy available even after providing electrical and thermal energy to the cell. In case of endothermic electrolysis, air is provided at a higher temperature to heat up the system and in case of exothermic operation, air is provided at lower temperature than SOEC to cool down the system. Figure 5.5 shows the thermoneutral voltage between 1000 K and 1500K. It can be assumed that thermoneutral voltage at 800°C (1073K) is about 1.29V.

5.2.2.1 Co-electrolysis (jet fuel)

For co-electrolysis, water reduction reaction (equation 5.2) and CO_2 reduction reaction (equation 5.3) occur at the cathode side. The oxide ions formed by these reactions migrate through the electrolyte to the anode surface, and are reduced into oxygen (O_2) according to the reaction 5.4.

$$2H_2O + 4e^- \rightarrow 2H_2 + 2O^{2-} \tag{5.2}$$

$$2CO_2 + 4e^- \rightarrow 2CO + 2O^{2-} \tag{5.3}$$

$$2O^{2-} \rightarrow O_2 + 4e^- \tag{5.4}$$

In addition to the electrochemical reaction, reverse water gas shift (RWGS) equation 5.5 also takes place to convert CO_2 to CO. Electrolyzing at high-temperature is more efficient as it can save 30% and 20% of the electricity needed to reduce CO_2 and water respectively as compared to low temperature electrolysis [42]. The syngas produced can be converted into synthetic fuel via Fisher-Tropsch process.

$$CO_2 + H_2 \leftrightarrow CO + H_2O \tag{5.5}$$

The electrolyzer works at a high temperature (1073 K) to avoid methane formation, with an $H_2O/CO_2/H_2$ inlet molar ratio equal to 45/45/10 in order to minimize the internal resistance of cells [42]. Input conditions for all the gases is given in table 5.4. To ensure hydrogen fraction of 10% in the SOEC input stream, syngas obtained from electrolysis cell is split and recirculated to the inlet. A design specification block is used to restrict the split such that the ratio of hydrogen is maintained. Amount of water and CO_2 are determined by using calculator block such that their ratio is 1:1. All these gases are expanded to atmospheric pressure and heated to 750°C before entering the electrolysis cell. The complete ASPEN PLUS model for co-electrolysis can be seen in appendix, figure A.2. Air at atmospheric pressure and heated to 900°C is added to SOEC. Since SOEC is modelled within endothermic region, air flow at 100°C higher than that of SOEC is used to avoid excessive temperature drop during its operation. $CO_2$and air are heated in heat exchangers by cooling the syngas obtained from reverse water gas shift reactor of gas processing unit (to be explained later) as seen in figure A.2.

Since ASPEN PLUS does not offer a pre-built electrolyzer, it will be designed as a combination of reactors available in ASPEN PLUS. Co-electrolysis is assumed to pass through 3 reactors each of which signifies a function performed by electrolyzer unit. The electrolysis cell is shown in figure 5.6.

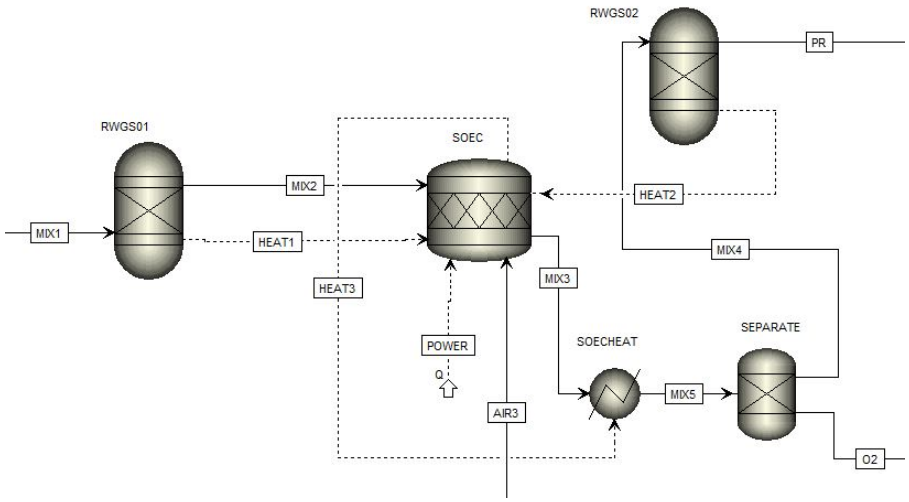

Figure 5.6: SOEC unit modelled with different reactors for Co-electrolysis

The first one simulated as Gibbs reactor is RWGS01, where reaction 5.5 takes place during the preheating of inlet gases. The second step is the electrochemical reduction of CO_2 and H_2O (equations 5.2 and 5.3) at 800°C in SOEC block. This step is modelled as R-Stoic reactor with pre-determined conversion rates of 0.75 for both CO_2 and H_2O, so that the total fuel utilization is also 0.75. The flow from SOEC is split in a separator block (SEPARATE) which acts as anode by letting out oxygen. Syngas stream flows to another R-Gibbs reactor (RWGS02) which acts as eletrolyzer exit point. Inlet parameters for SOEC are as shown in table 5.5

Table 5.5: Input parameters for SOEC design and dimensioning (co-electrolysis)

Variable	Value	Unit
I	572113	A
J	9212	A/sqm
ASR	2.06E-05	ohm/sqm
SOEC temperature	800	C
SOEC pressure	20	bar
UF	0.75	
N_{cell} /module	327	
A_{cell}	0.0474	sqm
N_{module}	4	

5.2.2.2 Steam electrolysis (ammonia)

For steam electrolysis, a mix of 90% steam and 10% hydrogen is required to prevent oxidation of Ni based electrode [5]. Hydrogen is obtained from product stream coming out of SOEC which is partially recirculated to the inlet. The mix of water and hydrogen is heated by using the heat from anode outlet stream (oxygen) before it enters the SOEC. For steam electrolysis reactions 5.2 and 5.4 are the reactions taking place. Figure A.3, available in appendix, shows the basic SOEC unit layout in electrolysis mode. Air enters the system at ambient temperature and is also preheated in the heat exchanger by hot air coming from the cell stack. A design specification block is used to maintain the temperature of the outlet stream from SOEC (stoichiometric block) at 800°C by adjusting the temperature of inlet air. In this case, since the voltage is in endothermic region, the air is made to enter at higher temperature than SOEC. Steam electrolysis is performed at 1 atm and temperature of 800°C. The inlet conditions for SOEC unit are mentioned in table 5.4.

SOEC consists of 2 reactors, R-Stoic which is used to model SOEC reactions and R-Gibbs signifies electrolyzer outlet boundary. The maximum steam conversion is set to 75%. After electrolyis reaction in SOEC, anode and cathode flows are separated in the separator. The mix of hydrogen and steam goes to the R-Gibbs (cathode) while oxygen and air goes out through the anode (Separator block). Hydrogen-steam mixture is then sent to flash separator where hydrogen is separated from steam by condensation. The hydrogen obtained is compressed and used further for ammonia production. Inlet parameters and size of SOEC is as shown in table 5.6.

Table 5.6: Input parameters for SOEC design and dimensioning (steam-electrolysis)

Variable	Value	Unit
I	605535	A
J	9212	A/sqm
ASR	2.06E-05	ohm/sqm
SOEC temperature	800	C
SOEC pressure	1.013	bar
UF	0.75	
Ncell /module	327	
Acell	0.0403	sqm
Nmodule	5	

5.2.3 Jet fuel production

5.2.3.1 Gas processing unit

This unit receives syngas from SOEC as well as gasification unit for the three cases as shown in figure 5.1. The syngas from gasification unit is reformed in Autothermal reformer (GF-ATR) modelled as R-Gibbs unit. Steam and oxygen are added for autothermal reforming of methane to syngas. Steam to carbon (S/C) ratio is set as 2. This is done to achieve lower H_2/CO ratio, closer to 1 [43]. This is favorable for syngas entering mixed alcohol synthesis reactor of jet fuel synthesis unit as explained previously in chapter-2. ATR unit is made to function with a temperature of 800°C. Similarly, the syngas obtained from electrolyzer cell is sent to autothermal reforming unit (ATR1) modelled as R-Gibbs reactor with S/C ratio of 2. Steam heated to 500°C and oxygen from electrolysis cell at 800°C are used as inputs for ATR1. Since, the pressure of syngas entering Rectisol unit is 35 bar, the pressure for ATR1 is maintained at 20 bar, same as the SOEC operative pressure. Gas processing unit model for integrated jet fuel production plant can be found in appendix, figure A.4.

Combined syngas is sent to reverse water gas shift reactor (RWGS) to produce CO such that ratio of H_2/CO is maintained at 1-1.2 before it enters the mixed alcohol reactor. RWGS is carried out through R-stoic reactor and conversion rate of CO_2 is given as 51.1% [44]. The reaction is endothermic, therefore thermodynamic equilibrium favors high conversion of CO_2 and H_2 at high temperatures above 850°C at atmospheric pressure [44]. The hot syngas is cooled down through several heat exchangers and stripped of water in a dehumidifier (Separator block). Dry syngas is then sent to Rectisol unit for CO_2 removal, the ASPEN PLUS modeling of which has been also described in previous studies [31]. In this model, Rectisol unit is shown as a separator block. All the processes which are part of Rectisol unit are not modelled in ASPEN PLUS as reactor blocks to keep the model simple. Table 5.7 shows conditions and compositions of streams entering and leaving the Rectisol unit while separating almost 98.9% CO_2.

Table 5.7: Inlet and outlet compositions and conditions for Rectisol process

	Syngas entering Rectisol (mole %)	Clean syngas leaving Rectisol (mole %)	Carbon dioxide stream from Rectisol (mole %)
CH_4	2.42	2.95	0.00
CO	39.51	48.14	0.00
CO_2	18.08	0.24	99.78
H_2	39.99	48.67	0.22
Temperature C	30	-45	-35
Pressure bar	35	60	6

During exergy analysis, electric power required by Rectisol unit will be considered by multiplying the CO_2 captured (kg/s) with the specific electric equivalent consumption from the processes shown in table 5.8. The CO_2 from Rectisol can be stored and reused as input for SOEC.

Table 5.8: Processes and related power consumption to be considered for Rectisol

Absorber raw syngas compressor (electric)	12.3	MW
Process compressors/expanders electric power	8	MW
Electric equivalent of Reboiler duty	5	MW
Refrigeration electric power	21.1	MW
Cooling water consumption (electric)	1.5	MW
Overall equivalent electricity consumption	47.9	MW
Specific Electric Equivalent Consumption	736.92	KJ/kgCO_2

5.2.3.2 Jet fuel synthesis unit

Finally, the syngas is cleaned and in the correct ratio to be sent to mixed alcohol synthesis (MAS) reactor. This syngas from Rectisol is heated to 300°C through heat exchangers using the heat from outlet stream of MAS. Mixed alcohol synthesis involves the reaction between CO and H_2 under high pressures (55-150 bar) and moderate temperatures (180-350°C) to produce a mixture of C_1 to C_6 mono-alcohols [11]. In addition, some mixed alcohol synthesis catalysts also catalyze the WGS reaction, resulting in the conversion of a significant portion of the CO to CO_2. Figure 5.7 depicts the entire Alcohol formation and separation process.

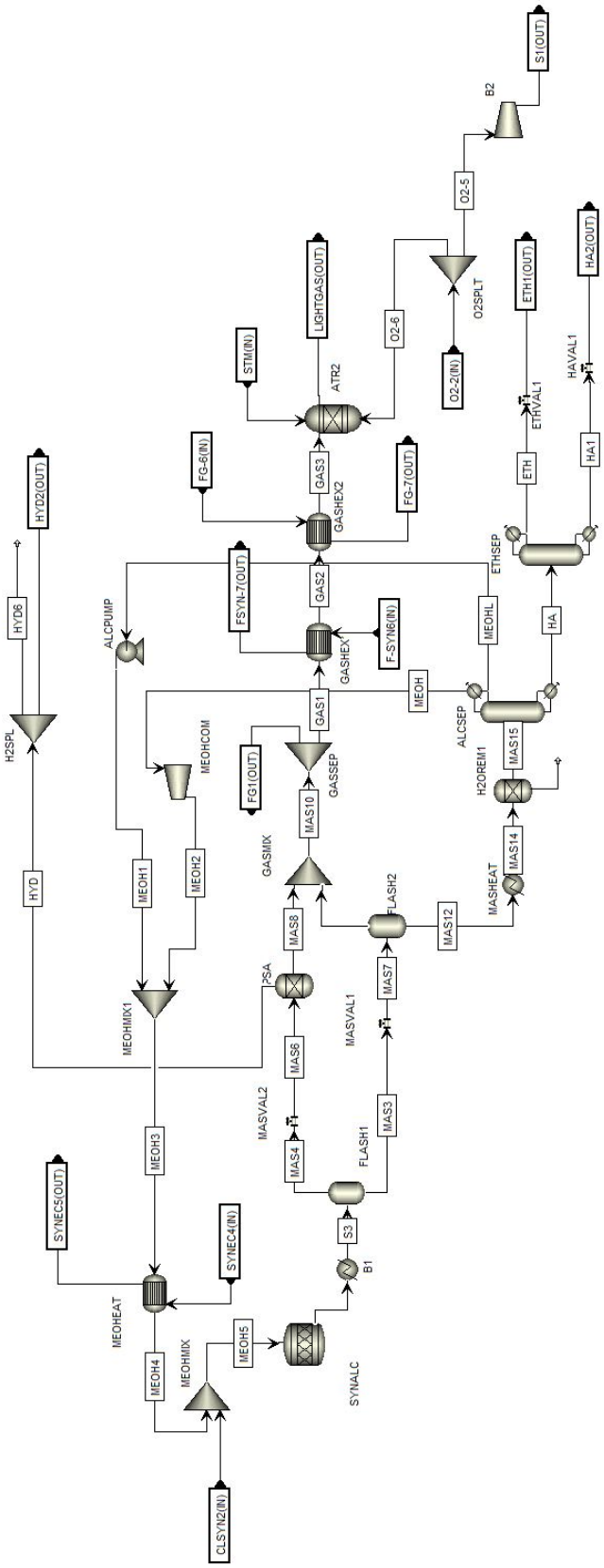

Figure 5.7: Mixed alcohol synthesis and methanol separation process modelled using ASPEN PLUS

Table 5.9: Process parameters for mixed alcohol synthesis, methanol & ethanol separation and Guerbet reaction [8]

Mixed Alcohol Synthesis		
Temperature	300	C
Pressure	60	bar
Catalyst	$K/Co/MoS_2$	
Methanol separation		
Reflux ratio	10	
Distillate to feed ratio	1.12	
No. of stages	85	
Feed stream stage	40	
Distillate vapor fraction	0.1	
Condenser type	Partial vapor liquid	
Reboiler type	Kettle	
Pressure	20	bar
Ethanol separation		
Reflux ratio	2	
Distillate to feed ratio	1.09	
No. of stages	20	
Feed stream stage	10	
Distillate vapor fraction	0	
Condenser type	Total	
Reboiler type	Kettle	
Pressure	20	bar
Guerbet reactor		
Temperature	150	C
Pressure	1	bar
Catalyst	$RuCl_2$	
Ethanol conversion	27.8	%
Butanol conversion	2.56	%

MAS is modelled as R-stoic reactor (SYNALC) with the reactions and conversion rates shown in table 5.10. This study assumes a modified FT catalyst ($K/Co/MoS_2$ catalyst) because of its relatively high alcohol selectivity and its main product mixture of linear alcohols [8, 11]. The inlet and design conditions for MAS are summarised in table 5.9.

Mixture of alcohols is cooled down and sent to a flash tank at 55°C. Heavier alcohols and water are separated which are further cooled down to 35°C and sent to another flash tank. A part of the light gases from FLASH1 and FLASH2 are mixed and 98% of it is recycled and sent to another autothermal reformer unit (ATR2) after heating the gases to 800°C. The reformate product is then recompressed and mixed with the original inlet syngas. 2% of light gases is purged from the system to limit the build-up of methane in the syngas entering the alcohol synthesis reactor. The purge gas is sent to the BURNER (R-Stoic) as fuel for the combustion. The liquid product from flash tanks is dewatered using a molecular sieve column (Separator block) and further purified in a series of distillation units to recover methanol, ethanol, propanol and butanol.

Table 5.10: Mixed alcohol synthesis reactions and conversion rates [11]

Reaction No.		Mol% CO Conversion (per pass):
1	$CO + H_2O \rightarrow CO_2 + H_2$	13.0%
2	$CO + 3\ H_2 \rightarrow CH_4 + H_2O$	4.5%
3	$2\ CO + 4\ H_2 \rightarrow C_2H_6 + H_2O$	0.5%
4	$CO + \ H_2 \rightarrow$ Methanol	4.1%
5	$2\ CO + 4\ H_2 \rightarrow$ Ethanol $+ H_2O$	11.4%
6	$3\ CO + 6\ H_2 \rightarrow$ Propanol $+ 2\ H_2O$	3.0%
7	$4\ CO + 8\ H_2 \rightarrow$ n-Butanol $+ 3\ H_2O$	1.0%
8	$5\ CO + 10\ H_2 \rightarrow$ n-Pentanol $+ 4H_2O$	0.5%
	Total CO Conversion	38%
Reaction No.	Reaction	Mole % Recycled Methanol Conversion (per pass):
9	Methanol $+ \ CO + 2\ H_2 \rightarrow$ ethanol $+ H_2O$	58%
10	Methanol $+ 2\ CO + 4H_2 \rightarrow$ Propanol $+ 2\ H_2O$	7%
11	Methanol $+ 3\ CO + 6\ H_2 \rightarrow$ n-Butanol $+ 3\ H_2O$	4.5%
12	Methanol $+ 4\ CO + 8\ H_2 \rightarrow$ n-Pentanol $+ 4H_2O$	2%
	Total Recycled Methanol Conversion	71.5%

Another part of the light gases is diverted to the Pressure Swing Adsorption process (PSA) for the production of pure H_2 which is required for hydrogenation of paraffins [8]. Methanol distillation column is modelled with RadFrac block where 99% of the methanol is recovered overhead at purity greater than 99%. The bottoms product from the methanol column (ALCSEP) is sent to a second distillation column (ETHSEP) where 99.95% of incoming ethanol is recovered in the overhead stream and 99% of the propanol is recovered in the bottom stream along with the higher alcohols. Design parameters for both methanol and ethanol distillation columns are presented in table 5.9 . MeOH from ALCSEP is compressed and recirculated to MAS whereas ethanol from ETHSEP is sent to the Guerbet reactor for condensation.

Ethanol undergoes condensation in Guerbet reactor which is modelled as R-Stoic reactor (GBREACT). The key parameters for Guerbet reaction and ethanol conversion rate to n-butanol are mentioned in table 5.9. $RuCl_2$ is used as catalyst for Guerbet reaction which shows a conversion rate of 30% for ethanol [8]. Product stream from Guerbet reactor is sent to water decanter and compressed before separating higher alcohols (propanol and n-butanol) from ethanol in a distillation column. RadFrac column is used to carry out the distillation with design parameters shown in table 5.11. The higher alcohols separation in this stage is necessary in order to avoid accumulation at the next stage. Ethanol rich solution is recycled to the ethanol inlet and higher alcohols are mixed with product stream from ETHSEP block.

Table 5.11: Process conditions for butanol separation, alcohol dehydration, oligomerisation and hydrogenation [8]

Butanol separation		
Reflux ratio	1.5	
Distillate to feed ratio	1.10	
No. of stages	12	
Feed stream stage	6	
Distillate vapor fraction	0	
Condenser type	Total	
Reboiler type	Kettle	
Pressure	2.5	bar
Alcohol dehydration		
Temperature	250	C
Pressure	1	bar
Catalyst	γ-alumina on Rh/alumina foam	
Alcohol conversion	80	%
Alkene selectivity	100	%
Oligomerisation Reactor		
Temperature	25	C
Pressure	1	bar
Catalyst	Cp_2ZrCl_2/MAO	
Butene conversion	100	%
C8 selectivity	27	%
C12 selectivity	26	%
C16 selectivity	47	%
Hydrogenation reactor		
Temperature	250	C
Pressure	30	bar
Catalyst	Pd	
Alkene conversion	100	%
Hydrogen inlet	1.629	kmol/hr

This mixed stream is heated before alcohol dehydration process simulated with R-Stoic block (ALCDEHYD). Design parameters for ALCDEHYD are also shown in table 5.11. The 1-butanol conversion was found to be 80% by adding a coating of γ-alumina onto the Rh/alumina foam and due to catalytic oxidative dehydration of 1-butanol, 88–99% of the olefins produced were butene isomers [34]. After water removal and separation of butene from other hydrocarbons in distillation column, increment of carbon chain is performed in the next process step where oligomer synthesis takes place. Oligomer synthesis of butene on Cp_2ZrCl_2/MAO catalyst based on patent by [36] results in 100% conversion to higher alkenes (C_8-C_{16}). However, selectivity for different alkenes is different and highest selectivity is observed for C_{12} oligomers [36]. Important parameters for R-stoic reactor (OLIGOMER) are described in table 5.11. Finally, via hydrogenation process, branched paraffins are produced, which are essential for the jet fuel and gasoline production. The hydrogen for the hydrogenation process is recovered from the unconverted syngas by means of the Pressure Adsorption Process (PSA). The hydrogenation reaction is assumed to

take place in 30 bar and 250°C [8]. Table 5.11 summarizes the design characteristics for hydrogenation block and table 5.12 represents parameters for final distillation column to produce jet fuel and gasoline.

Table 5.12: Input parameters for final distillation column for producing jet fuel and gasoline

Paraffin distillation		
Reflux ratio	0.1	
Distillate to feed ratio	1.16	
Condenser temperature	100.30	C
Reboiler temperature	240.98	C
No. of stages	10	
Feed stream stage	5	
Distillate vapor fraction	0.1	
Condenser type	Partial vapor liquid	
Reboiler type	Kettle	
Pressure	1	bar
$C_{12}H_{26}$ purity	91.2	%
$C_{16}H_{34}$ purity	99.8	%

5.2.4 Ammonia synthesis

5.2.4.1 Gas processing

Ammonia synthesis model is divided into gas processing, ammonia synthesis and recovery units. Gas processing is done to increase hydrogen content in syngas and remove oxygen compounds as they can poison ammonia synthesis reactor catalysts. Gas processing also ensures addition of appropriate amount of nitrogen in the system for ammonia production. Gas processing begins with treating the syngas in an autothermal reactor to convert methane into hydrogen and CO. Steam and air flow in this reactor, modelled as equilibrium reactor (R-Gibbs), is calculated using calculator block. Air addition is specified with design specification block to ensure addition of nitrogen in required amount. S/C ratio for ATR is set at 2 and it is made adiabatic by adjusting the inlet temperatures of steam and air as 621°C and 600°C respectively.

The temperature of ATR outlet is fixed to be 800°C and pressure as 1.3 bar. Figure 5.8 shows part of gas processing section including ATR and WGS reactors.

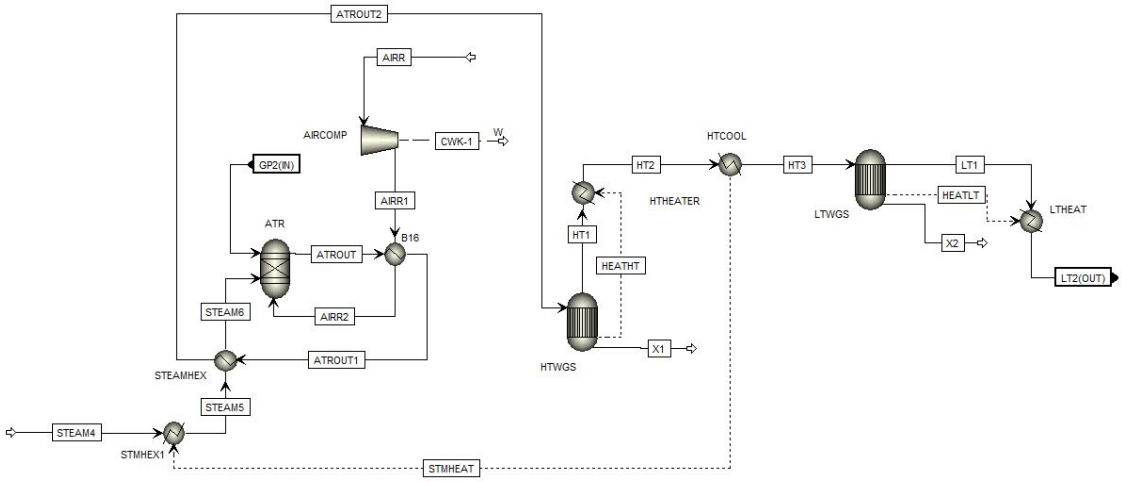

Figure 5.8: Syngas processing steps to increase hydrogen content of the gas

The product stream from ATR undergoes water gas shift through a series of high temperature shift (HTS) followed by a low temperature shift catalyst based reactor (LTS), with intercooling stage to increase the overall conversion. These reactors are designed adiabtic with R-Equil reactors. HTS is performed at 350°C followed by intercooling stage to carry out LTS at 200°C. The heat from intercooler is used to produce steam for ATR. Figure 5.9 shows the increase in hydrogen content of syngas stream through ATR and WGS units.

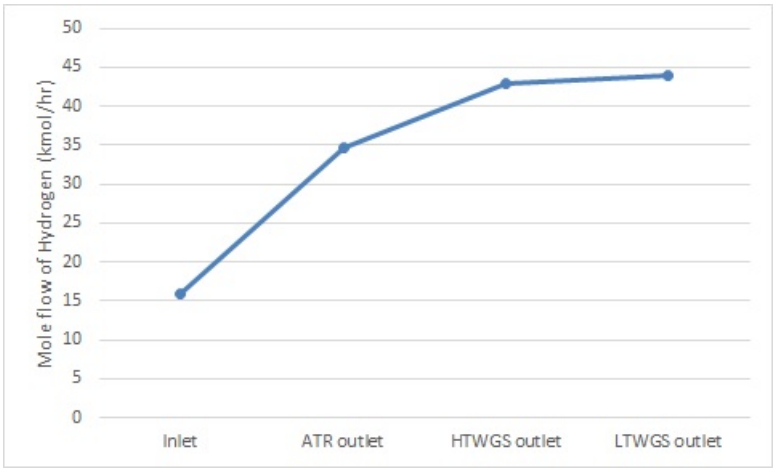

Figure 5.9: Increase in hydrogen mole flow from inlet of autothermal reformer to LTWGS outlet

After enhancing hydrogen content of the syngas, it is sent for cooling to separate water and further treated in Rectisol unit to remove CO_2. Cooling, compression and carbon capture unit are shown in figure A.5 in appendix. Syngas is cooled and water condensation takes place in a flash tank at a temperature of 29°C. After water removal, the dry gas is compressed with a two stage intercooled compression. Outlet temperature from the compression in 108 °C. CO_2 is then removed in Rectisol unit which is modelled as a

separator block to keep the model simple with outlet and inlet conditions of the Rectisol process taken from literature directly [31]. The only energy input required by the process is electricity to run the pumps that pressurize the physical solvent and compress and recirculate the gases which is calculated and taken in account in the energy balance of the plant. CO_2 stream purity achieved is 98% from rectisol unit. After carbon capture, there are still traces of CO and CO_2 in the syngas which are converted to methane through methanator. Methanator is designed as R-Stoic block and operates at pressure of 29 bar such that it attains the temperature which makes the process adiabatic. For this model, the temperature comes to be 258°C. Methanation is a process of converting CO and CO_2 to methane by hydrogen present in the stream. The syngas from methanator contains some water which is removed in a separator block before it enters into the ammonia synthesis unit.

5.2.4.2 Ammonia synthesis and recovery unit

Figure 5.10 shows the ASPEN PLUS model for ammonia synthesis section.

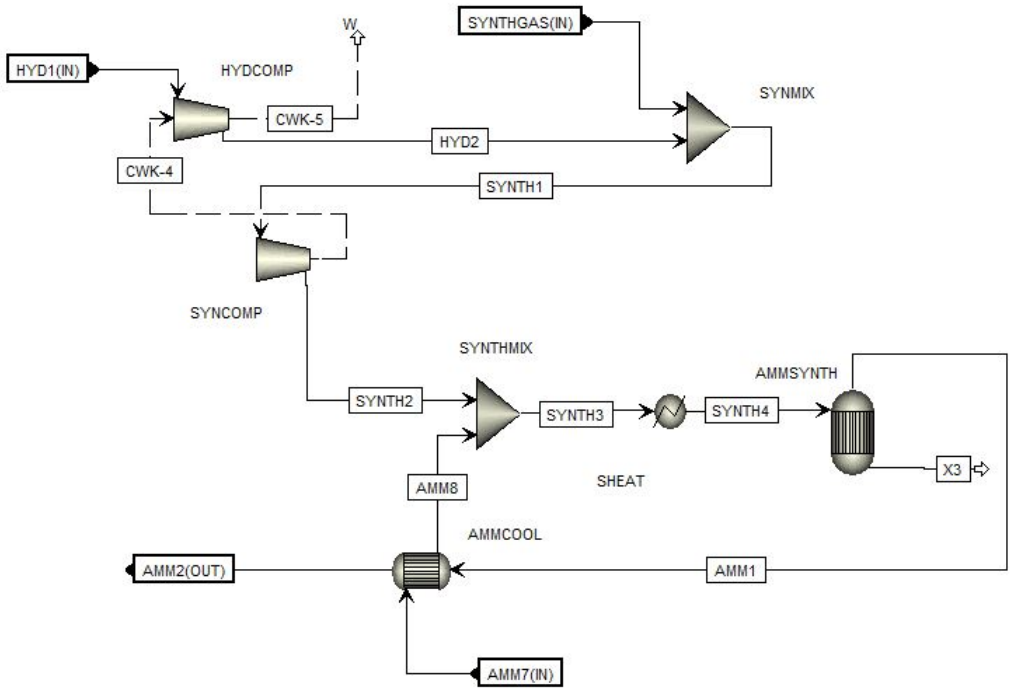

Figure 5.10: Ammonia synthesis unit

Ammonia formation takes place at high temperature and pressure, therefore syngas from gas processing unit is compressed to 200 bar and heated to 400°C before it enters ammonia synthesis reactor. Practically, ammonia synthesis never reaches equilibrium, hence the reactor is modelled with a quasi-equilibrium reactor (REquil with reaction and temperature approach specified) [6]. With a temperature approach of 75 K, the system operates at a

temperature lower than the equilibrium temperature, thus reducing the conversion rate to values in accordance with industrial operations. With a temperature of 475 °C and a pressure of 200 bar, conversion is in the range 10-20 %. Ammonia with unreacted hydrogen and nitogen is cooled by the stream from flash tank which is recirculated to ammonia synthesis inlet. Figure A.6 available in appendix shows ASPEN PLUS model for ammonia recovery section. Ammonia is further cooled by refrigeration to achieve a temperature of -25°C and sent to a flash tank (FLASHSEP) where ammonia condenses. The uncondensed gases are compressed and recirculated to the ammonia synthesis inlet. However, a 10% purge stream is taken out before recirculating the stream to avoid accumulation of gases. Although, 10% is very high for purge stream, due to accumulation of methane, less purge resulted into non-convergence. This can be solved by using hydrogen membrane to recover hydrogen which will be further discussed in chapter-7 (Future recommendations). The high-pressure liquid ammonia is sent to the product recovery section. The liquid ammonia is sent to flash tank at lower pressure (DEGAS), where more ammonia condenses. This liquid ammonia is further flashed at ambient pressure in another Flash tank (B22). The gaseous stream from both flash tanks (DEGAS and B22) are mixed and washed with water in a column to strip ammonia entrained in the gas. The aqueous solution of NH_3 is further sent to a stripper column to separate ammonia. This ammonia is sent to the product tank, where it condenses. Purge gases from the loop and the recovery are mainly composed of hydrogen and methane are sent to the burner for combustion.

5.2.5 Integration of SOEC, gasifier and fuel production units

After modelling all the units, they are integrated to form six different integrated plant models, two models (jet fuel & ammonia) each for three cases mentioned earlier in this chapter. The results obtained after modelling and simulation of the models described in this chapter are discussed in section 5.3.

For case-1, gasifier is designed for full load capacity. The amount of biomass added should be able to produce all the fuel required for 5 aircrafts per day. Assuming that the gasifier works for 24 hours, equation 5.6 gives the amount of fuel in kmol/hr required to be produced by gasifier.

$$Fuel_{hr,gasifier} = \frac{Fuel_{day}}{24} \tag{5.6}$$

In case-2, SOEC operated fuel production plant (without gasifier unit), fuel produced on a daily basis is calculated by equation 5.7. Bi-directional SOC units from 5 aircraft APUs are operated as electrolysis cells for only 8 hours per day, an assumption made previously. However, while modelling only one SOEC unit is considered as each aircraft is supposed to produce its own fuel.

$$Fuel_{day,SOEC} = Fuel_{hr,SOEC} \times 8 \tag{5.7}$$

For case-3, gasifier and SOEC are combined to produce fuel for 5 aircrafts per day. Since the fuel produced by SOEC on a daily basis is not enough to fuel five aircraft APUs, gasifier is integrated with it for case-3. Gasifier operates at full load for entire day with

one SOEC unit operating at full load for 8 hours as discussed previously in section 5.1 of this chapter. To calculate the hourly and daily fuel production capacity of integrated plant, equation 5.8 and 5.9 are used respectively.

$$Fuel_{hr,plant} = Fuel_{hr,gasifier} + Fuel_{hr,SOEC} \tag{5.8}$$

$$Fuel_{day,plant} = (24 \times Fuel_{hr,gasifier}) + (8 \times Fuel_{hr,SOEC}) \tag{5.9}$$

In case of jet fuel production, syngas from gasifier and SOEC combine to produce fuel for 5 aircrafts. For ammonia production, syngas from gasifier unit after gas processing is combined with hydrogen from SOEC unit to produce ammonia.

5.3 Results and discussions

Results for all the units developed are discussed here section by section. Inlet conditions and working parameters to be used for each reactor has been discussed in previous sections. However, the outlet compositions and calculated values for these models are provided in this section. All the results produced in this section are based on case-3 configuration of the model. (Refer case-3 from figure 5.1)

- Biomass gasification and gas cleaning unit results are based on full load capacity of gasifier (producing entire fuel for 5 aircraft APUs per day)
- SOEC unit results are based on full load capacity of one SOEC unit to produce either syngas or hydrogen (operating for 8 hours per day)
- Results for jet fuel gas processing and Fischer Tropsch process are considered by taking into account contribution of both gasifier and SOEC unit, as in case-3 configuration. Ammonia gas processing and ammonia synthesis results are also obtained in the same manner.

Exergy efficiency calculation and comparisons are shown in chapter-6 for all the cases.

5.3.1 Gasification unit

This unit comprises of gasifier and gas cleaning unit. Syngas produced by this unit is used to produce fuel in the stationary plant. Amount of biomass to be added is calculated using a design specification block, which pre-defines the amount of fuel (jet fuel/ammonia) to be produced. The amount of steam for gasifier and biodiesel, air and nitrogen for OLGA unit are calculated in a calculator block to maintain the ratio with amount of biomass added. These values for jet fuel and ammonia production are provided in table 5.13 .

Table 5.13: Calculated values for biomass and steam for gasifier and air, nitrogen and biodiesel input for OLGA unit for jet fuel and ammonia synthesis

	Jet Fuel	Ammonia	Units
Biomass flow	3485.02	1267.51	kg/hr
Steam flow	1402.27	510	kg/hr
Bio-diesel flow	21.30	7.75	kg/hr
Air flow	1504.66	547.25	kg/hr
Nitrogen flow	7055.86	2569	kg/hr

Syngas composition obtained from Gasification unit, with oulet pressure and temperature, is presented in table 5.14.

Table 5.14: Syngas composition obtained from gasification unit which comprises of gasifier and gas cleaning unit. Comparison made between jet fuel and ammonia plants.

Gasification unit outlet (kmol/hr)	**Jet Fuel**	**Ammonia**
C_2H_4	2.25	0.81
C_2H_6	1.01	0.37
CH_4	12.84	4.63
CO	32.77	11.83
CO_2	19.70	7.11
H_2	43.86	15.84
H_2O	54.44	19.66
H_3N	0.06	0.02
Total flow (kmol/hr)	166.93	60.28
Temperature C	836.467	447.15
Pressure bar	20	0.995

The syngas from gasifier unit is sent to gas processing unit before it enters fuel synthesis unit.

5.3.2 SOEC unit

Co-electrolysis, using CO_2 and H_2O as inputs, is adopted for syngas production in case of jet fuel plant. Steam electrolysis is adopted for ammonia production as it produces hydrogen as product, which can be sent to ammonia synthesis unit directly without gas processing. Compositions for hydrogen, steam, carbon dioxide and air for both co-electrolysis and steam electrolysis are different and are tabulated in table 5.15. Calculator and design specification blocks are used to calculate the amount of inlet mole flows of steam, hydrogen, CO_2 and the recirculated stream to maintain required ratios in inlet stream of SOEC as explained in section 5.2.

Table 5.15: Calculated molar compositions of inlet flows for co-electrolysis and steam electrolysis

Molar flow (kmol/hr)	Jet Fuel	Ammonia
Recirculated Hydrogen	3.83	1.91
Water inlet	12.34	15.01
Recirculated water	1.88	0.05
Carbon dioxide inlet	11.82	--
Recirculated CO2	2.40	--
Air	710.01	67.62

Co-electrolysis For obtaining the voltage and power required by SOEC, parameters like cell active area, number of cells, fuel utilization and current produced are kept same as that obtained from SOFC model as we use the same cell reversibly. A calculator block calculates the voltage and the power required by SOEC which is shown in table 5.16. Equation 2.32 is used to calculate Nernst potential for SOEC. Patial pressure of oxygen is calculated by multiplying its fraction at outlet of anode and cathode with SOEC operative pressure (20 bar).

Table 5.16: Voltage and power calculations for co-electrolysis

Variable	Value	Unit
V_{nst}	1.044	Volt
V	1.234	Volt
$P_{SOEC,req}$	705.66	KW
Total Voltage	403.59	Volt

Steam electrolysis The calculator block calculates the voltage and the power required by SOEC to perform electrolysis which is shown in table 5.17 .

Table 5.17: Voltage and power calculation for steam electrolysis

Variable	Value	Unit
V_{nst}	1.005	Volt
V	1.195	Volt
$P_{SOEC,req}$	723.36	KW
Total Voltage	390.11	Volt

Partial pressure of oxygen is calculated from its composition at outlet (anode and cathode) and operative pressure of SOEC. This is then used to calculate Nernst voltage. It can be observed from tables 5.16 and 5.17 that power required is higher for steam electrolysis than that for co-electrolysis. Although the voltage for steam electrolysis is lower than that for co-electrolysis, higher current causes higher power consumption for steam electrolysis.

5.3.3 Jet fuel synthesis

This section consists of results from gas processing and fuel synthesis unit as modelled in case-3. As discussed previously, gas processing unit comprises of ATR, RWGS and Rectisol units. Syngas from gasification unit is reformed in GF-ATR. Electrolyzer syngas is also reformed in ATR1 reactor. The syngas obtained from both the ATR units is mixed with recirculated stream from mixed alcohol synthesis section. The syngas hence obtained is sent to RWGS reactor. Molar flow of air and steam in ATR units is calculated by using calculator block. The final composition of syngas obtained before and after reforming is shown in table 5.18.

Table 5.18: Composition of syngas obtained before and after reforming. ATR1 represents reformer for syngas from SOEC unit and GF-ATR represents reformer for syngas from gasification unit

Component mole flow (kmol/hr)	ATR1 inlet	ATR1 outlet	GF-ATR inlet	GF-ATR outlet
CH_4	3.74	0.41	12.84	5.17
CO	10.80	4.16	32.77	27.53
CO_2	5.76	7.25	19.70	39.14
H_2	9.20	12.45	43.86	88.10
H_2O	4.52	20.07	54.44	115.87
Air flow	4.72		27.95	
Steam flow	21.02		82.69	

As the mixture of syngas from gas processing enters fuel synthesis unit, it undergoes a number of processes like mixed alcohol synthesis, alcohol dehydration, oligomerisation and dehydrogenation to form paraffins. The input conditions and conversion rates for all these reactors are provided in section 5.2. Table 5.19 gives the inlet and outlet composition in mole percent for the stream as it passes through different reactors to form various components.

Fuel synthesis unit also consists of various distillation columns for purifying products like methanol and ethanol etc. These products are then recirculated or sent for further processing. Similarly, the final step of jet fuel formation also incorporates distillation of higher paraffins. The parameters for purity of separation is given in section 5.2.

Final composition of jet fuel obtained is compared with literature in table 5.20.

Table 5.20: Comparison of jet fuel composition obtained in simulation, with literature

	Jet fuel (present study)	Jet fuel [9]
	Mole %	Mole %
C_8H_{18}	0.12	0.7
$C_{12}H_{26}$	45.53	41.5
$C_{16}H_{34}$	54.34	57.9

Table 5.19: Inlet and outlet composition (mole%) of product stream passing through different process steps in fuel synthesis unit

Components	Mixed alcohol synthesis		Guerbet reaction		Alcohol dehydration		Oligomerisation		Dehydrogenation	
Mole %	Inlet	Outlet	Inlet	Outlet	Inlet	Outlet	Inlet	Outlet	Inlet	Outlet
C_2H_4	--	--	--	--	--	1.21	--	--	--	--
C_2H_6	--	0.17	--	--	--	--	--	--	--	--
CH_4	2.89	6.95	--	--	--	--	--	--	--	--
CO	46.86	37.29	--	--	--	--	--	--	--	--
CO_2	0.50	9.04	--	--	--	--	--	--	--	--
H_2	47.36	32.00	--	--	--	--	--	--	--	--
H_2O	--	3.92	--	12.32	--	50	--	--	--	--
Methanol	2.39	3.67	3.68	3.64	--	--	--	0.01	0.01	0.01
Ethanol	--	5.64	90.93	66.30	2.42	--	--	--	--	--
Propanol	--	0.88	4.92	4.97	22.81	--	--	--	--	--
Butanol	--	0.31	0.46	12.76	71.13	--	--	--	--	--
Hexanol	--	0.13		0.01	3.64	--	--	--	--	--
Hexene	--	--	--	--	--	1.82	4.99	2.82	2.82	2.82
Butene	--	--	--	--	--	35.57	94.86	--	--	--
Propene	--	--	--	--	--	11.40	0.16	0.44	0.44	0.44
$C_{12}H_{24}$	--	--	--	--	--	--	--	28.92	28.92	--
$C_{16}H_{32}$	--	--	--	--	--	--	--	31.55	31.55	--
C_8H_{16}	--	--	--	--	--	--	--	36.25	36.25	--
C_8H_{18}	--	--	--	--	--	--	--	--	--	36.25
$C_{12}H_{26}$	--	--	--	--	--	--	--	--	--	28.92
$C_{16}H_{34}$	--	--	--	--	--	--	--	--	--	31.55

5.3.4 Ammonia synthesis

This section consists of results from gas processing and ammonia synthesis unit as modelled in case-3. The composition of syngas entering and leaving gas processing unit is shown in table 5.21. This inlet syngas is obtained from gasification unit. From the table it is clearly visible how gas processing unit removes all the oxygen species from syngas to obtain a product gas with only hydrogen and nitrogen as main components.

Table 5.21: Comparison of syngas entering and product gas leaving gas processing unit

Components (kmol/hr)	Syngas entering gas processing unit	Product gas leaving gas processing unit
C_2H_4	0.81	--
C_2H_6	0.37	--
CH_4	4.63	0.17
CO	11.83	--
CO_2	7.11	--
H_2	15.84	43.40
H_2O	19.66	--
N_2	--	18.05
H_3N	0.02	--

Product gas from gas processing unit is combined with hydrogen obtained from SOEC unit before it is sent to ammonia synthesis unit. In table 5.22 mole percent of inlet and outlet composition from ammonia synthesis reactor can be observed.

Table 5.22: Comparison of gas entering and leaving ammonia synthesis reactor on mole % basis

Components (mole%)	Inlet	Outlet
CH_4	0.62	0.70
H_2	74.19	64.38
H_2O	0.12	0.14
N_2	23.96	20.60
NH_3	1.10	14.18

The ammonia formed is then sent to recovery section. In this section ammonia is cooled, condensed and stored in ammonia tank after water removal. Some ammonia from this section with unreacted hydrogen and nitrogen is recirculated to the ammonia synthesis reactor. Purge gases are taken out as explained previously. Ammonia flow as obtained from ammonia synthesis and recovery unit is 27.05 kmol/hr with traces of water and methane.

5.3.5 Integrated fuel production

When SOEC and gasifier units are connected to fuel synthesis unit for fuel production, an integrated plant is formed. Calculations are done for three cases as defined previously. Comparison is made between jet fuel and ammonia production plants on the basis of fuel produced and amount of biomass required on a daily and hourly basis for all three cases. Table 5.23 shows the calculation for jet fuel and ammonia for all 3 cases.

Table 5.23: Fuel production and biomass consumption calculations for all 3 cases of fuel production plants (jet fuel & ammonia). Values are provided on both hourly and daily basis for all 3 cases

		CASE-1		CASE-2		CASE-3	
		Jet fuel	*Ammonia*	*Jet fuel*	*Ammonia*	*Jet fuel*	*Ammonia*
Hourly basis (kmol/hr)	*Fuel produced by SOEC units*	--	--	0.144	4.83	0.144	4.83
	Fuel produced by gasifier unit	0.833	22.216	--	--	0.833	22.216
	Biomass flow (kg)	3485.02	1267.51	--	--	3485.02	1267.51
	Total fuel produced	0.833	22.216	0.144	4.83	0.977	27.05
Daily basis (kmol/day)	*Fuel produced by SOEC units*	--	--	1.152	38.67	1.152	38.67
	Fuel produced by gasifier unit	20	533.20	--	--	20	533.20
	Biomass flow (kg)	83640.48	30420.24	--	--	83640.48	30420.24
	Total fuel produced	20	533.20	1.152	38.67	21.15	571.87

Although jet fuel integrated plant should be designed for 18.18 kmol/day fuel production, yet it is designed for 20 kmol/day as round figure value. From the table, it can be deducted

that for case-3, fuel produced is more than that required for 5 aircraft APU on a daily basis (refer table 5.1) . This is due to the fact that gasifier is operating at full load capacity even when SOEC unit is in operation, thereby increasing the fuel output. Since gasifier is designed for constant capacity production and it is not feasible to shut down on a daily basis, it operates throughout the day at designed capacity. It can also be observed that amount of fuel produced in case-2 by SOEC unit is not enough to carry out one day operation of an aircraft. SOEC units (case-2) provide syngas for production of only 32% of jet fuel and hydrogen for production of 36% of ammonia consumed by an aircraft in a day. Regarding biomass consumption, jet fuel production uses almost three times more biomass than ammonia production for the gasifier. For producing required amount of ammonia for one day aircraft operations, 133 kmol/hr syngas is required from biomass gasifier whereas for jet fuel production 275 kmol/hr of syngas is required. This difference is mainly due to Fischer Tropsch process selectivity to jet fuel (~40%).

5.4 Concluding remarks

This chapter detailed the modelling parameters and inputs required for stationary fuel plant. Three cases are discussed for both jet fuel and ammonia production. Different units like biomass gasification, gas cleaning, gas processing, jet fuel synthesis, ammonia synthesis and SOEC are modelled separately using several reactors and blocks in ASPEN PLUS. Important parameters like temperature, pressure, conversion rates, steam to carbon ratio and catalysts used for different reactor are mentioned. Complete parametric evaluation for distillation columns used in jet fuel synthesis is also done.

The models created are integrated in different arrangements according to the mentioned cases. It can be concluded that gasifier unit is designed for full load capacity for case-1 and case-3. SOEC unit is designed to work at full capacity for 8 hours, when aircraft is parked at the airport, in cases-2 and 3. Gasifier unit is integrated with SOEC unit for both ammonia and jet fuel plants in case-3. Gasifier operating on biomass and SOEC operating on excess electricity available from renewable sources has made the stationary plant completely independent of conventional methods for energy production like coal or natural gas. The stationary plant can be made self sufficient in terms of energy requirements with better heat integration and addition of steam cycle to produce power.

Chapter 6

Thermodynamic evaluation and comparison

This chapter discusses the thermodynamic analysis performed on all the models designed. Section 6.1 enumerates the exergy analysis and exergy calculations for SOFC-GT system designed with both jet fuel and ammonia. Based on the fuel used, the exergy destruction and losses will differ which will be compared. In section 6.2 and 6.3, exergy efficiency is calculated for stationary jet fuel plant and ammonia plant respectively. Three cases as shown below will be discussed for exergy calculations and comparisons.

- **CASE-1**: Biomass gasification based fuel production plant
- **CASE 2**: SOEC based fuel production plant
- **CASE 3**: SOEC and biomass gasification integrated fuel production plant

However, section by section exergy destruction is shown for case-3 only. Comparison between jet fuel and ammonia plants for all cases will be done in section 6.4. Section 6.5 concludes this chapter with a summary about the exergy performance of the models.

6.1 Exergy analysis of SOFC-GT system

Thermodynamic analysis for SOFC-GT consists of exergy calculations for each component used for jet fuel and ammonia operated SOFC-GT systems. Chemical and physical exergy for components present in analysed streams are obtained by calculating mole fractions and partial pressure of the component in the stream. Exergy analysis for SOFC-GT system is based on values obtained when the aircraft is on ground as explained in chapter-4. Chemical exergy is calculated by multiplying the mole fraction with the chemical exergy of the components as calculated in table A.1, available in appendix. Procedure to calculate

chemical exergy is explained in section 2.3.2 of chapter-2. Table A.1 also shows all the components which are used in gaseous streams for SOFC-GT and stationary plant as well.

Physical exergy for streams is calculated by summing physical exergy of each component in the stream using equation 2.35. It is calculated for temperature of the stream and partial pressure of the particular component in the stream. For these calculations, FluidProp is used to obtain enthalpy and entropy values for different basic components at particular pressure and temperature. However, these physical and chemical exergy calculation methods are used for gaseous streams only. For calculating chemical exergy of liquid fuel (jet fuel), equations 2.40 and 2.41 are used. Table 6.1 shows chemical exergy for jet fuel. For liquid fuel, physical exergy can be calculated by using enthalpy and entropy at inlet (T_0, P_0) and outlet (T,P), as acquired from ASPEN PLUS.

Table 6.1: Calculated values for chemical exergy for Jet fuel

	C_8H_{18}	$C_{12}H_{26}$	$C_{16}H_{34}$	Units
C	0.8404	0.8471	0.8479	
H	0.0788	0.0765	0.0751	
Molar mass	114.23	170	226.45	kg/kmol
fL	1.0563	1.0557	1.0554	
LHV	44429.0	44196.94	43942.20	KJ/kg
Ex-chem	5360896.43	7931981.32	10501795.15	KJ/kmol

Table 6.2 shows exergy of jet fuel inlet stream. Ammonia enters the SOFC-GT system in liquid form therefore chemical and physical exergy of ammonia is also calculated in the same way as that of jet fuel. Table 6.3 lists down chemical and physical exergy for ammonia inlet stream for ammonia based SOFC-GT system.

Table 6.2: Exergy calculation for Jet fuel inlet streams for SOFC-GT system in aircraft

	Mole flow (kmol/hr)	Mole fraction	Chemical exergy (kJ/kmol)	Physical exergy (KJ/kmol)
C_8H_{18}	0.002	0.007	37526	
$C_{12}H_{26}$	0.128	0.415	3291772	
$C_{16}H_{34}$	0.178	0.578	6070037	
Total	0.308	1	9399336	0
Temperature	25	C		
Pressure	1.013	bar		
Total exergy	804.94	KW		

Table 6.3: Exergy calculation for Ammonia inlet streams for SOFC-GT system for aircraft

	Mole flow (kmol/hr)	Mole fraction	Chemical exergy (kJ/kmol)	Physical exergy (KJ/kmol)
NH3	9.037	1	336761	6088
Total	9.037	1		342850
Temperature	-40	C		
Pressure	1.013	bar		
Total exergy	860.68	KW		

Major components of SOFC-GT system include compressors, heat exchangers, SOFC, burner (R-Stoic) and turbine. Major difference between jet fuel and ammonia based SOFC-GT system is that ammonia does not require pre-reforming before it enters the fuel cell unlike jet fuel which uses steam reformer. This component is one of the extra sources of exergy destruction for jet fuel based SOFC-GT as compared to ammonia. A water heat exchanger required to produce steam for steam reformer, also causes considerable exergy destruction for jet fuel based SOFC-GT system. Figure 6.1 show exergy destruction in each component for jet fuel and ammonia respectively.

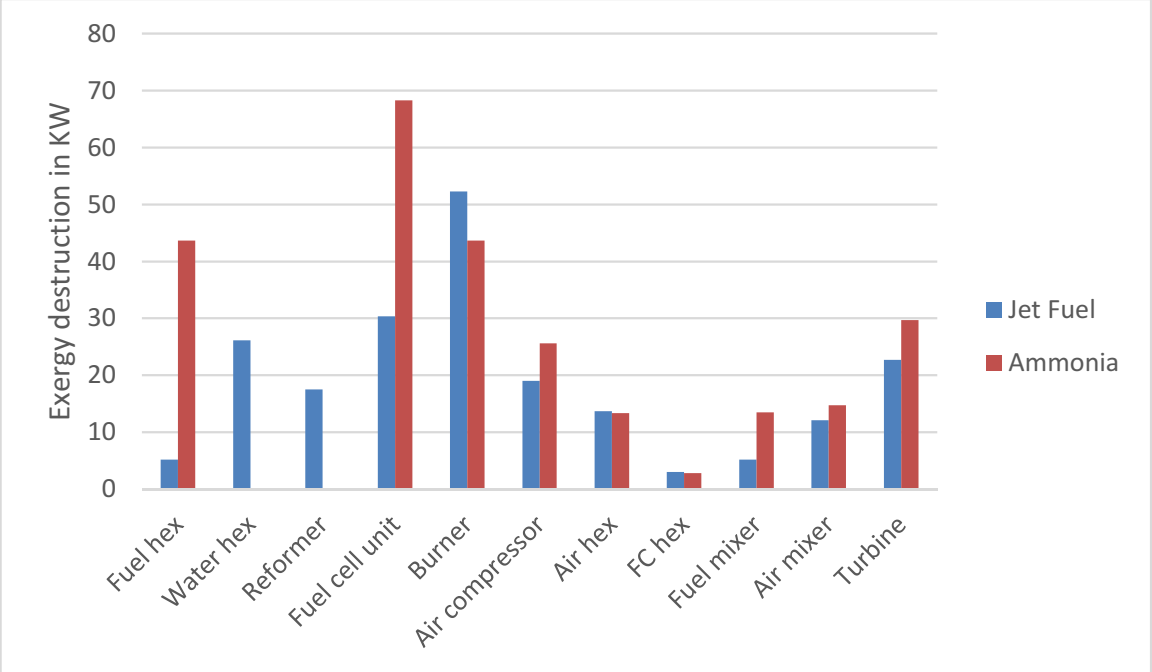

Figure 6.1: Exergy destruction in jet fuel and ammonia based SOFC-GT systems

Exergy destruction takes place in SOFC due to the internal losses manifested as voltage overpotentials. Within the SOFC, most of the chemical reactions occur, like reforming and electrochemical oxidation of hydrogen. It is well known that these processes are the most important source of irreversibilities causing exergy destruction. Compressor exergy destruction is attributed to isentropic or polytropic efficiency, compression ratio and fluid condition. Combustor shows considerable exergy destructions which are associated to the irreversibility of the combustion reactions, the amounts of reactants and the limited

temperature of the combustor [45]. Fuel pump, water pump, air and fuel recirculating stream compressors show negligible exergy destruction for both cases, hence not included in the exergy destruction figure. Exergy efficiency of SOFC-GT systems can be calculated as shown in equation 6.1.

$$\eta_{Ex,SOFC-GT} = \frac{P_{net}}{Ex_{fuel}} \tag{6.1}$$

Table 6.4 gives exergy summary and compares jet fuel to ammonia based SOFC-GT system based on efficiency.

Table 6.4: Exergy inlet, outlet, destruction and efficiency comparison for jet fuel and ammonia based SOFC-GT systems

	Total exergy inlet (KW)	Total exergy outlet (KW)	Exergy destruction (KW)	Exergy losses (KW)	Exergy efficiency (%)
Jet Fuel	806.37	500	223.42	82.94	62.01
Ammonia	862.50	500	276.01	85.34	57.97

6.2 Exergy analysis of jet fuel plant

Exergy analysis is carried out for three cases of jet fuel production for which three models are designed as explained in chapter-5. Integrated jet fuel production (case-3) is discussed in detail and results are shown in this section. For case-1 and case-2, similar procedure is adopted to calculate exergy efficiency but detailed results are not shown. However, comparison is done for exergy efficiency of all the cases. Following equations are used to calculate exergy efficiency of jet fuel plant for all three cases. (Note: Exergy of air is almost negligible hence not shown in the equations)

$$\eta_{Ex,jf1} = \frac{Ex_{prod,fuel}}{Ex_{biomass} + Ex_{biodiesel} + P_{aux}} \tag{6.2}$$

$$\eta_{Ex,jf2} = \frac{Ex_{prod,fuel}}{Ex_{CO2} + P_{SOEC,req} + P_{aux}} \tag{6.3}$$

$$\eta_{Ex,jf3} = \frac{\left[\left(8\,\text{hours} \times \frac{Ex_{prod,fuel}}{Ex_{biomass}+Ex_{biodiesel}+Ex_{CO2}+P_{SOEC,req}+P_{aux}}\right) + (16\,\text{hours} \times \eta_{Ex,jf1})\right]}{24\,\text{hours}} \tag{6.4}$$

CASE-3 detailed analysis: Complete section by section exergy analysis is performed for gasifier & SOEC integrated jet fuel plant (case-3) only. Integrated jet fuel plant is divided into sections as shown in figure 6.2 for exergy analysis. Inlet and outlet streams from each section are analyzed. GF-ATR, RWGS and Rectisol sections together form gas processing unit of jet fuel synthesis plant.

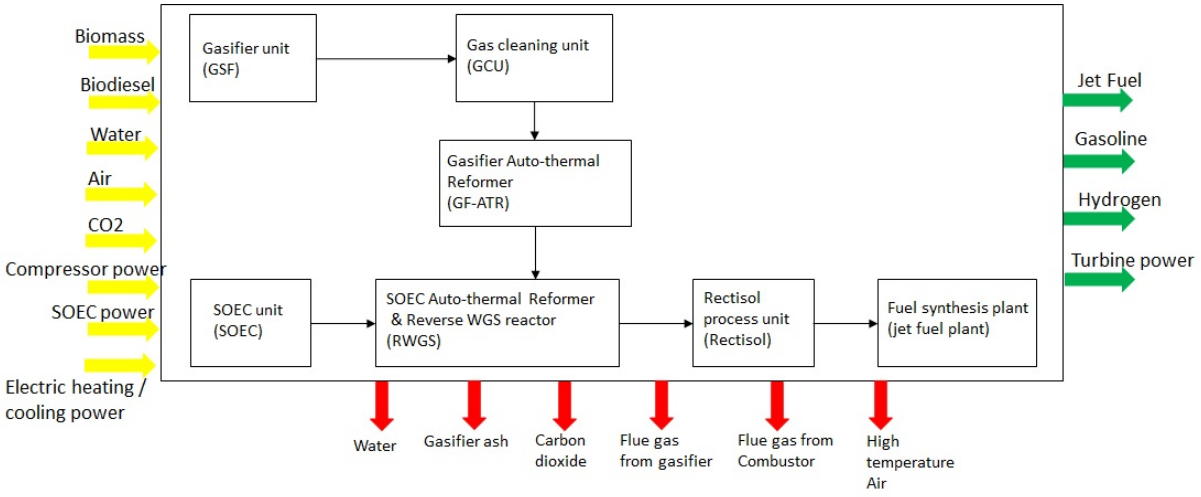

Figure 6.2: Division of integrated jet fuel production plant (case-3) for exergy analysis. The yellow markers show inlet exergy streams, green arrow shows product oultlet stream and red arrows show exergy losses

Exergy calculations for liquid and gaseous fuels have been discussed earlier, however, solid fuels such as biomass also possesses chemical exergy which is treated as inlet exergy stream. Biomass used for this study consists of birch wood and its composition has been tabulated in chapter-5 section 5.1.1. Equation 2.42 and 2.43 are used to calculate solid fuel exergy. Equation 2.46 is used to calculate the exergy destruction for each section.

Exergy flow diagram shows inlet exergy flows, exergy destruction, losses and exergy recirculation at each stage of integrated jet fuel plant (case-3) in figure 6.3. This figure shows exergy destruction, exergy losses and exergy output (products) as percent of total exergy inlet. Since calculation of exergy of multi-component two-phase streams is too complex, jet fuel synthesis unit with burner is taken as one complete section for analysis. This is done to ensure that inlet and outlet streams from this section are either 100% liquid or 100% vapor.

Gasifier section (GSF) shows highest exergy destruction as 30.5% fuel is converted in the combustor to produce heat for gasifier system. The combustion process is typically characterised by large entropy generation due to limited temperature of reaction. Next highest exergy destruction is observed in fuel synthesis section. This may be due to improper utilization of energy stored in rejected streams. These streams are burnt to generate heat and produce flue gas. These streams consists of purge gas from ethanol distillation, distilled waste stream from butanol separation and paraffin distillation columns. Exergy destruction in fuel synthesis section may also be due to numerous processes involved for jet fuel production. RWGS section consists of ATR and Reverse water gas shift reactors which are responsible for major exergy destruction in this section.

Gasoline and hydrogen are also produced by the fuel synthesis unit with Jet fuel and all are considered as product streams. Figure 6.4 shows the exergy distribution of different product streams obtained from jet fuel plant.

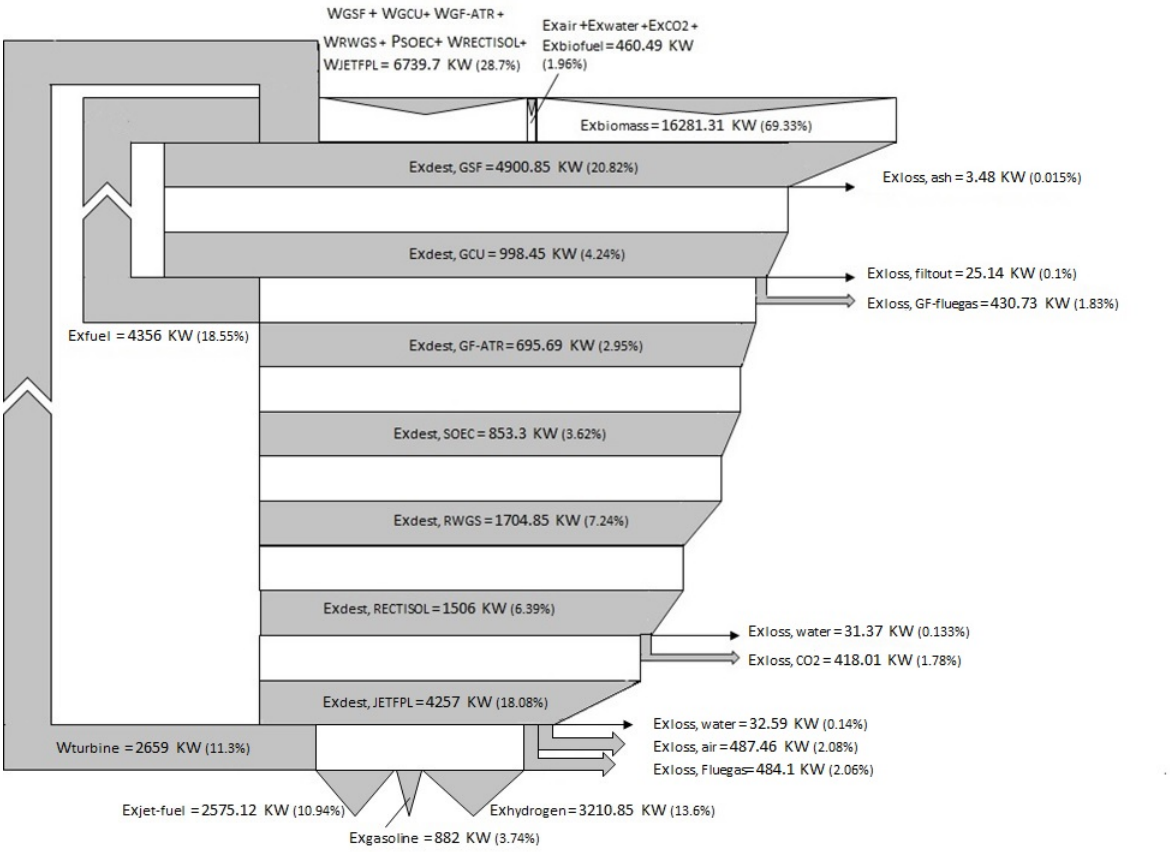

Figure 6.3: Exergy flow diagram showing exergy flows in integrated jet fuel production plant (case-3). This diagram is representing 8 hour operation when both gasifier and SOEC units are operational.

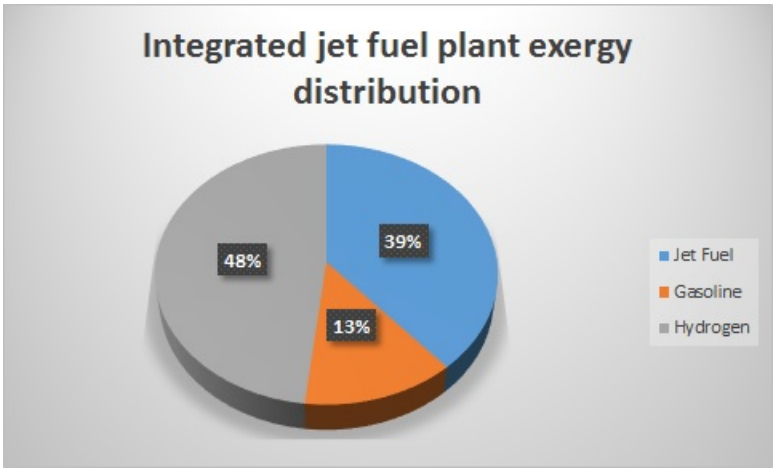

Figure 6.4: Distribution of different product streams for jet fuel plant

All the outlet streams which are exhausted to the environment are considered losses. The exergy efficiency of the plant is calculated for two scenarios: a) Only jet fuel as product and b) Jet fuel, gasoline and hydrogen, all are considered as products. The comparison is made for all three cases for both the scenarios as shown in table 6.5.

Table 6.5: Exergy efficiency comparison of jet fuel production plant for all three cases. Two scenarios are considered: a) Only Jet fuel as product b) Jet fuel+gasoline+hydrogen as products

	Exergy Efficiency (%)	
	Jet fuel as only product	***Jet fuel, gasoline & hydrogen as products***
Case-1	10.81	30.57
Case-2	6.19	24.79
Case-3	10.94	28.33

The table shows comparable exergy efficiencies for case-1 and case-3 for both senarios. Since gasifier unit contributes around 85% in fuel production for case-3, exergy efficiency for case-1 and case-3 are comparable with a minor effect of SOEC efficiency.

Exergy efficiencies for case-2 are lesser in both scenarios as compared to case-1 & 3. Since conditions (temperature, pressure and composition) at the inlet of gas processing section and outlet of jet fuel synthesis section are also similar for case-1 and case-2, jet fuel production process is equally efficient in terms of gas processing and fuel synthesis for both the cases. With this, it can be deducted that gasifier and gas cleaning units (case-1) are more efficient than SOEC unit (case-2) for syngas production. SOEC unit consists of compressors and heat exchangers, with high electrical power input. Due to conservative selection of mechanical efficiency for compressors and turbines, significant amount of exergy is destroyed. These components also have isentropic efficiency of 80% which results in further exergy destruction. Also SOEC unit itself adds considerable exergy destruction in this case.

6.3 Exergy analysis of Ammonia plant

Ammonia exergy analysis is done in a similar way as jet fuel exergy analysis. Three models for three different cases as explained in beginning of the chapter have been designed for ammonia production as well. Detailed exergy analysis is performed for integrated ammonia plant (case-3) only. For other two cases, exergy efficiency calculations are performed and all cases are compared. Following equations are used to calculate exergy efficiency of ammonia plant for all three cases.

$$\eta_{Ex,am1} = \frac{Ex_{prod,fuel}}{Ex_{biomass} + Ex_{biodiesel} + P_{aux}} \tag{6.5}$$

$$\eta_{Ex,am2} = \frac{Ex_{prod,fuel}}{P_{SOEC,req} + P_{aux}} \tag{6.6}$$

$$\eta_{Ex,am3} = \frac{\left[\left(8\,\text{hours} \times \frac{Ex_{prod,fuel}}{Ex_{biomass}+Ex_{biodiesel}+P_{SOEC,req}+P_{aux}}\right) + (16\,\text{hours} \times \eta_{Ex,am1})\right]}{24\,\text{hours}} \tag{6.7}$$

CASE-3 detailed analysis: Figure 6.5 shows the division of integrated ammonia plant in sections for exergy analysis.

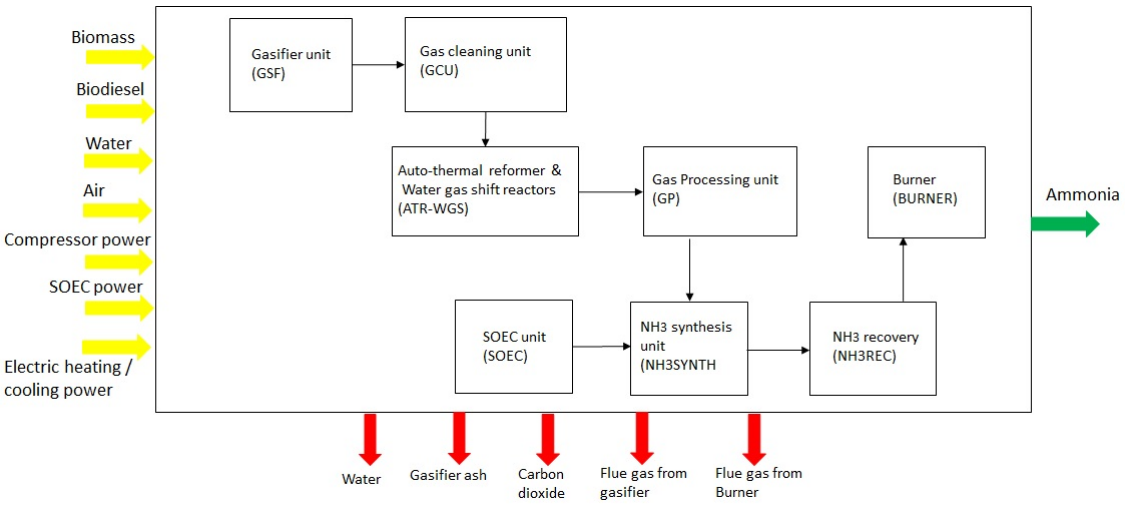

Figure 6.5: Division of integrated ammonia production plant (case-3) for exergy analysis. The yellow markers show inlet exergy streams, green arrow sho

Exergy flow diagram shows inlet exergy flows, exergy destruction, losses and exergy recirculation at each stage of integrated ammonia plant (case-3) in figure 6.6. This figure shows exergy destruction, exergy losses and exergy output (products) as percent of total exergy inlet.

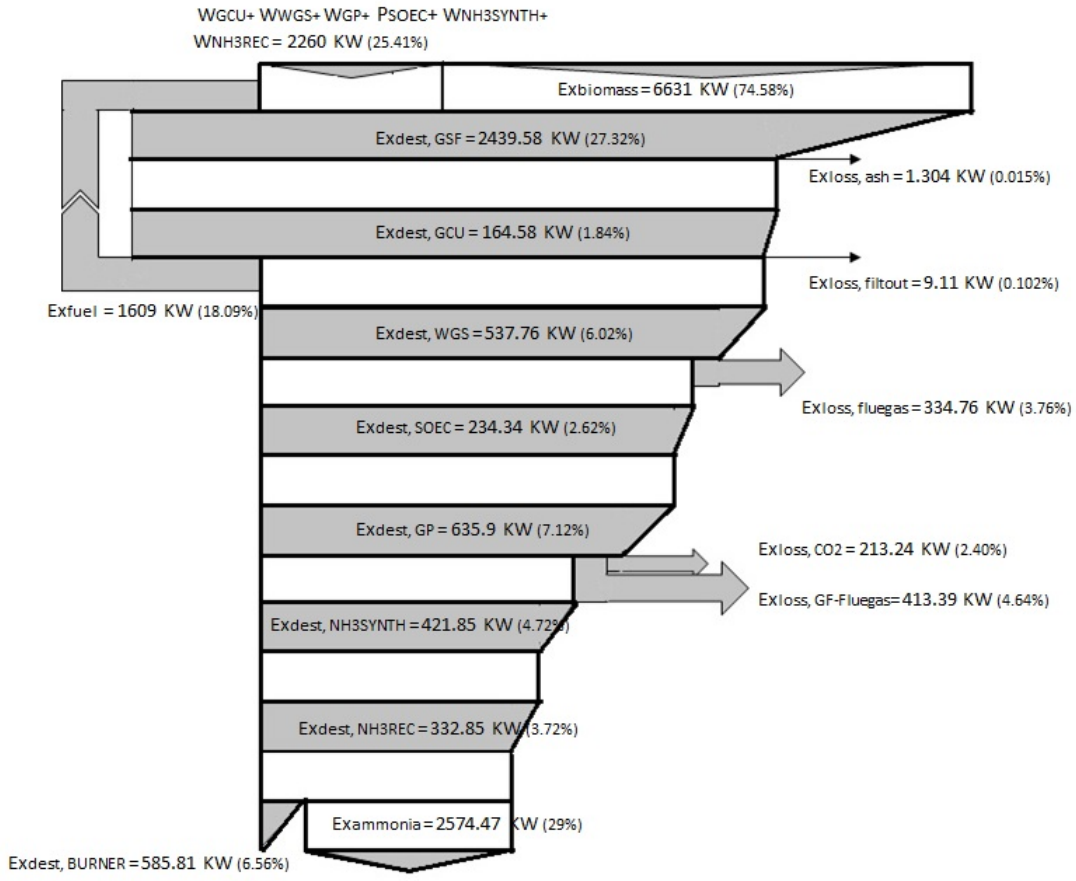

Figure 6.6: Exergy flow diagram showing exergy flows in integrated ammonia production plant (case-3). This diagram is representing 8 hour operation when both gasifier and SOEC units are operational.

Highest destruction is in gasifier unit (GSF) as 30.5% fuel is recirculated to the combustor to produce heat for gasifier system. ATR-WGS section consists of Auto thermal reformer which is responsible for major exergy destruction in this section. Gas processing (GP) unit contains Rectisol process and NH_3 recovery section (NH3REC) has purge of 10%, containing high hydrogen content which is not recovered and burnt to produce heat in the burner. This exergy destruction can be minimized by recovery of hydrogen from purge gas by adding an extra unit.

Exergy efficiency of ammonia production plant for all three cases are compared in table 6.6. Ammonia is the only product stream obtained from ammonia production plant unlike jet fuel production plant where multiple products are obtained. Ammonia plant efficiency for case-2 is higher as compared to other cases due to absence of gasifier, gas cleaning unit and gas processing unit. ATR-WGS and GP sections shown in figure 6.5 together form the energy intensive gas processing unit of ammonia production plant. Gasifier with gas processing unit results in major exergy destruction. Therefore elimination of these units increases efficiency of SOEC based plant.

Table 6.6: Comparisons of exergy efficiencies for all three cases of ammonia production

	Exergy efficiency (%)
Case-1	24.02
Case-2	37.39
Case-3	28.83

Since contribution of fuel production from gasifier is around 80% for case-3, the exergy efficiency for case-1 and case-3 are comparable.

Plant efficiency can be increased by ~ 6-7% by reducing the purge to 3%. While modelling the system, 3% purge resulted in errors and accumulation of components like methane in the system. This results in loss of hydrogen which is a potential fuel. To reduce this loss, a hydrogen membrane can be added after the purge to recover 80% hydrogen. This hydrogen can be further compressed and recirculated to ammonia synthesis reactor. This process can be taken up as a future optimisation and exergy calculations can be done to obtain higher efficiencies and lower biomass requirement for ammonia production.

6.4 Comparison of jet fuel and ammonia plants

Comparison is made between integrated jet fuel and ammonia plants based on case-3 configuration, designed to operate at full capacity producing enough fuel for five aircrafts for one day operations. Both the plants will be compared on basis of fuel used in terms of biomass, major exergy inlets, outlets, destruction processes and losses. Table 6.7 shows these comparisons for integrated jet fuel and ammonia plant.

Table 6.7: Exergy inlet, outlet and losses compared between integrated jet fuel and ammonia plants (case-3)

	Integrated Jet fuel	Integrated Ammonia	Units
Major exergy Inlet			
Biomass	16281.31	6574.71	KW
Biodiesel	242.64	88.19	KW
CO2	107.01	0.00	KW
Water	1.99	1.25	KW
Air	23.09	4.75	KW
SOEC power requirement	705.66	723.36	KW
Other power requirements	8693.69	1502.93	KW
Major exergy Outlet			
Fuel	2575.14	2574.48	KW
Hydrogen	3210.85	0.00	KW
Gasoline	882.06	0.00	KW
Carbon capture	418.01	210.24	KW
Exhaust losses	1004.16	748.40	KW
Total exergy destruction	17094.91	5352.69	KW

A comparison is made between exergy efficiencies between jet fuel and ammonia production plants for all three cases based on two scenarios: a) Considering jet fuel and ammonia as products and b) Considering (jet fuel + gasoline + hydrogen) and ammonia as product streams.

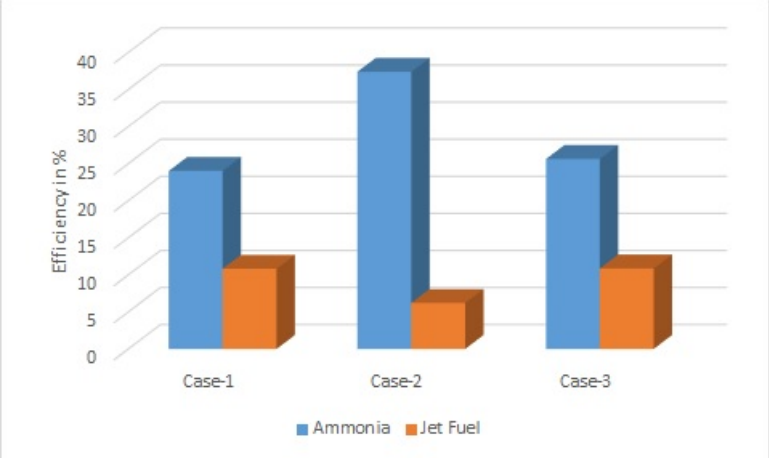

Figure 6.7: Exergy efficiency comparison between jet fuel and ammonia for all three modes of plant operation considering jet fuel and ammonia as only products

Jet fuel production efficiency in all cases is much lower than ammonia production as observed from figure 6.7. This is due to more products formed during jet fuel synthesis as compared to ammonia synthesis. Jet fuel forms just 39% of the total products formed, hence the lower exergy efficiency. In other words, the limited selectivity of jet fuel lowers the exergy efficiency.

Exergy efficiency comparison for another scenario (b) is made between both types of fuel production plants as shown in figure 6.8.

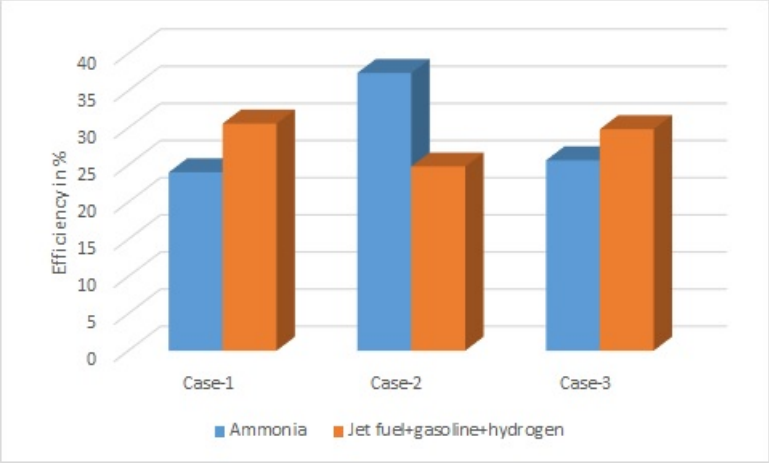

Figure 6.8: Exergy efficiency comparison for jet fuel and ammonia plants for all three modes of operation considering (jet fuel, gasoline and hydrogen) and ammonia as products

It is observed that for case-1, jet fuel presents a better option than ammonia. The major reason is higher exergy destruction encountered in gas processing unit of the ammonia as compared to jet fuel production plant. [1]In addition to that, gasifier and gas cleaning units of jet fuel production plant show slightly lower exergy destructions as compared to ammonia production plant. This is due to better heat integration achieved in this section of jet fuel production plant .

For case-2, when only the SOEC units are used as syngas or hydrogen sources, ammonia is more efficient. This is due to the elimination of the inefficient syngas processing section from ammonia production plant. For jet fuel, syngas from SOEC has to undergo processing so gas processing section cannot be eliminated completely for jet fuel production plant.

For case-3, jet fuel production shows higher exergy efficiency than ammonia. For case-3, both SOEC and gasifier contribute to fuel synthesis during 8 hours when aircraft is parked. From figures 6.3 and 6.6, it can be seen that both plants have comparable exergy efficiencies for 8 hour operation. For rest of the 16 hours of the day, only gasifier operates at full capacity. Gasifier operated jet fuel production plant (case-1) is more efficient than ammonia as expalined before. Therefore, according to equations 6.4 and 6.7, jet fuel is more efficient than ammonia exergetically, since gasifier is operational for longer time and contributes more to the exergy efficiency.

[1]Considering figure 6.6 (case-3) for ammonia production, approximately 24% of exergy is destroyed in syngas processing unit (ATR-WGS+GP). This value is only representative of amount of syngas required to produce hydrogen for 65% ammonia production. Remaining hydrogen is produced by SOEC, which does not need processing.

However, for case-1, gas processing unit has to deal with 100% syngas to produce hydrogen for required ammonia production. This will lead to increased exergy destruction in this unit which will consequently reduce the efficiency of the ammonia plant. For jet fuel production, 100% syngas has to pass through gas processing unit (RWGS+Rectisol) in both case-1 & case-3, hence exergy destruction in this unit remains same (refer figure 6.2).

6.5 Conclusion

From this chapter, conclusions can be drawn for exergy efficiency of SOFC-GT systems and stationary fuel production plants. Exergy efficiency of SOFC-GT for jet fuel and ammonia are 62% and 58% respectively, which is higher than conventional turbine based aircraft APU systems. In terms of stationary plant models, exergy efficiency of jet fuel production (only jet fuel as product) in all 3 cases is lower than that for ammonia production. Hydrogen and gasoline are two more products which are obtained from jet fuel production plant. Jet fuel contributes only 39% to the total product exergy and hence exhibits very low exergy efficiency. Considering all useful products from jet fuel synthesis, case-1 and case-3 show higher efficiency for jet fuel production than ammonia unlike case-2, which shows ammonia as more efficient.

In case of ammonia production, with reduction of purge gas from 10% to 3% and better heat integration, an exergy efficiency of ~40% is possible. Jet fuel synthesis unit shows high exergy destruction which may be due to numerous processes involved or conversion of energy contained in waste streams from distillation columns into heat by burning them in the combustor. Gasifier unit for both jet fuel and ammonia shows high exergy destruction as 30.5% fuel is recirculated to the combustor to provide heat for gasifier. Exergy efficiencies of case-3 models are relatively closer to case-1 for both jet fuel and ammonia as gasifier unit contributes more than 75% for fuel production. It is also known from these results that SOEC units will not be able to produce entire fuel for one day operation of aircrafts in 8 hours, hence gasifier has to operate at full load capacity to produce enough fuel.

Chapter 7

Conclusion

7.1 Conclusion

To achieve the goal of 80% decarbonization by 2050, aircraft industry has to switch to cleaner fuels and more efficient APU systems to lower greenhouse gas emissions. Bi-directional SOC systems can be designed to be used as SOFC-GT systems for aircraft APU to reduce emissions and achieve high efficiency than conventional gas turbine based APU systems. Being bi-directional, these SOC units have potential functionalities during periods of non-operation, for instance when aircraft is parked at the airport. For these periods, the SOC APU units can be used in the airport to produce sustainable fuels. The integration of these units would reduce the capital investment in new, flexible, cleaner and more efficient fuel production plants.

One of the aims of this study is to investigate the potential of integration of these bi-directional SOC APU units in the airport stationary fuel production plant during the night period (8 hours) when the aircrafts are parked. Small aircrafts like A320 & B737 with power requirement of 500 KWe are considered. Jet fuel and ammonia are considered as fuel alternatives for SOFC-GT based APU system. Modelling and sizing analysis of these systems shows a fuel consumption of 3.6 kmol of jet fuel and 106 kmol of ammonia per day for SOFC-GT based aircraft APU. Five SOC APU units (5 aircrafts) can be integrated with this plant to produce syngas for the jet fuel plant or hydrogen for the ammonia plant. Due to the limited production of syngas or hydrogen by SOEC units as well as the limited period of excess electricity from the electric grid, a gasifier fed by biomass is also integrated as complementary source of syngas. These aspects led to investigation of three different plant designs:

- Case-1: Gasifier+fuel synthesis. No excess electricity available
- Case-2: SOEC+fuel synthesis. Operating only on excess electricity from renewable energy sources
- Case-3: Gasifier+SOEC+Fuel synthesis. A mix of both the technologies

Jet fuel synthesis based on Fischer Tropsch process is modelled to produce jet fuel as the main product whereas ammonia is produced by the conventional Haber Bosch process. With jet fuel, a significant amount of gasoline and hydrogen are also produced in Fischer Tropsch process.

Case-1 and case-3 are designed to produce entire fuel (jet fuel or ammonia) required by 5 aircraft APUs per day by determining the gasifier capacity. Results determine that jet fuel production uses almost three times more biomass than ammonia. Since biomass is a limited resource, its utilization can play a crucial role in fuel selection. Case-2 is modelled only with SOEC units operating for 8 hours when aircraft is parked. Results show that SOEC units (case-2) can provide syngas for production of only 32% of jet fuel and hydrogen for production of 36% of ammonia consumed by an aircraft APU in a day.

Thermodynamic evaluation for all 3 cases reveal that exergy efficiencies vary from case to case. Two scenarios are analysed for exergy comparisons.

a) *Ammonia and Jet fuel are considered as products:* Ammonia shows higher exergy efficiency than jet fuel production in all cases.

b) *Ammonia and (jet fuel +gasoline +hydrogen) are considered as products*: Jet fuel presents a better option for case-1 due to the more efficient gas processing and gasifier units. However, in case-2, when only SOEC units are used, ammonia seems to be a better choice due to the elimination of exergetically inefficient syngas processing section from ammonia synthesis. In case-3, for which exergy efficiency is a time weighted average of case-1 and case-2 exergy efficiencies (refer equations 6.4 and 6.7), jet fuel is more efficient than ammonia exergetically. This is because gasifier is operational for longer time (16 hrs) than SOEC units (8 hrs) and contributes more to the exergy efficiency of the plant for one day operation.

It should also be highlighted that higher ammonia plant efficiencies (~40%) are achievable by reducing the purge gas percentage and better heat integration. Further work in this regard can be undertaken to optimize and increase the efficiency of ammonia production plant as shown in section 7.2 of this chapter.

Regarding the utilization of jet fuel or ammonia as fuel for the aircraft APU unit, it can be concluded that use of jet fuel for SOFC-GT based aircraft APU system shows better exergy efficiency of 62% than ammonia (58%). In addition to being exergetically more favorable, jet fuel also has higher energy density and lower volume with no additional storage space required.

Since, the scope of this study includes only thermodynamic evaluation, results and conclusions are provided based purely on that. Economic analysis is required to understand the better option among the two fuel alternatives for both SOFC-GT system and stationary fuel production plants.

Nonetheless, other conclusions can be disclosed. Gasoline and hydrogen produced by jet fuel plant can be used to extend the plant to other purposes by integration of a vehicle pump station and therefore contributing for a cleaner road transportation sector.

7.2 Future recommendations

Both the stationary plant models have streams of flue gas leaving at high temperature. These streams can be made to produce steam to be used in a steam cycle to retrieve ~30% of flue gas exergy. This can result in increment of efficiency of stationary plants by ~2-3%. The model can also be optimised for better heat integration. This can be taken up as future research project.

Ammonia production model can be optimised by reducing purge to increase overall plant exergy efficiency. This will also reduce biomass consumption for ammonia production. Purge can be reduced by using hydrogen membranes to separate hydrogen from purge gas and recirculating to ammonia synthesis reactor. Another method to reduce purge gas percent is to avoid accummulation of methane. This can be done by making the purge stream pass through methane membranes [32]. However, there will still be some loss of hydrogen and nitrogen in this case, but maximum amount will be recycled back to ammonia synthesis. This can lead to increase in ammonia production and exergy efficiency of ~40% can be achieved for ammonia plants.

Section by section exergy analysis can be unertaken for Jet fuel synthesis part of integrated jet fuel plant. It can be divided into smaller sections like mixed alcohol synthesis, ethanol separation and Guerbet reactor, alcohol dehydration, oligomerisation and dehydrogenation with final distillation process. This will give a clearer idea about the exergy destruction and losses in different sections of jet fuel synthesis unit. To achieve this, understanding of the procedure for calculating chemical and physical exergy of multi-phase multi component streams is required. Also physical and chemical exergy calculation of higher and more complex hydrocarbons can be studied in detail as further extension of this project. Validation and comparison can be made with existing jet fuel plants to understand the accuracy of the simulations. There can also be made some changes in the production method to reduce carbon emissions and make these plants self sufficient in terms of energy requirements.

Lastly, this needs a special mention that the technologies discussed in this thesis are aimed as starting point for discussion on massive shift in air transport industry from conventional, fossil based technologies to sustainable technology. This project can be further extended to include a complex energy network comprising of aircrafts, airports and power plants as main points of operation. This system should enable the use of bi-directional SOC APU systems for providing electricity to the airport or to the grid. Use of bio waste from airport can be used for biofuel production. Other technologies, which are more efficient and economic can be integrated with the present work to make it more feasible.

References

[1] Airbus a320 aircraft systems description and diferences between a318, a319 and a320.

[2] Stephan Eelman. Fuel cell apu in commercial aircraft-an assessment of sofc and pemfc concepts.

[3] P.V. Aravind. Solid oxide fuel cells for next generation power plants: An introduction, 2014.

[4] Giulia Botta. Thermodynamic and exergy analysis of reversible solid oxide cell systems. In *ECS Conference on Electrochemical Energy Conversion & Storage with SOFC-XIV (July 26-31, 2015)*. Ecs, 2015.

[5] Rafael Cuellar. Analysis of 5 mw hydrogen power system with thermal energy storage. 2013.

[6] Piga Bruno. Simulation and exergy analysis of ammonia production and use for a sofc-gt powered uav: a thermodynamic well-to-wake analysis. Master's thesis, POLITECNICO DI TORINO, Dipartimento di Energia, 2014.

[7] Hermann Hofbauer, Gunter Veronik, Thomas Fleck, Reinhard Rauch, Herbert Mackinger, and Erich Fercher. *The FICFB-gasification process*. Springer, 1997.

[8] Konstantinos Atsonios, Michael-Alexander Kougioumtzis, Kyriakos D Panopoulos, and Emmanuel Kakaras. Alternative thermochemical routes for aviation biofuels via alcohols synthesis: Process modeling, techno-economic assessment and comparison. *Applied Energy*, 138:346–366, 2015.

[9] Greg A Whyatt and Lawrence A Chick. *Electrical Generation for More Electric Aircraft Using Solid Oxide Fuel Cells*. 2012.

[10] A. Fernandes, T. Woudstra, and P.V. Aravind. System simulation and exergy analysis on the use of biomass-derived liquid-hydrogen for sofc/gt powered aircraft. *International Journal of Hydrogen Energy*, 40(13):4683 – 4697, 2015.

[11] Y Zhu, M.A. Gerber, S.B. Jones, and D.J. Stevens. *Analysis of the Effects of Compositional and Configurational Assumptions on Product Costs for the Thermochemical Conversion of Lignocellulosic Biomass to Mixed Alcohols.* Washington, D.C : United States. Dept. of Energy, 2009.

[12] Jim Skea. Roadmap 2050: A practical guide to a prosperous, low-carbon europe, european climate foundation (2010)., 2012.

[13] Christopher J Steffen, Joshua E Freeh, and Louis M Larosiliere. Solid oxide fuel cell/gas turbine hybrid cycle technology for auxiliary aerospace power. In *ASME Turbo Expo 2005: Power for Land, Sea, and Air*, pages 253–260. American Society of Mechanical Engineers, 2005.

[14] Kaushik Rajashekara, James Grieve, and David Daggett. Hybrid fuel cell power in aircraft. *Industry Applications Magazine, IEEE*, 14(4):54–60, 2008.

[15] Joshua E Freeh, Christopher J Steffen, and Louis M Larosiliere. Off-design performance analysis of a solid-oxide fuel cell/gas turbine hybrid for auxiliary aerospace power. In *ASME 2005 3rd International Conference on Fuel Cell Science, Engineering and Technology*, pages 265–272. American Society of Mechanical Engineers, 2005.

[16] K.M. Spencer and C.A. Martin. Investigation of potential fuel cell use in aircraft. In *IDA Document D-5043*. INSTITUTE FOR DEFENSE ANALYSES, Dec 2013.

[17] Rong Lan and Shanwen Tao. Ammonia as a suitable fuel for fuel cells. *Frontiers in Energy Research*, 2:35, 2014.

[18] Adam Wojcik, Hugh Middleton, Ioannis Damopoulos, et al. Ammonia as a fuel in solid oxide fuel cells. *Journal of Power Sources*, 118(1):342–348, 2003.

[19] Ryan P O'Hayre, Suk-Won Cha, Whitney Colella, and Fritz B Prinz. *Fuel cell fundamentals.* John Wiley & Sons New York, 2006.

[20] J Hanna, WY Lee, Y Shi, and AF Ghoniem. Fundamentals of electro-and thermochemistry in the anode of solid-oxide fuel cells with hydrocarbon and syngas fuels. *Progress in Energy and Combustion Science*, 40:74–111, 2014.

[21] S Basu and Anil Verma. Fuel cell technology. 2014.

[22] Enrique Querol, Borja Gonzalez-Regueral, and Jose Luis Perez-Benedito. *Practical approach to exergy and thermoeconomic analyses of industrial processes.* Springer Science & Business Media, 2012.

[23] SC Kaushik and Omendra Kumar Singh. Estimation of chemical exergy of solid, liquid and gaseous fuels used in thermal power plants. *Journal of Thermal Analysis and Calorimetry*, 115(1):903–908, 2014.

[24] Ricardo Rivero, Consuelo Rendon, and Leodegario Monroy. The exergy of crude oil mixtures and petroleum fractions: calculation and application. *Int. J. Appl. Thermodyn*, 2:115–123, 1999.

[25] Michael J Moran, Howard N Shapiro, Daisie D Boettner, and Margaret B Bailey. *Fundamentals of engineering thermodynamics*. John Wiley & Sons, 2010.

[26] Woudstra N. J.J.C. van Lier. Thermodynamic for energy systems. Delft University Press, ISBN 90-407-2037-1.

[27] Jian Zheng, James Jon Strohm, and Chunshan Song. Steam reforming of liquid hydrocarbon fuels for micro-fuel cells. pre-reforming of model jet fuels over supported metal catalysts. *Fuel Processing Technology*, 89(4):440–448, 2008.

[28] Ke Qin, Anker Degn Jensen, Peter Arendt Jensen, and Weigang Lin. *Entrained Flow Gasification of Biomass*. PhD thesis, Technical University of DenmarkDanmarks Tekniske Universitet, Risø National Laboratory for Sustainable EnergyRisø Nationallaboratoriet for Bæredygtig Energi, 2012.

[29] Principle of olga tar removal system.

[30] Steven Phillips and Timothy J Eggeman. *Thermochemical ethanol via indirect gasification and mixed alcohol synthesis of lignocellulosic biomass*, volume 112. Citeseer, 2007.

[31] Manuele Gatti, Emanuele Martelli, Francois Marechal, and Stefano Consonni. Review, modeling, heat integration, and improved schemes of rectisol-based processes for {CO2} capture. *Applied Thermal Engineering*, 70(2):1123 – 1140, 2014. PRES13 Process Integration.

[32] Ke Liu, Chunshan Song, Velu Subramani, et al. *Hydrogen and syngas production and purification technologies*. Wiley Online Library, 2010.

[33] A.S Ndou, N Plint, and N.J Coville. Dimerisation of ethanol to butanol over solid-base catalysts. *Applied Catalysis A: General*, 251(2):337 – 345, 2003.

[34] Ivan C Lee, Jeffrey G St Clair, and Adam S Gamson. Catalytic oxidative dehydration of butanol isomers: 1-butanol, 2-butanol, and isobutanol. Technical report, DTIC Document, 2011.

[35] C3-c4 oligomerization for gasoline, December 2009.

[36] Michael E Wright, Benjamin G Harvey, and Roxanne L Quintana. Highly efficient zirconium-catalyzed batch conversion of 1-butene: a new route to jet fuels. *Energy & Fuels*, 22(5):3299–3302, 2008.

[37] Steven F Rice and David P Mann. Autothermal reforming of natural gas to synthesis gas reference: Kbr paper# 2031. 2007.

[38] Douglas Falleiros Barbosa Lima, Fernando Ademar Zanella, Marcelo Kaminski Lenzi, and Papa Matar Ndiaye. *Modeling and Simulation of Water Gas Shift Reactor: An Industrial Case*.

[39] Mustafa Cavcar. The international standard atmosphere (isa). *Anadolu University*, 26470, 2000.

[40] R Deuchler. Load management–strategies for dealing with temporary oversupply of variable renewable electricity. 2013.

[41] Christoph Pfeifer, Reinhard Rauch, Dariusz Hofbauer, Hermann, Claire Courson, and Alain Kiennemann. *Hydrogen-rich gas production with a Ni-catalyst in a dual fluidized bed biomass gasifier*. Citeseer, 2004.

[42] Youssef Redissi and Chakib Bouallou. Valorization of carbon dioxide by co-electrolysis of co 2/h 2 o at high temperature for syngas production. *Energy Procedia*, 37:6667–6678, 2013.

[43] M Khoshnoodi and YS Lim. Simulation of partial oxidation of natural gas to synthesis gas using aspen plus. *Fuel Processing Technology*, 50(2):275–289, 1997.

[44] Vassily Abidin, Chakib Bouallou, and Denis Clodic. Valorization of co2 emissions into ethanol by an innovative process. *Chemical Engineering Transactions*, 25:1–6, 2011.

[45] Yannay Casas, Luis E Arteaga, Mayra Morales, Elena Rosa, Luis M Peralta, and Jo Dewulf. Energy and exergy analysis of an ethanol fueled solid oxide fuel cell power plant. *Chemical Engineering Journal*, 162(3):1057–1066, 2010.

Appendix A

ASPEN PLUS models and tables

A.0.1 Gasifier unit

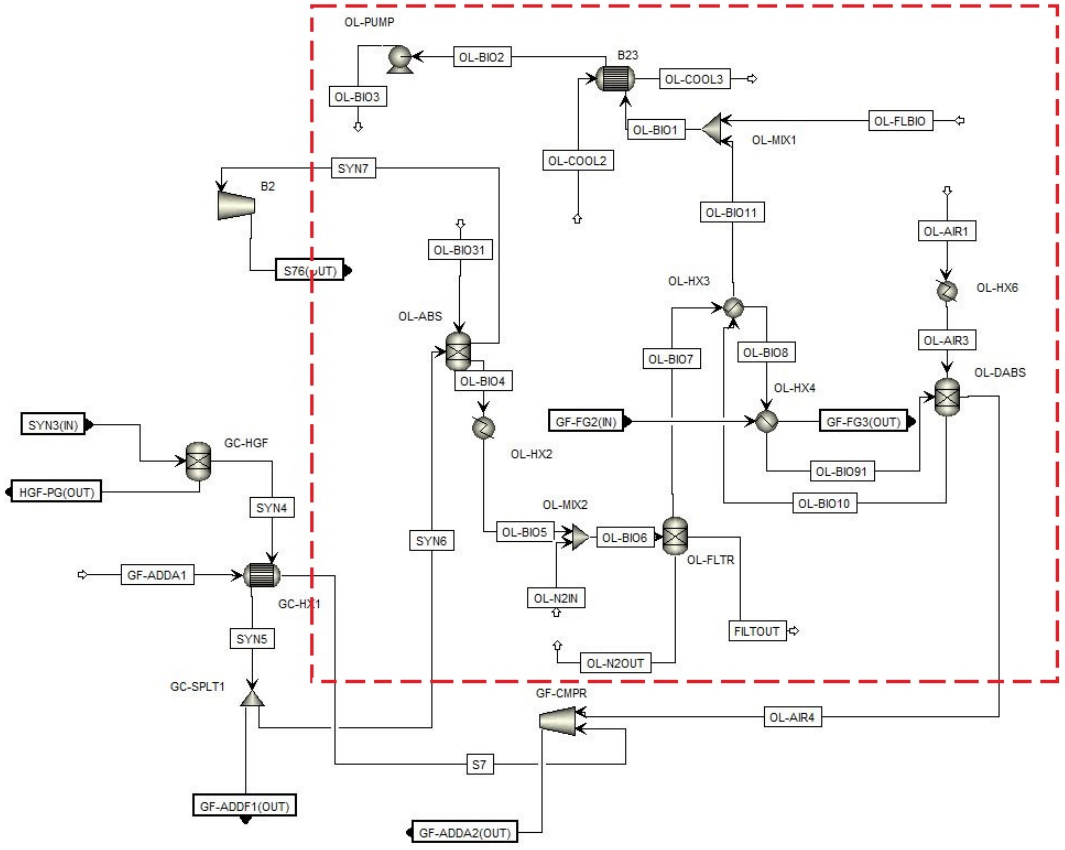

Figure A.1: Gas cleaning unit with OLGA unit highlighted with red boundary

A.0.2 SOEC unit - Co-electrolysis

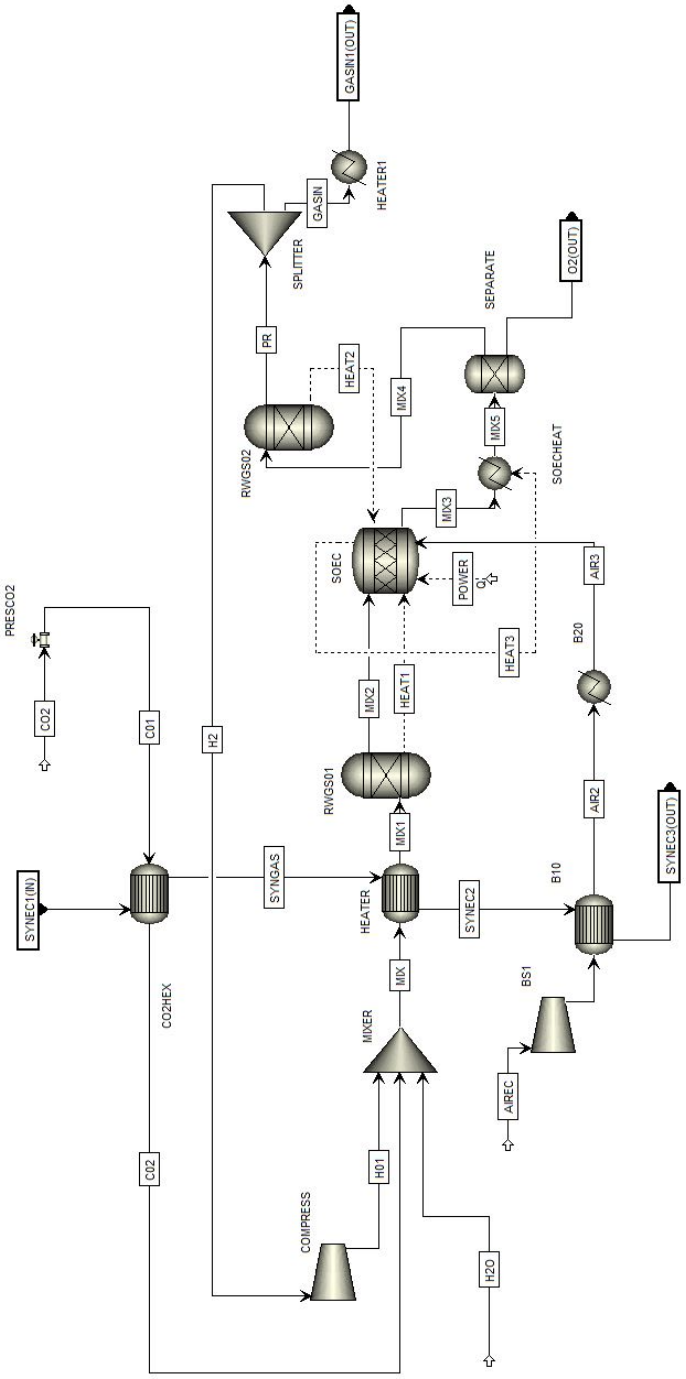

Figure A.2: Basic layout of SOEC undergoing co-electrolysis

A.0.3 SOEC unit - steam electrolysis

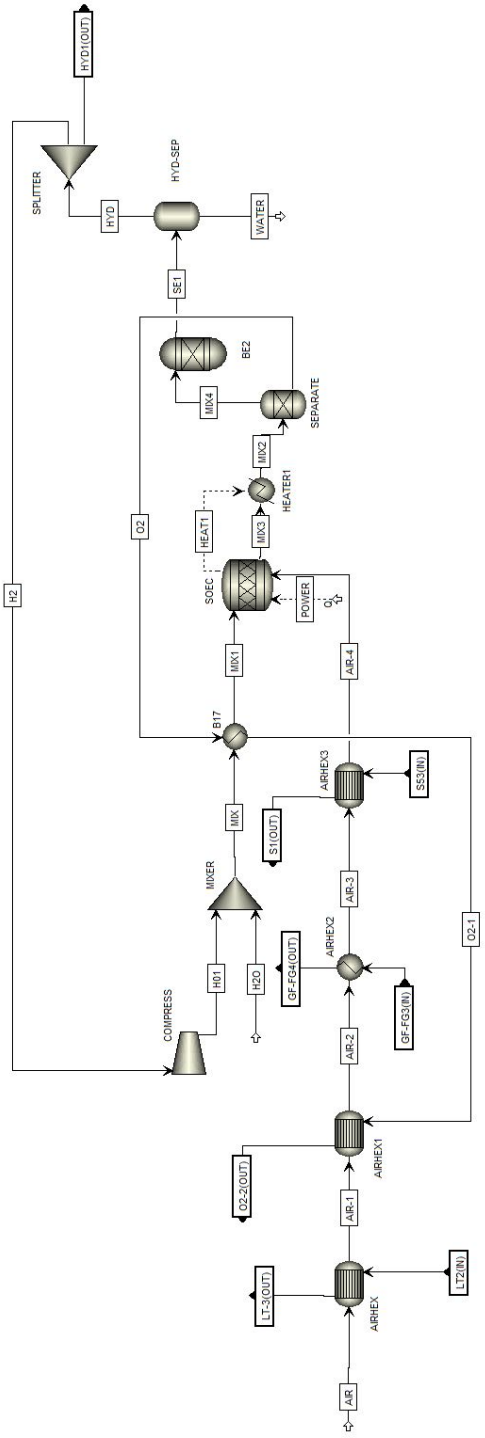

Figure A.3: Basic layout of SOEC undergoing steam electrolysis

A.0.4 Gas processing unit - Jet fuel Plant

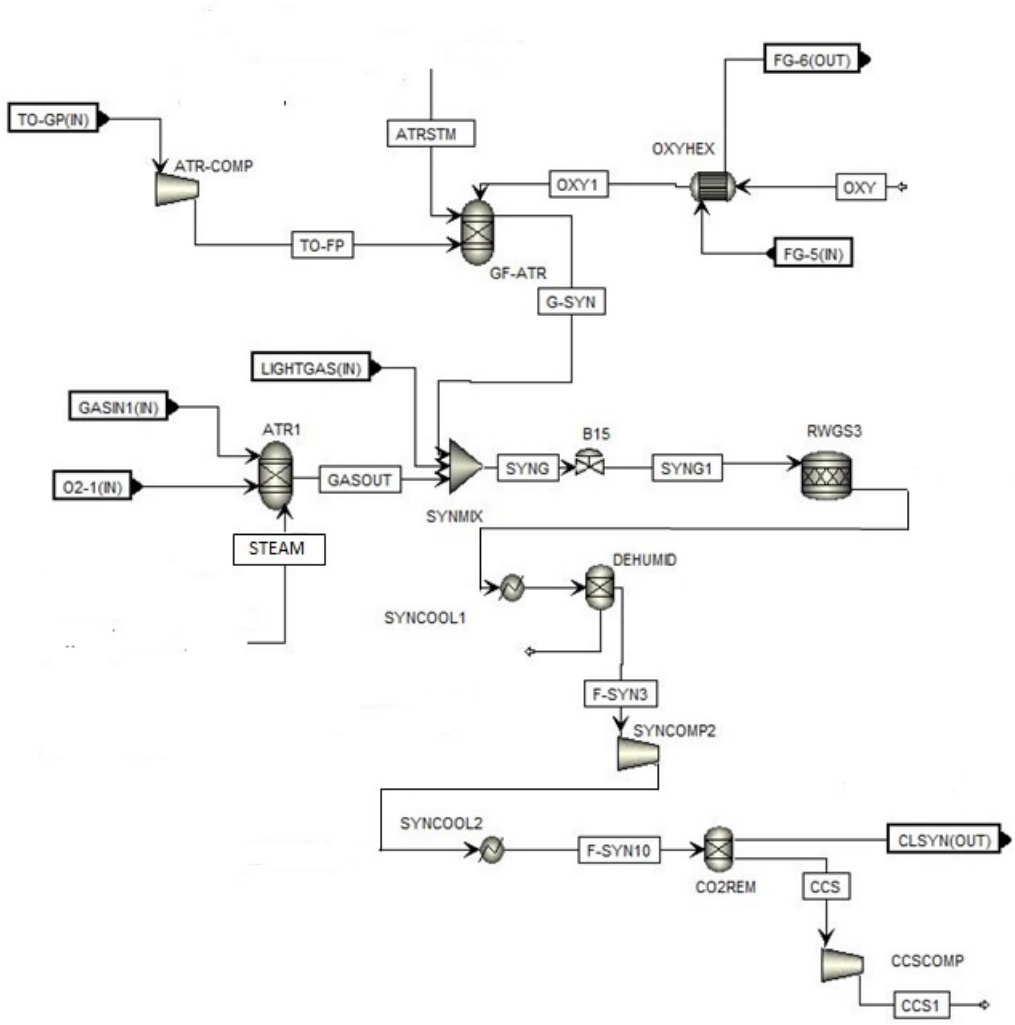

Figure A.4: Gas processing unit model for integrated jet fuel production plant

A.0.5 Ammonia gas processing unit

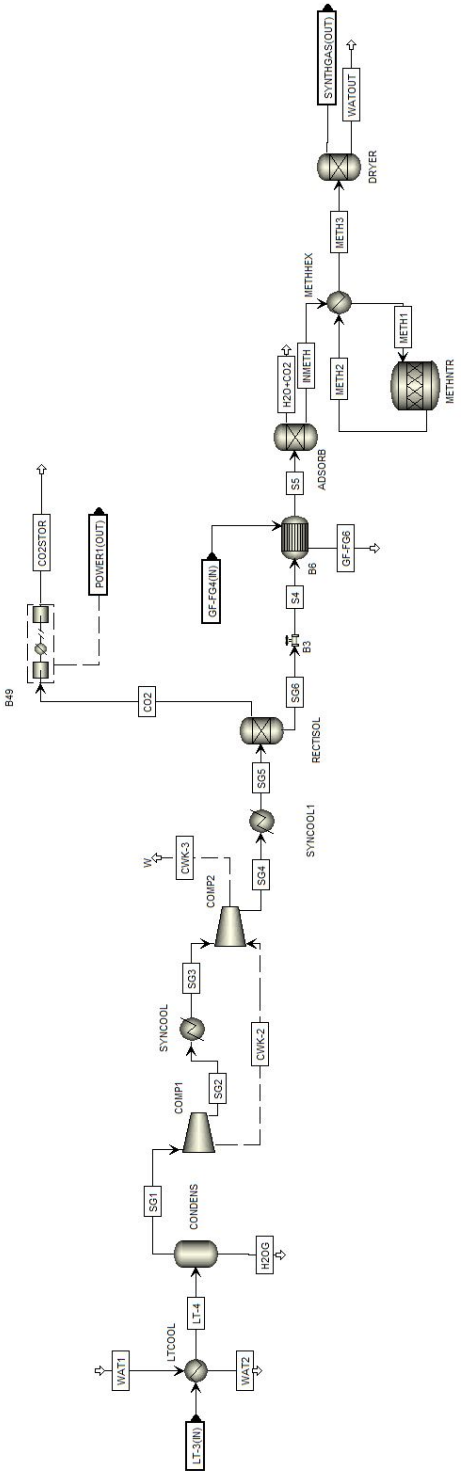

Figure A.5: Cooling, compression and carbon capture sections of gas processing unit

A.0.6 Ammonia recovery unit

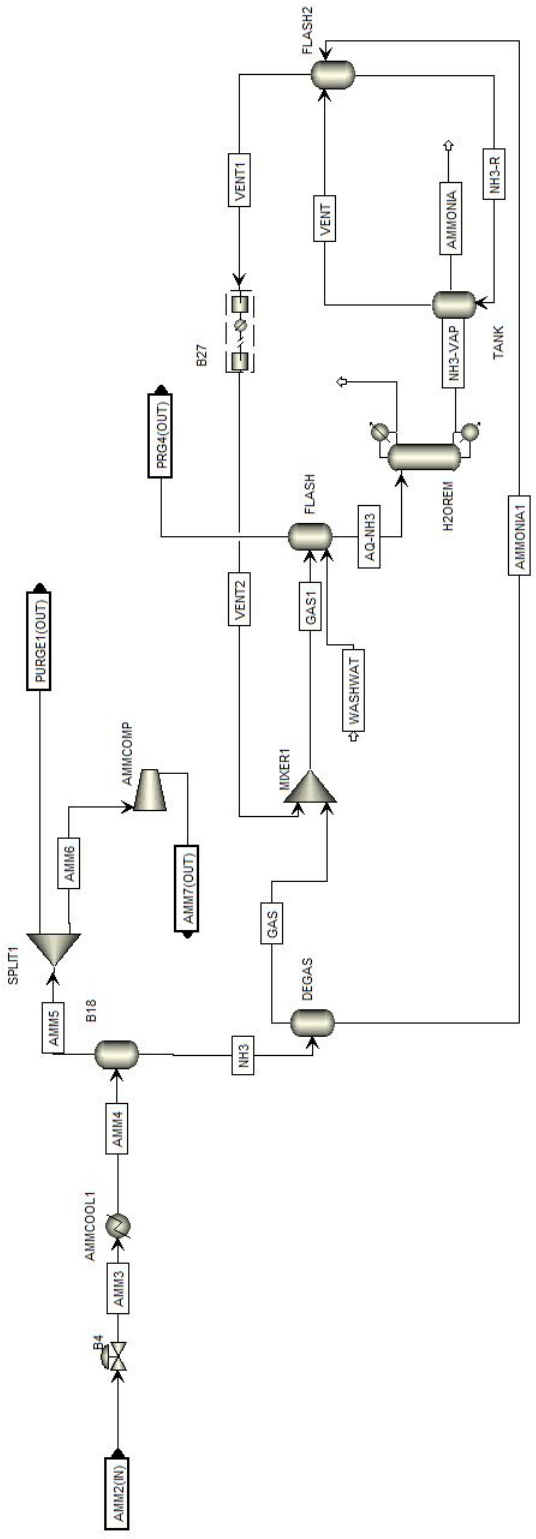

Figure A.6: Ammonia recovery and storage unit

A.0.7 Exergy tables

Table A.1: Chemical exergy and formation enthalpy & entropy of components formed during jet fuel or ammonia production

STD	Chemical Exergy calc				Physical Exergy calc		
Comp.	3	4a	4b	total	h0	s0	Mmolar
	kJ/kmol				KJ/kmol	KJ/kmol.K	kg/kmol
Ar	0.0	11674.1	0.0	11674.1	0.0	154.7	39.9
C2H4	1314293.8	57548.0	-11856.3	1359985.6	52461.0	219.2	28.1
C2H6	1441632.6	66135.74	-13832.3	1493936.0	-84674.5	229.4	30.1
CH4	800738.8	37361.724	-7904.2	830196.4	-74876.2	186.1	16.0
CO	257226.4	20186.31	-1976.0	275436.7	-110525.2	197.5	28.0
CO2	0.0	20186.31	0.0	20186.3	-393498.4	213.7	44.0
H2	228583.2	8587.7	-1976.0	235194.8	3.0	130.6	2.0
H2O gas	0.0	0.0	0.0	0.0	1890.3	6.6	18.0152
H2O liq	0.0	0.0	0.0	0.0	1890.3	6.6	18.0
N2	0.0	692.2	0.0	692.2	-0.3	191.5	28.0
NH3	326498.0	13227.6	-2964.1	336761.6	-45899.7	192.6	17.0
O2	0.0	3952.1	0.0	3952.1	-0.4	205.0	32.0